

Fig. 1. (a) TG and (b) DTG curves for decomposition of pure lignin (\blacktriangle), PA (—), and the 0.3 P/L mixture (\triangle) in nitrogen. The thermal treatment is also shown on the plot.

has been described by several authors [29,30]. Negligible weight losses were observed while lignin was held 2 h long at 650 °C in nitrogen, hence the x-axis in Fig. 1 was limited to a maximum value of $t = 140$ min.

PA losses water at higher temperatures than pure lignin due to the different nature of the water eliminated. Water from lignin corresponds only to moisture whereas water from PA comes from moisture and the water generated by H_3PO_4 thermal degradation into P_2O_5 . Indeed, when orthophosphoric acid is heated it dehydrates to form pyrophosphoric acid, $H_4P_2O_7$, as a result of the condensation of two phosphoric acid molecules. Continued heating leads to a mixture of orthophosphoric and polyphosphoric ($H_{n+2}P_nO_{3n+1}$) acids called superphosphoric acid. At higher temperatures metaphosphoric acid, HPO_3 , is formed and it decomposes to P_2O_5 [31]. Thus, a maximum weight-loss rate was observed at 170 °C and the sample continued losing weight up to 300 °C, which can be attributed to the successive dehydration reactions to P_2O_5 . As temperature increased above 300 °C, weight loss continued at slower rate due to the sublimation of P_2O_5 that starts at this temperature [31]. Sublimation continued steadily up to $T = 580$ °C where a sharp increase in the weight-loss rate of the sample was observed, due to P_2O_5 melting and evaporation at 580–585 °C [31]. The sample weight when temperature arrived at 650 °C was of 52% and, as the temperature was held for 2 h, the sample was totally evaporated.

The 0.3 P/L mixture showed an intermediate behavior between those shown by lignin and PA. Fig. 2(a) and (b) shows experimental and calculated TG and DTG curves of the 0.3 P/L mixture; the calculation was made on the basis of a weighted combination of the experimental curves of pure PA and pure lignin. Doing so, the calculated carbon yield measured during heating was found to be lower than the

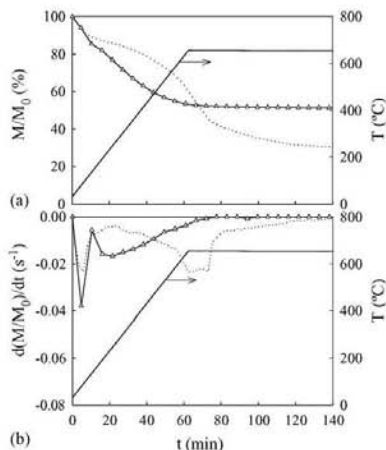


Fig. 2. (a) TG and (b) DTG curves for the decomposition of the 0.3 P/L mixture experimental (\triangle) and calculated (—) assuming a weighted combination of the TG and DTG curves for PA and lignin.

experimental one. However, when temperature was held at 650 °C for 2 h the calculated carbon yield decreased under the experimental one, 29 and 51%, respectively. The experimental weight-loss was higher than that calculated at temperatures lower than 150 °C and between 200 and 450 °C, and the weight of the sample was almost constant at temperatures higher than 600 °C.

These results clearly indicate that lignin reaction with PA during impregnation results in a complex mixed substrate, and that the PA/lignin mixture decomposes according to a reaction path, which is different from that of pure lignin. The PA-impregnated lignin follows a different reaction path during decomposition from that observed in pure lignin. Reaction of lignin with PA starts at room temperature as soon as the components are mixed since, according to the DTA curve given in Fig. 3, the temperature of the P/L sample increases immediately. This observation is in agreement with Lai [32]

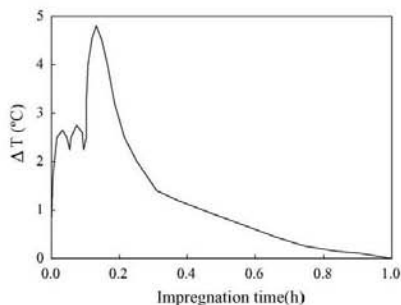


Fig. 3. DTA as a function of the impregnation time of the 1.4 P/L mixture in air and at room temperature. The first two peaks are artefacts only related to the stirring of the formerly inhomogeneous P/L mixture.

who reported the cleavage of aryl ether bonds in accompanied by dehydration, degradation and condensation reactions together with the formation of ketones by hydrolysis of ether linkages at low temperatures. PA promotes dehydration producing an important reordering of the structure and decreasing the volatile compounds emitted during decomposition and so increasing the carbon yield. Therefore, the first weight loss at temperatures lower than 150 °C can be attributed to the increase of dehydration and the higher rate of mass loss between 200 and 450 °C can be attributed to the decomposition of the depolymerized fractions of lignin that degrade at lower temperature than 'pure' lignin. The mass loss rate calculated as the weighted combination of the curves for PA and lignin is very different from the experimental one at temperatures higher than 500 °C (see Fig. 2). Whereas the weight of the sample remained approximately constant at 51% the calculated weight decreases steadily up to 29% due to P₂O₅ evaporation at temperatures above 580 °C. This result agrees with the total reaction of PA with lignin once they are mixed with a P/L of 0.3.

3.1. Effect of the impregnation time

In order to study the effect of the impregnation time, two samples with a P/L = 1.4 and impregnation times of 1 and 22 h were pyrolysed with a heating rate of 10 °C min⁻¹ up to 600 °C in nitrogen. TG curves showed nearly the same evolution with temperature. The char yield at 600 °C was of 56 and 55% for the samples with 1 and 22 h of impregnation time, respectively. This little difference is within the uncertainties of the method and it is difficult to conclude from these results that impregnation time has a real effect on the char yield.

Fig. 3 shows a DTA curve of a sample during the impregnation time with a P/L = 1.4 in air and at room temperature. The temperature difference between the sample and the reference is seen to be almost zero after 1 h impregnation time, evidencing that no chemical reaction still occurs after that time. Therefore, the expected differences, if there are, will be of minor importance for carbons prepared with impregnation times longer than 1 h. In that sense, DTA results are in good agreement with TG-DTG analysis and hence the effect of the other operating conditions can be studied using only 1 h impregnation time.

3.2. Effect of intermediate isothermal periods

Yoon et al. [33] reported an increase of char yield by maintaining the sample at constant temperature for a certain period of time at the beginning of the weight loss. Therefore, we have studied the effect of including isothermal periods at 150 and 300 °C, temperatures at which maximum weight-loss rates in PA-lignin mixtures were observed.

The PA-lignin decomposition was studied for a sample with a P/L = 1.4 and an impregnation time of 1 h, intercalating isothermal periods of 15, 30 and 60 min at 150 °C. Fig. 4 shows the mass loss of these samples and that of the ref-

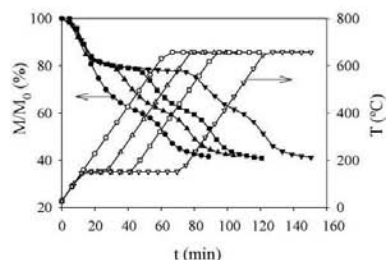


Fig. 4. TG curves of the 1.4 P/L mixture in nitrogen when intercalating isothermal periods at 150 °C (●) 0 min-reference, (▲) 15 min, (■) 30 min, (▼) 60 min). The thermal treatment is also shown on the plot ((○) 0 min-reference, (△) 15 min, (□) 30 min, (▽) 60 min).

erence sample without including isothermal periods. Except for the step at 150 °C, the shape of the curves was essentially the same with a slight variation in the slope of the mass loss between 250 and 400 °C due to the higher extent of lignin degradation with longer isothermal periods. Thus, the differences observed at the end of the isothermal period at 150 °C were small 81, 79 and 77% after 15, 30 and 60 min, respectively. However, once the temperature arrived to 650 °C and after holding for 30 min the char yield was of 42, 41 and 41% for the same samples, respectively, and also of 41% for the reference sample. Therefore, intercalating isothermal periods does not produce changes in the char yield.

Although the differences of char yield upon addition of an isothermal period at 150 °C were not very important, including an isothermal step at this temperature can be of practical interest. Biomass is usually ground and pelletized before carbonization for commercial purposes. As the maximum weight-loss rate corresponding to moisture vaporization during the decomposition of lignin takes place at approximately 150 °C, the rapid water vaporization could crack-up the pellet. Carbonization of lignin in pellets indeed evidenced that intercalating an isothermal period between 100 and 150 °C allows a steady vaporization of lignin moisture, finally leading to pellets free of cracks.

We also studied the PA-lignin decomposition with a P/L = 1.4 and with the inclusion of isothermal periods of 1 h at 150 or 300 °C. The inclusion of an isothermal period of 1 h at 150 °C or at 300 °C did not produce any change in the char yield that was about 41% after holding for 30 min once the temperature arrived to 650 °C. These results are in agreement with the works of Rodríguez-Reinoso et al. [34] and Tascón et al. [35] who found no change in carbon yield with inclusion of intermediate isothermal periods during the course of decomposition of viscose rayon cloth and apple pulp, respectively.

3.3. Effect of phosphoric acid to lignin mass ratio (P/L)

Fig. 5 shows the DTG curves of PA-lignin mixtures, varying P/L from 0.3 to 1.8. As the P/L increased, the tempera-

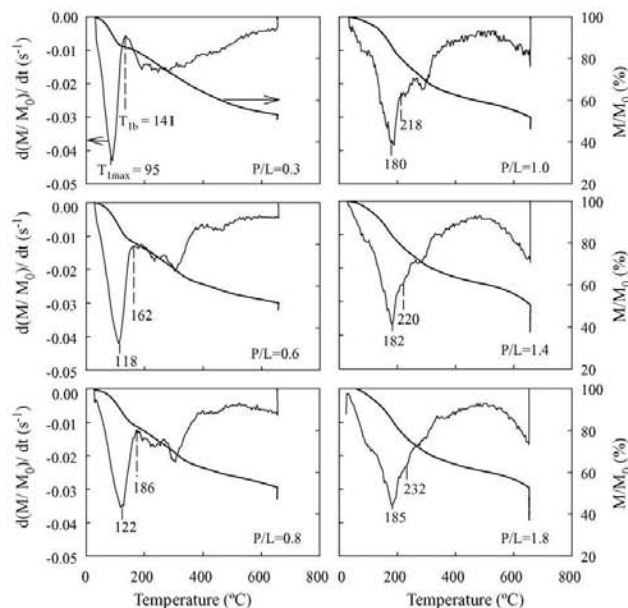


Fig. 5. TG and DTG curves of the decomposition of PA/lignin mixtures, varying P/L from 0.3 to 1.8, heating at $10\text{ }^{\circ}\text{C min}^{-1}$ up to $650\text{ }^{\circ}\text{C}$ and holding the final temperature for 2 h.

ture at which the rate of weight loss was maximal raised up to $P/L = 1.0$. At $P/L \geq 1.0$, $T_{1\text{max}}$ remains practically unchanged at a temperature of around $180\text{--}185\text{ }^{\circ}\text{C}$. We can also observe in the figure that increasing P/L from 0.3 to 0.8 makes the lignin to be completely degraded at decreasingly lower temperatures, from 620 to about $400\text{ }^{\circ}\text{C}$. By contrast, $P/L \geq 1.0$ lead to almost identical end of degradation temperatures, lower than $400\text{ }^{\circ}\text{C}$.

Jagtøyen and Derbyshire [21] reported that CO_2 and CO begin to evolve from biomass in presence of PA just below about $100\text{ }^{\circ}\text{C}$ and their production increases sharply to achieve a maximum at about $200\text{ }^{\circ}\text{C}$. In Fig. 5, it may be observed that $T_{1\text{max}}$ becomes higher than the temperature of maximal rate for PA dehydration ($170\text{ }^{\circ}\text{C}$) and so there is not a clear difference between dehydration of the PA-lignin mixture, dehydration of the PA in excess and lignin degradation with increasing P/L. However, it seems clear that there is a P/L value where PA totally reacts with lignin and so higher P/L should not produce any effect on the decomposition of lignin. In order to confirm the existence of this optimum P/L, the inflexion point of the TG curve after $T_{1\text{max}}$ was assumed to mark the end of the dehydration peak, and hence to correspond to the limiting temperature $T_{1\text{b}}$ between dehydration and decomposition. The percentage of mass loss due to the reaction of PA with lignin, $\%ML_{P/L}$, could thus be quantified, and was calculated as follows:

$$\%ML_{P/L} = \frac{ML_{T_{1b}} - [X_P ML_P + X_L ML_L]}{ML_{T_{1b}}} \times 100$$

where $ML_{T_{1b}}$ is the percentage of mass loss at the inflexion point of the curve, T_{1b} , for a mixture PA-lignin. ML_P and ML_L stand for the water loss of PA and lignin respectively when pyrolyzed independently. X_P and X_L are the weight fraction of PA and lignin in the PA-lignin mixture at a given P/L.

Fig. 6 shows the $\%ML_{P/L}$ calculated as defined above as a function of P/L. The mass loss due to the addition of PA increases nearly linearly between a P/L of 0 and 0.8 and remains approximately constant for $P/L \geq 1.0$ within the error in the estimation of $ML_{T_{1b}}$. This figure confirms that it exits a maximum of acid that can react with lignin. Using $P/L \geq 1.0$ does not increase dehydration: the acid in excess degrades

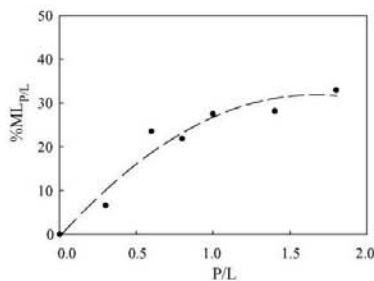


Fig. 6. Percentage of mass loss due to the reaction of PA with lignin as a function of P/L.

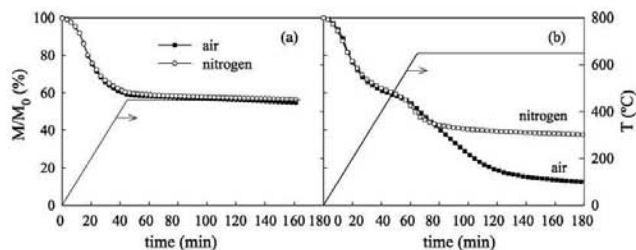


Fig. 7. TG curves of the 1.4 P/L mixture in nitrogen and air when heating at $10^{\circ}\text{C min}^{-1}$ up to (a) 450°C and (b) 650°C , and holding the final temperature for 2 h.

up to P_2O_5 and evolves, which is confirmed by the weight loss produced at $\text{P/L} \geq 1.0$ and at temperatures higher than 550°C observed in Fig. 5.

It may be seen from Fig. 5 that, at $\text{P/L} = 0.3$, the plateau indicating that no more reaction takes place while the material is heated (i.e., the lignin degradation is finished), occurs near 600°C . Increasing P/L makes the end of the degradation occur at decreasing temperatures as far as P/L remains below 1.0. The DTG curves for $\text{P/L} \geq 1.0$ evidenced the same behavior, i.e., the lignin degradation took place at lower ($<400^{\circ}\text{C}$) and almost identical temperatures, and the weight-loss rate was nearly constant at temperatures from 450 to 550°C . The melting and vaporization of P_2O_5 of the unreacted PA could explain the increase in weight-loss rate from 550 to 650°C . This observation supports the hypothesis of an optimum on P/L at values between 0.8 and 1.0 as argued above. It seems clear that since PA reacts with lignin, the optimum P/L will depend on the lignin origin.

3.4. Effect of the gaseous atmosphere

Materials impregnated with PA are usually pyrolyzed in nitrogen. However, earlier studies have shown that chemical activation with PA in air produced carbons with the greatest total number of functional groups when compared with activation under nitrogen flow [25,36,37]. Therefore, excluding obvious economical concerns, activation in air is an interesting option when activated carbons are used for the removal of metals in water treatment because metal uptake appears to be directly correlated with the number of functional groups [36].

To study the effect of the gaseous atmosphere in the process, a sample of PA-impregnated lignin was heated at $10^{\circ}\text{C min}^{-1}$ up to 450 or 650°C in air and in nitrogen and both final temperatures were held for 2 h. Fig. 7(a) shows TG curves of PA-lignin decomposition with $\text{P/L} = 1.4$ in nitrogen and air when heating at $10^{\circ}\text{C min}^{-1}$ up to 450°C . The TG curves for these two experiments exhibit exactly the same shape, i.e., the sample losses weight in the same way and independently of the atmosphere used. Moreover, there was no significant weight loss for 2 h once the temperature of the sample arrived to 450°C .

Fig. 7(b) shows the same as in Fig. 7(a) but the final temperature was 650°C , held 2 h long. Again, the TG curves for both nitrogen and air atmospheres exhibit exactly the same shape up to 650°C . However, if temperature was held at 650°C for a longer time, the samples behaved differently in air and in nitrogen. The sample pyrolyzed in nitrogen showed a sharp decrease in the weight from 51 to 43% during the first 15 min and afterwards the weight remained approximately constant with time. On the contrary, the sample pyrolyzed in air showed a continuous decrease during 80 min reaching a mass percentage of 14.5% meaning the total combustion of the sample. Indeed, due to the phosphatation of the ashes, a residual mass higher than that given in Table 1, 9.5%, was recovered. The low mass variation (8%) of the sample pyrolyzed in nitrogen can be attributed to the P_2O_5 vaporization whereas the low char yield in air is the result of the P_2O_5 vaporization of the PA used in excess and the combustion of unprotected carbon. Examining Fig. 7, one can extract a conclusion of practical and economical importance: char yield is nearly independent of the gaseous atmosphere at moderate temperatures and with the adequate P/L.

4. Conclusions

When lignin and PA are mixed together, they react completely in less than 1 h and longer impregnation times or inclusion of isothermal periods do not have any influence on the char yield. The product of the reaction between PA and lignin pyrolyses following a reaction path different from that of pure lignin. PA acts on lignin increasing dehydration and anticipating its complete degradation at temperatures as low as 400°C . There exists an optimum P/L at values between 0.8 and 1.0 that allows the complete reaction of lignin, and further increases in P/L do not produce changes on the pyrolysis process. H_3PO_4 in excess dehydrates progressively into P_2O_5 which finally melts and evaporates. P_2O_5 protects carbon from oxidation and once evaporated at temperatures higher than 580°C the carbon is totally oxidized in air whereas the char yield in nitrogen remains constant. Char yield is nearly independent of the gaseous atmosphere at moderate decomposition temperatures as long as lignin has reacted completely with PA.

Acknowledgements

This research was made possible in part by financial support from MCYT (project PPQ2002-04201-CO02) and DURSI (2001SGR00323). V. Fierro acknowledges the MCYT and the Universitat Rovira i Virgili (URV) for the financial support of her 'Ramón y Cajal' research contract. V. Torné-Fernández acknowledges the URV for her PhD grant.

References

- [1] V.D. del Bagno, R.L. Miller, J.J. Watkins, On site production of activated carbon from Kraft Black Liqueur, U.S. EPA Report no. 600/2-78-191 (1978).
- [2] J. Rodríguez-Mirasol, T. Cordero, J.J. Rodríguez, *Carbon* 31 (1993) 87–95.
- [3] E. Gonzalez Serrano, T. Cordero, J. Rodríguez-Mirasol, J.J. Rodríguez, *Ind. Eng. Chem. Res.* 36 (1997) 4832–4838.
- [4] H. Teng, T.S. Yeh, L.Y. Hsu, *Carbon* 36 (1998) 1387–1398.
- [5] M. Jagtoyen, F. Derbyshire, *Carbon* 31 (1993) 1185–1192.
- [6] H. Benadi, D. Legras, J.N. Rouzaud, F. Béguin, *Carbon* 36 (1998) 306–309.
- [7] J. Laine, A. Calafat, M. Labady, *Carbon* 27 (1989) 191–195.
- [8] M. Molina-Sabio, F. Rodríguez-Reinoso, F. Caurila, M.J. Sellés, *Carbon* 34 (1996) 457–462.
- [9] B.S. Girgis, A.A. El-Hendawy, *Micropor. Mesopor. Mater.* 52 (2002) 105–117.
- [10] A.A. El-Hendawy, S.E. Samra, B.S. Girgis, *Colloid Surf. A* 180 (2001) 209–221.
- [11] B.S. Girgis, M.F. Ishak, *Mater. Lett.* 39 (1999) 107–114.
- [12] F. Suárez-García, A. Martínez-Alonso, J.M.D. Tascón, *J. Anal. Appl. Pyrolysis* 63 (2002) 283–301.
- [13] F. Suárez-García, A. Martínez-Alonso, J.M.D. Tascón, *Carbon* 39 (2001) 1111–1115.
- [14] M.C. Baquero, L. Giraldo, J.C. Moreno, F. Suárez-García, A. Martínez-Alonso, J.M.D. Tascón, *J. Anal. Appl. Pyrolysis* 70 (2003) 779–784.
- [15] B.S. Girgis, S.S. Yunis, A.M. Soliman, *Mater. Lett.* 57 (2002) 164–172.
- [16] T. Vemersson, P.R. Bonelli, E.G. Cerrella, A.L. Cukiernan, *Bioreour. Technol.* 83 (2002) 95–104.
- [17] J. Guo, A.C. Lua, *Sep. Purif. Technol.* 30 (2003) 265–273.
- [18] R.A. Shawabkeh, D.A. Rockstraw, R.K. Ehada, *Carbon* 40 (2002) 781–786.
- [19] Y. Diao, W.P. Walawender, L.T. Fan, *Bioreour. Technol.* 81 (2002) 45–52.
- [20] C.A. Toles, W.E. Marshall, M.M. Johns, L.H. Wartelle, A. McAloon, *Bioreour. Technol.* 71 (2000) 87–92.
- [21] M. Jagtoyen, F. Derbyshire, *Carbon* 36 (1998) 1085–1097.
- [22] H. Benaddi, T.J. Bandoz, J. Jagiello, J.A. Schwarz, J.N. Rouzaud, D. Legras, F. Béguin, *Carbon* 38 (2000) 669–674.
- [23] C. Toles, S. Rimmer, J.C. Hower, *Carbon* 34 (1996) 1419–1426.
- [24] F. Carrasco-Marín, M.A. Alvarez-Merino, C. Moreno-Castilla, *Fuel* 75 (1996) 966–970.
- [25] A.M. Puziy, O.I. Poddubnaya, A. Martínez-Alonso, F. Suárez-García, J.M.D. Tascón, *Appl. Surf. Sci.* 200 (2002) 196–202.
- [26] A.M. Puziy, O.I. Poddubnaya, B. Gawdzik, M. Sobiesiak, D. Dziadko, *Appl. Surf. Sci.* 196 (2002) 89–97.
- [27] J. Hayashi, A. Kazehaya, K. Muroyama, A.P. Watkinson, *Carbon* 38 (2000) 1873–1878.
- [28] J. Rodríguez-Mirasol, T. Cordero, J.J. Rodríguez, *Carbon* 34 (1996) 43–52.
- [29] J.A. Caballero, A. Marcilla, J.A. Conesa, *J. Anal. Appl. Pyrol.* 44 (1997) 75–88.
- [30] J.J.M. Órfão, F.J.A. Antunes, J.L. Figueiredo, *Fuel* 78 (1999) 349–358.
- [31] *Handbook of Chemistry and Physics*, 72nd ed., CRC press, Boca Raton, Florida, 1985, p. B-119.
- [32] Y.Z. Lai, in: D.N.S. Hon, N. Shirashi (Eds.), *Wood and Cellulosic Chemistry*, 10, Marcel Dekker, New York, 1991, p. 455.
- [33] S.H. Yoon, B.C. Kim, Y. Korai, I. Mochida, *Proceedings of the 22nd Biennial Conference on carbon. Extended Abstract and Program*, San Diego, California, 1995, p. 218.
- [34] C. Pastor, F. Rodríguez-Reinoso, H. Marsh, M.A. Martínez, *Carbon* 3 (1999) 1275–1283.
- [35] F. Suárez-García, A. Martínez-Alonso, J.M.D. Tascón, *J. Anal. Appl. Pyrolysis* 62 (2002) 93–109.
- [36] C.A. Toles, W.E. Marshall, M.M. Johns, *Carbon* 37 (1999) 1207–1214.
- [37] C.A. Toles, W.E. Marshall, M.M. Johns, *J. Chem. Technol. Biotechnol.* 72 (1998) 255–263.

5.1.3. Kraft lignin as a precursor for microporous activated carbons prepared by impregnation with orto-phosphoric acid: synthesis and textural characterisation

Este artículo se ha publicado en el journal *Microporous and Mesoporous Materials* en 2006 en el volumen 92, páginas 243 a 250.



Kraft lignin as a precursor for microporous activated carbons prepared by impregnation with ortho-phosphoric acid: Synthesis and textural characterisation

V. Fierro ^{a,*}, V. Torné-Fernández ^a, A. Celzard ^b

^a *Departament de Enginyeria Química, Universitat Rovira i Virgili, Avda dels Països Catalans, 26, 43007 Tarragona, Spain*

^b *Laboratoire de Chimie du Solide Minéral, Université Henri Poincaré—Nancy I, UMR—CNRS 7555, BP 239, 54506 Vandoeuvre-lès-Nancy, France*

Received 25 October 2005; received in revised form 12 January 2006; accepted 19 January 2006

Available online 3 March 2006

Abstract

Activated carbons were prepared by activation of Kraft lignin with ortho-phosphoric acid at various temperatures (400–650 °C), weight ratios of ortho-phosphoric acid to lignin (P/L = 0.7–1.75) and impregnation times (1–48 h). The resulting carbons were characterised by elemental analysis, N₂ adsorption at 77 K and SEM. The results indicate that the pyrolysis of lignin impregnated with ortho-phosphoric acid produces essentially microporous carbons, with a percentage of the total micropore volume approximately constant (80%), whatever the carbonisation temperature. The fraction of ultramicropores decreases with increasing temperature whereas that of supermicropores reaches a maximum at 600 °C. The maximum surface area (1305 m²/g) and pore volume (0.67 cm³/g) are reached at 600 °C, while pyrolysis of acid-impregnated lignin at temperatures higher than 600 °C produces a significant reduction of both pore volume and BET surface area due to: (i) the shrinkage of the material caused by the degradation of the phosphate and polyphosphate bridges and (ii) the oxidation of the carbon caused by the loss of the protecting P₂O₅. Increasing the P/L ratio increases the carbon yield and involves changes in the total volume of pores, the pore size distribution and the BET surface area. There exists an optimum P/L ratio which probably depends on the activation temperature, an excess of ortho-phosphoric acid beyond this optimum value reducing the surface area and the pore volume of the resultant activated carbon. Increasing the impregnation time, the surface area and the pore volume are lowered, and such an effect is more severe at higher activation temperatures.

© 2006 Elsevier Inc. All rights reserved.

Keywords: Activated carbon; Ortho-phosphoric acid activation; Porosity; Surface area

1. Introduction

The conversion of wood chips to pulp for manufacturing paper generates huge quantities of by-product lignins. Various processes can be used to remove and isolate lignin. The Kraft process produces black liquor, a residue composed of lignin (30–40%) and other inorganic compounds. This residue is used as in-house fuel for the recovery of

energy and of the remaining inorganic reactants. As progress has been taken to maximise production, the recovery furnaces in an ever-increasing number of mills have become overloaded; the result is that all the by-product lignin can no longer be used in its traditional role as a fuel. Unfortunately the necessary capital investment usually precludes construction of a new recovery furnace so that there is little prospect of rectifying the situation in the majority of recovery-loaded mills. The separation of lignin and its use as precursor for activated carbons (ACs) could be an alternative to incineration.

ACs have already been synthesised by physical activation of eucalyptus Kraft lignin by CO₂ partial gasification [1] and by chemical activation of this precursor using zinc

* Corresponding author. Present address: Laboratoire de Chimie du Solide Minéral, Université Henri Poincaré—Nancy I, UMR—CNRS 7555, BP 239, 54506 Vandoeuvre-lès-Nancy, France. Tel.: +33 383684000; fax: +33 383684619.

E-mail address: Vanessa.Fierro@lcsm-uhp.nancy.fr (V. Fierro).

chloride [2]. Chemical activation of Kraft lignin with $ZnCl_2$ within the thermal range 400–500 °C allowed obtaining high surface area ACs with predominantly microporous structure. At 500 °C and impregnation ratio $ZnCl_2$ /lignin of 2.3 w:w, the maximum of mesoporosity ($0.59 \text{ cm}^3/\text{g}$) and microporosity ($1.04 \text{ cm}^3/\text{g}$) and a corresponding BET surface area of $1800 \text{ m}^2/\text{g}$ were obtained. However, the use of $ZnCl_2$ has declined due to environmental problems [3], and ortho-phosphoric acid is preferred as activating-dehydrating agent.

The use of ortho-phosphoric acid as activating agent has been reported for various agricultural by-products [4–17], wood [18,19], natural [20,21,3] and synthetic [22,23] carbons. The ortho-phosphoric acid impregnating the material plays a double role according to Jagtoyen and Derbyshire [18]: (i) it produces the hydrolysis of the lignocellulosic matters and the subsequent extraction of some components, thus weakening the material, which swells and (ii) the acid occupies a volume which inhibits the contraction of the material during the heat treatment, by forming phosphate and polyphosphate bridges that connect and cross-link biopolymer fragments, thus leaving a porosity when it is extracted by washing after carbonisation.

To the best of our knowledge, there is only one paper [24] in which the possibility of chemical activation of Kraft lignin with H_3PO_4 , among other activating agents, has been examined. The authors carried out carbonisation at a temperature held for 1 h within the range 500–900 °C, under N_2 flow. Maximum surface areas of more than $1300 \text{ m}^2 \text{ g}^{-1}$ were reached at 600 °C.

Our previous studies, dealing with the analysis of the thermal decomposition of Kraft lignin impregnated with ortho-phosphoric acid, were carried out using thermogravimetry (TG–DTG) [25,26]. In these papers, we got significant insight in the activation process and in the role of P_2O_5 , up to its evaporation at 580 °C, in protection against carbon oxidation. Thus, ortho-phosphoric acid was found to increase the carbon yields in two ways: (i) increase of dehydration and promotion of a structural rearrangement of the solid, which also reduces the emission of volatile compounds and (ii) prevention of combustion in the air atmosphere.

In this paper, the preparation at a larger scale and the characterisation of the ACs derived from Kraft lignin (KL), using chemical activation with ortho-phosphoric acid in air, are reported. Our purpose was to examine the influence of preparation conditions (activation temperature, ortho-phosphoric/lignin weight ratio and impregnation time) on carbon yield, surface area and pore size distribution.

2. Experimental

2.1. Starting materials

Kraft lignin (KL) was provided by Lignotech Iberica S.A. The proximate analysis was carried out according to

ISO standards, following the weight losses of the material at 100 °C in air (moisture, ISO-589-1981), at 900 °C in a non-oxidising atmosphere (volatile matter, ISO-5623-1974) and at 815 °C in air (ashes, ISO-1171-1976). An 85 wt.% H_3PO_4 solution (Panreac, Spain) was used as activating agent. The ultimate analysis of the pristine lignin was carried out in an EA1108 Carlo Erba Elemental Analyser.

2.2. Preparation and characterisation of the ACs

Lignin was mixed with various amounts of H_3PO_4 in the range of 0.7–1.75 acid to lignin weight ratio (P/L) on a wet basis. The slurry was left for impregnation times varying from 1 to 48 h at room temperature in air, and then transferred to a furnace DUM Model 10CAF where carbonisation was carried out under air atmosphere. The furnace was heated at $10 \text{ }^\circ\text{C min}^{-1}$, up to 150 °C, which temperature was held for 1 h to allow free evolution of water. Afterwards the oven was heated at $10 \text{ }^\circ\text{C min}^{-1}$ up to the final carbonisation temperature, ranging from 400 to 650 °C, which was held for 2 h. To remove the excess of H_3PO_4 after carbonisation, the activated carbon was extensively washed with distilled water until a neutral pH was met (a CyberScan PC 510 pH-meter with a Hamilton-electrode ‘Fluhtrode’ was used). Then, the samples were dried overnight in an oven at 105 °C.

C, H, S and N contents of the ACs were measured using an EA1108 Carlo Erba Elemental Analyser. P content was determined by scanning electron microscopy (SEM) with a JEOL JSM-6400 equipped with an energy dispersive X-ray (EDX) microanalyser. Oxygen was calculated by difference.

Surface area and pore size distributions were determined from the corresponding nitrogen adsorption–desorption isotherms obtained at 77 K with an automatic instrument (ASAP 2020, Micromeritics). The samples were previously outgassed at 523 K for several hours. N_2 adsorption data at relative pressures ranging from 10^{-5} to 0.99 (in a set of values previously fixed) were analysed according to: (i) the BET method [27] for calculating the apparent surface area, S_{BET} and (ii) the α_s method [28] (using Carbopack F Graphitised Carbon Black as reference material [29]) for calculating the micropore volume, $V_{\alpha_{\text{micro}}}$, and the ultramicropore volume, $V_{\alpha_{\text{ultra}}}$. The total pore volume, $V_{0.99}$, was calculated from nitrogen adsorption at a relative pressure of 0.99. ACs were examined by scanning electron microscopy (SEM) operating at magnifications of $\times 400$ and $\times 7000$.

3. Results and discussion

3.1. Characterisation of the raw material

Table 1 shows the proximate and ultimate analyses of lignin. The high sulfur content (2.2%) in KL is originated both from the Kraft or sulfate process, based on the action of NaOH and Na_2S for separating cellulose from the other

Table 1
 Lignin analyses (wt.%)

Proximate (wt.%, humid basis)		Elemental (wt.%, ash and moisture free)	
Moisture	14.45	Carbon	59.46
Ash	9.50	Hydrogen	5.07
Volatile matter	44.93	Nitrogen	0.05
Fixed carbon ^a	31.12	Sulfur	2.15
		Oxygen ^a	33.27

^a Estimated by difference.

wood constituents, and from organically bound sulfur (up to 1.5%) [30].

Fig. 1 shows SEM images of KL at different magnifications. KL particles are small, and have a rounded (even spherical) shape with widely open volumes inside. Such morphology is probably due to the concentration process of lignin from black liquors, which is done by evaporation; due to their surface tension, the particles take a spherical—thermodynamically more stable form. A more detailed observation reveals that the surface of the KL particles is very rough.

We observed that reaction of lignin with ortho-phosphoric acid starts at room temperature, and as soon as the components are mixed together, the temperature of the vessel increases [25]. Lai [31] indeed reported the cleavage of aryl ether bonds accompanied by dehydration, degradation and condensation reactions together with the formation of ketones by hydrolysis of ether linkages at low temperatures.

In order to understand the effect of the preparation conditions on the ACs produced by activation of KL with ortho-phosphoric acid, activation temperature (400–650 °C), weight ratio of acid to lignin (P/L = 0.7–1.75) and impregnation time (1–48 h) were systematically varied.

3.2. Effect of the activation temperature

The effect of activation temperature was studied from 400 to 650 °C using KL impregnated with ortho-phosphoric acid for 1 h and with a P/L ratio of 1.4.

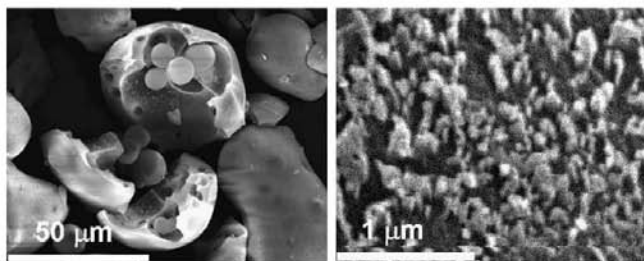


Fig. 1. SEM images of Kraft lignin at different magnifications.

Fig. 2 shows the variation of carbon yield with activation temperature. Increasing the temperature, the carbon yield decreases from 49% at 400 °C to 8% at 650 °C. There are two sharp decreases in carbon yield, one from 400 to 450 °C and the other between 550 and 650 °C, whereas the slope is lower between 450 and 550 °C. The corresponding weight loss mechanisms were explained in our previous studies [25,26] carried out in a thermogravimetric device. The first sharp weight loss corresponds to the loss of most of the volatile matter. The second one would correspond: (i) to the volatilisation of the P₂O₅ coming from the H₃PO₄ in excess and (ii) to the resultant carbon combustion once the formerly protecting P₂O₅ is lost.

Table 2 shows the elemental analysis of the ACs prepared according to the experimental conditions used in this study. As temperature is increased up to 550 °C, there is an increase in C and a decrease in O and H contents, due to an increasing degree of aromaticity. At activation temperatures higher than 550 °C, the C/H ratio remains nearly constant, indicating no further changes in the chemical composition, which again confirms the aforementioned process explaining the variations of carbon yield. The P content in the ACs decreases with temperature, indicating a degradation of the phosphate and polyphosphate groups.

Fig. 2 also shows the BET apparent surface area of the ACs prepared at different activation temperatures. The BET surface area increases between 400 and 600 °C up to

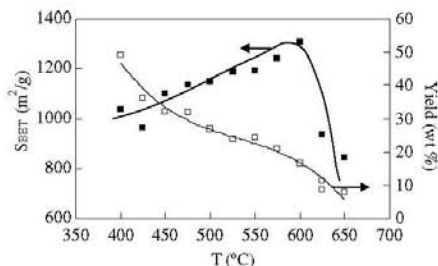


Fig. 2. BET surface area and carbon yield of the activated carbons as a function of the activation temperature (P/L = 1.4 and 1 h impregnation time).

Table 2
 Activation conditions and elemental analysis of the resultant ACs

Activation conditions			Elemental analysis						
T (°C)	P/L (w/w)	t _i (h)	C (%)	H (%)	C/H	N (%)	S (%)	P (%)	O ^a (%)
400	1.4	1	76.19	2.03	37.53	0.12	0.65	n.d.	n.d.
425	1.4	1	76.26	1.84	41.45	0.16	0.73	n.d.	n.d.
450	1.4	1	78.03	1.59	49.08	0.20	1.08	1.20	17.90
475	1.4	1	78.02	1.58	49.38	0.22	0.98	n.d.	n.d.
525	1.4	1	79.54	1.41	56.41	0.23	0.68	0.80	17.34
550	1.4	1	79.97	1.29	61.99	0.20	0.66	n.d.	n.d.
575	1.4	1	80.51	1.35	59.64	0.27	0.88	n.d.	n.d.
600	1.4	1	80.82	1.27	63.64	0.29	0.79	0.60	16.23
625	1.4	1	79.06	1.40	56.47	0.46	0.66	n.d.	n.d.
650	1.4	1	78.14	1.24	63.02	0.59	0.85	0.60	18.58
450	0.7	1	77.23	2.02	38.23	0.25	0.80	1.10	18.60
450	1.0	1	77.83	1.78	43.72	0.25	1.20	0.9	18.04
450	1.2	1	77.95	1.92	40.60	0.19	0.66	1.3	17.98
450	1.75	1	76.23	1.91	39.91	0.19	0.77	2.3	18.60
450	1.4	48	78.25	1.66	47.14	0.20	0.54	n.d.	n.d.
600	1.4	2	80.42	1.41	57.04	0.31	0.42	n.d.	n.d.
600	1.4	6	79.9	1.19	67.16	0.32	0.89	n.d.	n.d.
600	1.4	48	78.75	1.23	64.02	0.36	1.04	n.d.	n.d.

^a Estimated by difference; n.d. not determined.

a maximum value of $1305 \text{ m}^2 \text{ g}^{-1}$ observed at $600 \text{ }^\circ\text{C}$ and the surface areas are considerably reduced at higher temperatures. These results are consistent with the two sharp decreases in carbon yield observed previously. The steady increase of surface area with temperature up to $600 \text{ }^\circ\text{C}$ would correspond to the evolution of compounds produced from the cross-linking reactions. The latter preserve the structure of the polymer at the same time as the BET surface area and the porosity increase up to $600 \text{ }^\circ\text{C}$. At higher temperatures, the degradation of the phosphate and polyphosphate bridges, already observed by the decrease of P content in the ACs with temperature [25,26], would weaken the structure; the resultant collapse would then lower both the BET surface area and the pore volume. Moreover, the loss of the protecting P_2O_5 and the combustion of the carbon could also explain this reduction in the surface and the porosity. Hayashi et al. [24] also reported that $600 \text{ }^\circ\text{C}$ is the optimum temperature for surface development in ACs prepared by ortho-phosphoric acid activation of KL, in good agreement with our results.

Fig. 3 shows adsorption isotherms of N_2 at 77 K measured on ACs prepared at different temperatures from 400 to $650 \text{ }^\circ\text{C}$. All the isotherms are of type I. That of the carbon prepared at $400 \text{ }^\circ\text{C}$ has a very small upward bending at the highest pressures, indicating an essentially microporous character with some contribution of wider pores (meso- and macropores). As activation temperature increases, the knee of the isotherm widens and the plateau is not clearly reached, indicating pore widening. The isotherm of the carbon prepared at $650 \text{ }^\circ\text{C}$ shows the lowest N_2 adsorption capacity, due to the reduction of both its surface and its pore volume.

Fig. 4 shows the application of the α_s method to the N_2 isotherms of the ACs prepared at 400 , 500 , 600 and $650 \text{ }^\circ\text{C}$, which allows to calculate $V_{\alpha\text{micro}}$ and $V_{\alpha\text{ultra}}$. Fig. 5 shows

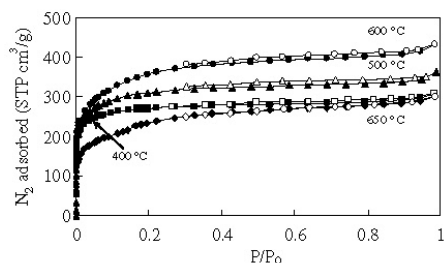


Fig. 3. Nitrogen adsorption (full symbols) and desorption (empty symbols) isotherms of activated carbons prepared at different temperatures (P/L – 1.4 and 1 h impregnation time).

the evolution of $V_{0.99}$, $V_{\alpha\text{micro}}$ and $V_{\alpha\text{ultra}}$ as a function of activation temperature. $V_{\alpha\text{ultra}}$ always decreases with increasing temperature whereas the volume of supermicropores, calculated as the difference between $V_{\alpha\text{micro}}$ and $V_{\alpha\text{ultra}}$, reaches a maximum at $600 \text{ }^\circ\text{C}$. At temperatures higher than $600 \text{ }^\circ\text{C}$, there is a reduction of all the pore volumes. This reduction in the total porosity would be due to: (i) the collapse of the structure produced by the loss of phosphate and polyphosphate bridges and the resultant weakening of the structure at temperatures higher than $600 \text{ }^\circ\text{C}$ and (ii) the oxidation of the carbon caused by the volatilisation of the protecting P_2O_5 .

SEM photographs of the ACs prepared at different temperatures, with a constant P/L ratio of 1.4 and an impregnation time of 1 h, are shown in Fig. 6. This figure shows well-defined macropores and the presence of small grains at the surface; these grains are more hardly seen in the AC prepared at $650 \text{ }^\circ\text{C}$, which also presents a smoother surface. It can be observed that increasing activation temperature, the small grains agglomerate, or soften, to form

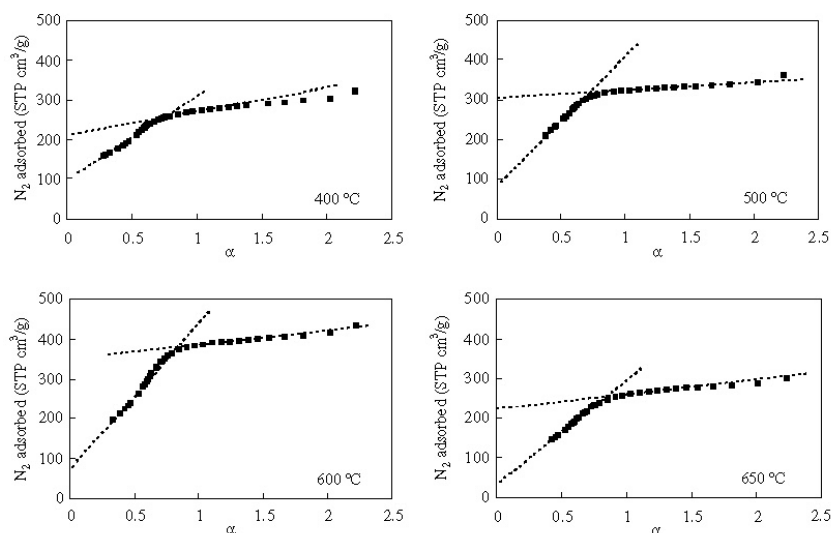


Fig. 4. α_c plots of N_2 adsorption at 77 K on ACs prepared at: (a) 400, (b) 500, (c) 600 and (d) 650 °C (P/L = 1.4 and 1 h impregnation time).

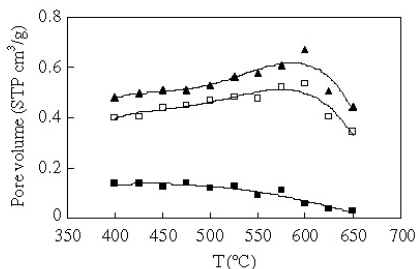


Fig. 5. Effect of the activation temperature on the pore volumes: $V_{0.99}$ (\blacktriangle), $V_{\alpha\text{micro}}$ (\square) and $V_{\alpha\text{ultra}}$ (\blacksquare) of the ACs.

bigger spheres until becoming nearly undistinguished with the surface at 650 °C. This finding is consistent with a lowering of the surface area at high temperatures.

3.3. Effect of the impregnation ratio

Porosity is generated with ortho-phosphoric acid remaining intercalated in the internal structure of the biopolymer material in the form of phosphate and polyphosphate compounds [32], hindering the shrinkage. As P/L increases, it is reasonable to expect, on one hand, an increase in the volume filled by polyphosphate compounds as long as ortho-phosphoric acid can react with lignin, but also, on the other hand, a weakening of the structure due to the attack of the excess acid. The effect of the P/L ratio was studied using carbons impregnated during 1 h at five differ-

ent P/L ratios, ranging between 0.7 and 1.75, and activated at 450 °C.

Fig. 7(a) shows the variation of carbon yield with the P/L ratio. The carbon yield increases from 21% at P/L = 0.7–32% at P/L = 1.4. The latter value of carbon yield is nearly identical to the amount of fixed carbon determined in Table 1, once more confirming the protecting role of the phosphoric acid against carbon oxidation in air at the experimental activation temperatures. It was found that P/L values higher than 1.4 do not produce further increase of carbon yield at 450 °C. The P/L ratio not only affects the char yield but also the apparent surface area and the pore size distribution. Fig. 7(a) also shows the variation of the apparent surface areas with the P/L ratio. The highest value is reached at P/L = 1.2–1.4, and further increases in the P/L ratio produces a decrease in the BET surface area.

Nitrogen adsorption isotherms measured on ACs prepared at several P/L ratios are of type I, just like those already presented in Fig. 3. At P/L = 0.7, the activated carbons are essentially microporous with some contribution of wider pores (meso- and macropores). Increasing the P/L ratio produces the development of porosity in the mesoporous region, evidenced by the widening of the knee of the isotherms. Fig. 7(b) shows the variation of $V_{0.99}$, $V_{\alpha\text{micro}}$ and $V_{\alpha\text{ultra}}$ of the ACs with the P/L ratio used for activation. The highest micropore to total volume ratio is found at the lowest P/L ratio used. As P/L ratio increases up to P/L = 1.4, the $V_{0.99}$ and $V_{\alpha\text{micro}}$ increases but the $V_{\alpha\text{ultra}}$ decreases. Within the inherent error in the N_2 adsorption measurements and despite the heterogeneity of the AC samples, a P/L ratio between 1.2 and 1.4 seems to be an optimum when carbonisation is carried out at 450 °C.

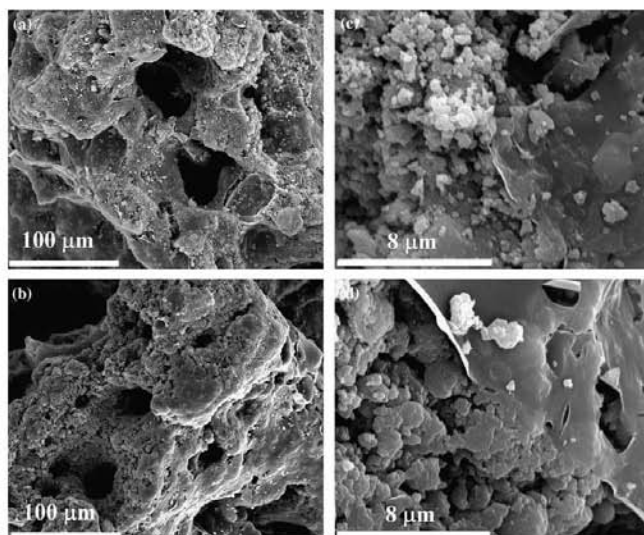


Fig. 6. SEM images of the activated carbons prepared at 450 (a, c) and 650 °C (b, d) at different magnifications (P/L = 1.4 and 1 h impregnation time).

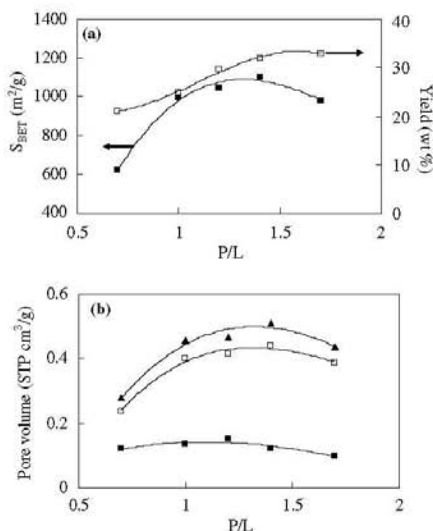


Fig. 7. Effect of the P/L ratio: (a) on the BET surface area and the carbon yield; (b) on the pore volumes $V_{0.99}$ (▲), V_{micro} (□) and V_{ultra} (■) of the ACs prepared at 450 °C and 1 h impregnation time.

P/L between 1.2 and 1.4 allowed to obtain carbons with high surface areas ($S_{BET} = 1049$ and $1101 \text{ m}^2 \text{ g}^{-1}$, respectively) and total pore volumes ($V_{0.99} = 0.469$ and $0.511 \text{ cm}^3 \text{ g}^{-1}$, respectively). Higher P/L ratios reduce the total pore volume and in a similar extent in the entire pore diameter interval.

It has been shown above that the use of P/L ratios in the range 1.2–1.4 allows obtaining ACs with high surface areas and porosity. The use of lower P/L ratios produces ACs having a higher contribution of micropores to the total porosity but also lower surface areas. The use of P/L = 1.75 reduces the total porosity and surface area, probably by the attack of the structure by the acid in excess. Thus, an optimum amount of ortho-phosphoric acid that can react exists, and higher P/L ratios produce an extensive breaking of biopolymer bonds, the shrinkage of the structure and consequently the reduction of the surface area and the total volume of pores.

Fig. 8 shows SEM photographs of the ACs prepared at 450 °C, with P/L = 0.7 and 1.75 and 1 h impregnation time at different magnifications, that can be compared with Fig. 6(a) and (c) corresponding to the AC prepared at P/L = 1.4 and 450 °C. The aspects of the surface of the ACs prepared with P/L ratios of 0.7 and 1.75 are very similar to each other, both at $\times 400$ and at $\times 7000$ magnification, with little grains agglomerated in bigger particles. The use of intermediate P/L ratios (see Fig. 6(a) and (c)) gives ACs with rough surfaces where small individual grains can be observed at $\times 7000$ magnification. These SEM observations agree well with the analysis done by N_2 adsorption.

Increasing the temperature or the P/L ratio seems to have the same effect on the pore texture. V_{ultra} always decreases with increasing activation temperature and P/L ratio, and there is an optimum value for both variables, allowing to obtain high surface areas and pore volumes. If the temperature or the P/L ratio are higher than their respective optimum, the surface area and the pore volume decrease, probably because of the collapse of the porous

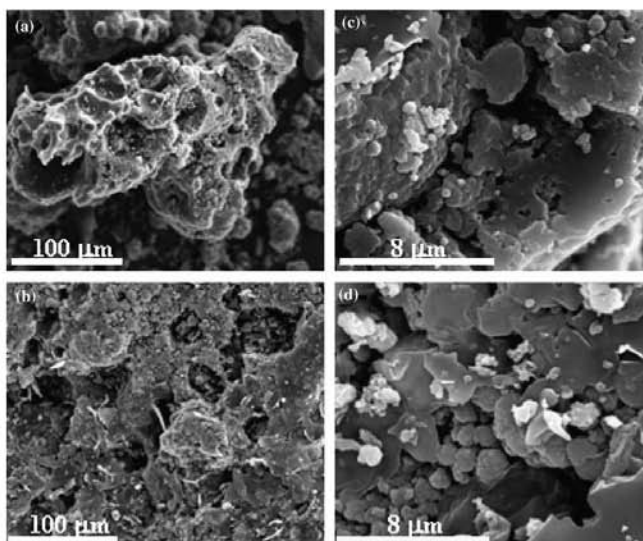


Fig. 8. SEM images of the activated carbons prepared at P/L = 0.7 (a, c) and 1.75 (b, d) at different magnifications ($T = 450\text{ °C}$ and 1 h impregnation time).

structure by the weakening of the phosphate bridges or by the excessive attack of the polymeric matrix, respectively.

3.4. Effect of the impregnation time

ACs were prepared within the range 450–600 °C with P/L = 1.4 and impregnation times ranging from 1 to 48 h. There was no significant difference in the carbon yield with impregnation time, although a very small decrease of carbon yield with increasing impregnation time was observed.

Fig. 9 shows the variation of the BET surface area for carbons prepared with different impregnation times at 450, 525 and 600 °C. Higher impregnation times lead to lower BET surface areas, the magnitude of this lowering being more important as the temperature increases. The

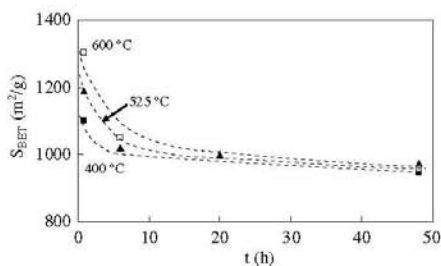


Fig. 9. Effect of the impregnation time on the BET surface area for carbons prepared at 450, 525 and 600 °C.

apparent surface area decreases from 1305 to 956 $\text{m}^2\text{ g}^{-1}$ from 1 to 48 h impregnation time, respectively, for ACs prepared at 650 °C. These changes in surface area and porosity are of less importance at low temperatures, and so the surface area is only reduced by 150 $\text{m}^2\text{ g}^{-1}$ at 450 °C when the impregnation time is extended from 1 to 48 h. The effect of time seems to be more important at the first moments of the impregnation of lignin with phosphoric acid, since BET surface areas values are nearly constant after 6 h impregnation time. Higher impregnation times promote the diffusion of ortho-phosphoric acid in the material and its role in the cross-linking reactions. Since KL is a powder, the ortho-phosphoric acid reacts rapidly with it, but it seems that it could also damage the polymeric structure at impregnation times higher than 1 h, thus leading to lower pore volumes and lower surface areas.

4. Conclusions

In the present study, activated carbon was produced by chemical activation of Kraft lignin, using H_3PO_4 as the activating agent. The results evidenced that pyrolysis of Kraft lignin impregnated with ortho-phosphoric acid produces essentially microporous ACs with high apparent surface areas and reasonable carbon yields.

Increasing the temperature of activation from 400 to 600 °C leads to the decrease of the volume of ultramicropores but to the increase of the total microporosity. The optimum temperature for porosity development in lignin-derived ACs was found to be 600 °C. Temperatures higher than 600 °C reduce both the volume of pores and the BET

surface areas due to the shrinkage and the oxidation of the material.

The ortho-phosphoric acid to lignin (P/L) ratio strongly affects the pore structure. Low impregnation ratios, i.e., P/L = 0.7, promote the creation of micropores whereas P/L ratios equal to or higher than 1.2 slightly affect the pore size distribution. P/L ratios higher than 1.4 decrease the surface area and the total volume of pores, possibly due to the attack of the polymeric matrix by the excess of ortho-phosphoric acid. The value of the P/L ratio has a clear effect on the total volume of pores: there is an optimum P/L = 1.2–1.4 for the development of porosity when the activation temperature is 450 °C.

Increasing the impregnation time lowers the BET surface area and the total pore volume. Moreover, impregnation time also affects the pore size distribution of the ACs. The effect of impregnation time is more important at higher temperatures, due to the decomposition of phosphate and polyphosphate bridges cross-linking parts of the carbon structure.

Acknowledgements

This research was made possible in part by financial support from the Spanish Government (MCYT, project PPQ2002-04201-CO02), the Catalan Regional Government (DURSI, 2001SGR00323 and 2002AIRE) and the ALFA Program of the E.U. (project ALFA II 0412 FA FI). V.F. acknowledges the MCYT and the Universitat Rovira i Virgili (URV) for the financial support of her 'Ramón y Cajal' research contract. V.T.F. acknowledges the URV for her PhD grant. The authors are grateful to Lignotech Iberica S.A. for supplying the Kraft lignin.

References

[1] J. Rodríguez-Mirasol, T. Cordero, J.J. Rodríguez, *Carbon* 31 (1993) 87.
[2] E. Gonzalez Serrano, T. Cordero, J. Rodríguez-Mirasol, J.J. Rodríguez, *Ind. Eng. Chem. Res.* 36 (1997) 4832.
[3] H. Teng, T.S. Yeh, L.Y. Hsu, *Carbon* 36 (1998) 1387.
[4] J. Laine, A. Calafat, M. Labady, *Carbon* 27 (1989) 191.

[5] M. Molina-Sabio, F. Rodríguez-Reinoso, F. Caturla, M.J. Sellés, *Carbon* 34 (1996) 457.
[6] B.S. Girgis, A.N.A. El-Hendawy, *Micropor. Mesopor. Mater.* 52 (2002) 105.
[7] A.N.A. El-Hendawy, S.E. Samra, B.S. Girgis, *Coll. Surf. A: Physicochem. Eng. Asp.* 180 (2001) 209.
[8] B.S. Girgis, M.F. Ishak, *Mater. Lett.* 39 (1999) 107.
[9] F. Suárez-García, A. Martínez-Alonso, J.M.D. Tascón, *J. Anal. Appl. Pyrol.* 63 (2002) 283.
[10] F. Suárez-García, A. Martínez-Alonso, J.M.D. Tascón, *Carbon* 39 (2001) 1111.
[11] M.C. Baquero, L. Giraldo, J.C. Moreno, F. Suárez-García, A. Martínez-Alonso, J.M.D. Tascón, *J. Anal. Appl. Pyrol.* 70 (2003) 779.
[12] B.S. Girgis, S.S. Yunis, A.M. Soliman, *Mater. Lett.* 57 (2002) 164.
[13] T. Vernersson, P.R. Bonelli, E.G. Cerrella, A.L. Cukierman, *Bioreour. Technol.* 83 (2002) 95.
[14] J. Guo, A.C. Lua, *Sep. Purif. Technol.* 30 (2003) 265.
[15] R.A. Shawabkeh, D.A. Rockstraw, R.K. Bhada, *Carbon* 40 (2002) 781.
[16] Y. Diao, W.P. Walawender, L.T. Fan, *Bioreour. Technol.* 81 (2002) 45.
[17] C.A. Toles, W.E. Marshall, M.M. Johns, L.H. Wartelle, A. McAloon, *Bioreour. Technol.* 71 (2000) 87.
[18] M. Jagtoyen, F. Derbyshire, *Carbon* 36 (1998) 1085.
[19] H. Benaddi, T.J. Bandosz, J. Jagiello, J.A. Schwarz, J.N. Rouzaud, D. Legras, F. Béguin, *Carbon* 38 (2000) 669.
[20] C. Toles, S. Rimmer, J.C. Hower, *Carbon* 34 (1996) 1419.
[21] F. Carrasco-Marín, M.A. Alvarez-Merino, C. Moreno-Castilla, *Fuel* 75 (1996) 966.
[22] A.M. Puziy, O.I. Poddubnaya, A. Martínez-Alonso, F. Suárez-García, J.M.D. Tascón, *Appl. Surf. Sci.* 200 (2002) 196.
[23] A.M. Puziy, O.I. Poddubnaya, B. Gawdzik, M. Sobiesiak, D. Dziadko, *Appl. Surf. Sci.* 196 (2002) 89.
[24] J. Hayashi, A. Kazehaya, K. Muroyama, A.P. Watkinson, *Carbon* 38 (2000) 1873.
[25] V. Fierro, V. Torné-Fernández, D. Montané, A. Celzard, *Thermo. Acta.* 433 (2005) 142.
[26] D. Montané, V. Torné-Fernández, V. Fierro, *Chem. Eng. J.* 106 (2005) 1.
[27] S. Brunauer, P.H. Emmett, E. Teller, *J. Am. Chem. Soc.* 60 (1938) 309.
[28] K.S.W. Sing, *Carbon* 27 (1989) 5.
[29] M. Kruk, Z.J. Li, M. Jaroniec, W.R. Betz, *Langmuir* 15 (1999) 1435.
[30] C.H. Hoyt, D.W. Goheen, in: K.V. Sarkanen, C.H. Ludwig (Eds.), *Lignins*, Wiley-Interscience, New York, 1971, p. 833 (Chapter 20).
[31] Y.Z. Lai, in: D.N.S. Hon, N. Shirashi (Eds.), *Wood and Cellulosic Chemistry*, vol. 10, Marcel Dekker, New York, 1991, p. 455.
[32] M. Jagtoyen, F. Derbyshire, *Carbon* 31 (1993) 1185.

5.1.4. Influence of the demineralisation on the chemical activation of Kraft lignin with orthophosphoric acid

Este artículo ha sido enviado al Journal of Hazardous Materials durante el año 2006.

Influence of the demineralisation on the chemical activation of Kraft lignin with orthophosphoric acid

V. Fierro^{1*◇}, V. Torné-Fernández¹, A. Celzard², D. Montané¹

¹*Departament de Enginyeria Química, Universitat Rovira i Virgili, Avda dels Països Catalans, 26, 43007 Tarragona, Spain*

²*Laboratoire de Chimie du Solide Minéral, Université Henri Poincaré - Nancy I, UMR - CNRS 7555, BP 239, 54506 Vandoeuvre-lès-Nancy, France*

Abstract

Preparation of activated carbons (ACs) produced from the thermal decomposition of mixtures of orthophosphoric acid (PA) and either as-received Kraft lignin, KL, or demineralised one, KL_d, has been investigated. Activation with PA has been studied for a PA/lignin ratio of 1 (daf basis) and 1h carbonisation time at final temperatures of 400, 500 and 600 °C. The yield, surface area, porosity and surface chemistry (acidic and basic groups) have been determined. All ACs were found to be essentially microporous, with surface areas higher than 800 m²/g and a maximum value of nearly 1200 m²/g for the carbon prepared at 600 °C from KL. In order to study the influence of temperature on yield, surface area, porosity and functional groups of the ACs prepared from KL and KL_d, the latter precursors were analysed by Fourier transform infrared spectroscopy (FT-IR), scanning electron microscopy (SEM) and X-ray diffraction (XRD). We have concluded that the very different characteristics of the ACs obtained from KL and KL_d are due to the presence or absence of mineral matter during carbonisation, but mainly to the demineralisation process itself, which produces a polymerisation of the raw lignin.

Keywords: Kraft Lignin; Activated carbon; H₃PO₄; demineralisation

1. Introduction

The Kraft method produces black liquor, a residue comprising lignin (30 - 40 %) and other inorganic compounds, which is used as in-house fuel for the recovery of both energy and residual inorganic matter. An interesting alternative is the production of activated carbons by physical [1] or chemical activation [2-4].

Kraft lignin has a high content of inorganic/mineral matter that usually ranges between 6 and 15% on dry ash-free (daf) basis. Since the mineral matter does not directly contribute to the specific surface area and porosity of the resultant active carbons it can be considered as an inert material, which decreases the adsorption capacity per unit mass. The demineralisation and/or abatement of inorganic compounds from carbonaceous precursors are thus thought to be necessary for the production of porous carbons with high surface areas [5]. This is particularly true for biomass, having higher inorganic contents than other precursors like synthetic polymers, and being recognised as a good feedstock for the production of cheap porous carbon materials. Thus, commercial activated carbons with low ash contents are prepared either by acid washing of the products, or by a suitable selection of the raw precursors [6]. Hence, in the case of precursors loaded with mineral matter, it may be wondered if the ashes should be removed before (i.e., in the precursor) or after (i.e., in the product) carbonisation and activation.

Indeed, it is well established that the presence of alkaline and alkaline earth elements in coal affects the reactivity of chars, and that the catalytic effect of inorganic matter depends on their concentration, dispersion and chemical form in the coal matrix [7]. It is also the case with biomass, since Fengel and

Wegener [8] suggested that the inorganic species naturally occurring in wood catalyse its pyrolysis. Since well-dispersed cations like sodium or calcium are good for activation of carbon by steam or CO₂ [9-10] and are abundant in lignin [11], a demineralisation pre-treatment would be *a priori* harmful for obtaining efficient adsorbents.

It has been reported that sodium promotes demethoxylation, demethylation and dehydration of lignin [12-13], and so the non-existence of these reactions could affect the final char yield. Furthermore, it has been recently shown [14] that when lignin is demineralised from 5.7 to 1% and afterwards pyrolysed at 300 °C, the char yield decreases from ca. 71 to 51% (on a daf basis), respectively. Authors indicated that the partial removal of sodium and potassium enhanced the de-volatilisation of lignin at the expense of char formation. DeGroot and Shafizadeh [15] observed a similar decrease in the char yield of wood after the latter was acid-washed. However, the presence of inorganic matter in lignin was found to be useful in reducing its plasticity and hindering its swelling in the carbonisation stage when pyrolysed under N₂ atmosphere [1].

The growing interest in the conversion of woods and its derivatives for producing alternative fuels, chemicals and products of high added value, as activated carbons are, requires a fundamental understanding of the processes involved. Lignin as a precursor of activated carbons is the subject of an increasing number of papers [4, 16-19] and, due to the high content of ashes in lignin, their effect on the pyrolysis process and on the product of carbonisation is worth studying. In this work, the physico-chemical properties of activated carbons produced from the thermal decomposition of mixtures of orthophosphoric acid (PA) and either as-received Kraft lignin, KL, or demineralised one, KL_d, were investigated.

2. Experimental

2.1 Precursor materials

Kraft lignin (KL) was supplied by Lignotech Iberica S.A. (Spain) in the form of fine dark brown particles. The removal of the inorganic matter of KL was achieved as follows: batches of 100 gr were introduced in 2 L of water, leading to black suspensions of pH 9.5. Lignin was precipitated by adding H_2SO_4 until the pH decreased to 1. The precipitate was gently washed with distilled until the pH of the rinse remained constant and close to 6, and finally dried overnight at 105 °C. The lignin prepared in this way ~~is~~ was nearly mineral-free and was termed demineralised Kraft lignin (KL_d).

2.2 Active carbon preparation

An 85 wt. % H_3PO_4 aqueous solution (Panreac, Spain) was used as activating agent. The weight ratio PA/precursor of all mixtures was 1.0 on a daf basis. The slurry was left for 1h impregnation time at room temperature in air, then transferred into a furnace DUM Model 10CAF where carbonisation was carried out under air atmosphere. The furnace was heated at 10 °C min⁻¹, up to 150 °C which temperature was held for 1h to allow free evolution of water. Next, the oven was heated at 10 °C min⁻¹ up to the carbonisation temperatures: 400, 500 and 600 °C, which were maintained for 1h. The excess of H_3PO_4 was removed after carbonisation by thorough washing with distilled water. As shown below, the resultant activated carbons were nearly free of ashes.

2.3 Characterisation of lignins and ACs

2.3.1 Proximate and ultimate analysis

Analysis of C, H, S and N content in the activated carbons (ACs) was done using a Carlo Erba EA-1108 instrument and oxygen was calculated by difference. The proximate analysis was carried out by thermogravimetric analysis in a Perkin-Elmer TGA 7 microbalance equipped with a 273–1273 K programmable temperature furnace, upon following the weight losses at 110 °C/air (moisture), 900 °C/non-oxidising atmosphere (volatile matter), 900 °C/air (fixed carbon); ash content was obtained by difference.

2.3.2 FTIR analysis

Infrared spectra of KL, KL_d and their derived ACs were recorded in the near IR region (4000–600 cm⁻¹) with a spectral resolution of 4 cm⁻¹, a scan speed of 2 mm/s and after 200 scans. The equipment used was a Fourier transform infrared (FTIR) spectrophotometer JASCO FT/IR-680 equipped with a diamond-composite attenuated total reflectance (ATR) cell.

2.3.3 SEM analysis

The surface morphology of KL and KL_d was studied by scanning electron microscopy (SEM) with a JEOL JSM-6400. The microscope was equipped with an energy dispersive X-ray (EDX) microanalyser that was used to observe the dispersion of the mineral matter in KL and KL_d.

2.3.4 Surface area and porosity

Surface area and porosity were determined from the corresponding nitrogen adsorption–desorption isotherms obtained at 77 K with an automatic instrument (ASAP 2020, Micromeritics). The samples were previously outgassed at 523 K for several hours. N₂ adsorption was studied within two pressure ranges. First, for P/P₀ lower than 10⁻³, N₂ were dosed to the sample in fixed amount of 3 cm³/g and the corresponding values of P/P₀ at equilibrium were recorded. The Horvath–Kawazoe (HK) model was applied to the adsorption data in order to obtain the micropore size distribution. Next, N₂ adsorption data for P/P₀ ranging from 10⁻⁵ to 0.99 (in a set of values previously fixed) were analysed according to: (i) the BET method for calculating the specific surface area, A_{BET} ; (ii), the Dubinin-Radushkevich (DR) for calculating the micropore volume, V_{DR} , the characteristic energy of N₂ with respect to carbon, E_0 , and the average width of the slit-shaped micropores, L_0 ; and (iii) the α_s method [20-21] for calculating the the ultramicropore volume, $V_{\alpha,\text{ultra}}$ and the micropore volume, $V_{\alpha,\text{micro}}$. The total pore volume, $V_{0.99}$, was calculated from nitrogen adsorption at a relative pressure of 0.99. The mesopore volume, V_{mp} was calculated as the difference between $V_{0.99}$ and V_{DR} .

3. Results and discussion

3.1 Characterization of KL and KL_d

Table I shows the proximate and ultimate analyses of KL and KL_d. It may be seen that the initial ash content of KL (11.1 % dry basis) was nearly totally removed (0.2 % dry basis) after the treatment with H₂SO₄. The high sulphur

content (2.2 %) in KL originates both from the Kraft or sulphate process, based on the action of NaOH and Na₂S for separating cellulose from the other wood constituents, and from organically bound sulfur (up to 1.5 %) [22]. XRD studies of lignin evidenced the presence of the phase Na₂CO₃ · 2 Na₂SO₄, further confirmed by microprobe analysis. The demineralisation of lignin produced a decrease of both S (down to 0.5 %) and O (from 33.3 to 27.8 %) contents. This finding is not surprising since both sodium carbonate and sulphate are very soluble in aqueous solutions. Analysis by SEM-EDX showed that S and Na are uniformly distributed in the polymeric matrix before and after the demineralisation treatment.

Figure 1 shows the IR spectra of KL and KL_a. The two lignins show a broad band at 3000 – 3600 cm⁻¹, attributed to the hydroxyl groups in phenolic and aliphatic structures, and bands centered around 2975-2945 cm⁻¹, predominantly arising from CH stretching in aromatic methoxyl groups and in methyl and methylene groups of side chains. Both bands decrease after acid treatment. The very weak bands centered near 2300 cm⁻¹ are assigned to carbon–oxygen groups due to ketene [23].

The most characteristic infrared bands of lignin are found at about 1510 and 1600cm⁻¹ (aromatic ring vibrations) and between 1470 and 1460 cm⁻¹ (C-H deformations and aromatic ring vibrations). [24]. The intensity of these bands, however, is strongly influenced by neighbouring functional groups. The band centred at 1585 cm⁻¹ in KL spectrum is the result of the aromatic ring vibrations at 1600 cm⁻¹ and coordinated carbonates [25], already evidenced by XRD analysis. Low absorption around 1650 cm⁻¹ in KL spectrum, resulting in the asymmetry and broadening of the more intense band at 1600 cm⁻¹, may originate from both carbohydrates impurities and water associated with lignin. [26]. The higher intensity of the 1510 cm⁻¹ band compared with the 1600 cm⁻¹ band in the spectra indicates that KL comes

from softwood. The intensive bands of the carbonyl groups appear in the range between 1660 and 1725 cm^{-1} . The exact position of the bands depends on whether the C=O groups are in conjunction with the aromatic ring (position below 1700 cm^{-1}) or not (position above 1700 cm^{-1}). After acid-washing, the carbonates are completely removed from lignin; as a consequence, the intensity of the 1585 cm^{-1} band decreased and was shifted to 1600 cm^{-1} . The KL_d spectrum also exhibits an intense band centered at 1729 cm^{-1} , which indicates C=O (ketones, aldehydes or carboxyl groups) not associated with aromatic rings.

The spectral region below 1400 cm^{-1} is more difficult to analyse, since most bands are complex, with contribution from various vibration modes. However, this region contains vibrations that are specific to the different monolignol units and allows the structural characterisation of lignins. The spectra of both samples show the characteristic vibrations of the guaiacyl unit (1269 cm^{-1} : guaiacyl ring breathing and C=O stretching; 1140 cm^{-1} : C-H in-plane deformation; 860 and 824 cm^{-1} : C-H out-of-plane vibrations in position 2, 5 and 6 of guaiacyl units) but the intensities of the bands vary significantly with the samples. The importance of guaiacyl characteristic vibrations increased after acid washing.

Both spectra also show a weak band at 1369 cm^{-1} originated by phenolic OH and aliphatic C-H in methyl groups and a strong vibration at 1215–1220 cm^{-1} that can be associated with C-C plus C-O plus C=O stretching. The aromatic C-H deformation at 1031 cm^{-1} appears as a complex vibration associated with the C-O, C-C stretching and C-OH bending in polysaccharides. Carbohydrates that remained in KL could be also the origin of the vibrations in the spectral region 1000–1300 cm^{-1} [26].

In summary, the most important changes introduced by acid-washing is the reduction of the amount of hydroxyl groups with the concomitant increase of the number of C=O functions, as well as the elimination of carbonates.

According with these findings, Yasuda et al.[27-28] demonstrated that the acid treatment of lignin produces its cross-linking, an increase of the phenol / aliphatic hydroxyl fraction, and a decrease of the total hydroxyl content of the lignin fractions.

Figure 2 shows SEM images of KL and KL_d at different magnifications. Differences in particle shapes and sizes may be observed. KL particles are smaller, and have a rounded (even spherical) shape with widely open volumes inside. Such morphology is probably due to the concentration process of lignin from black liquors, which is done by evaporation; due to their surface tension, particles take a spherical - thermodynamically more stable - form. After acid washing, KL_d particles are much bigger and sharp, and look broken. A more detailed observation reveals that the surface of KL particles is rough, whereas that of the KL_d is nearly smooth. Such different morphologies between KL and KL_d are probably due to the method used for lignin separation (evaporation or sedimentation-filtration) although changes in the polymer structure due to demineralisation process can not be excluded.

3.2 Characterisation of the activated carbons produced

3.2.1 Carbon yield and elemental composition

Table II shows the carbon yield (daf basis) and the proximate and ultimate analyses of the carbons. Carbon yields of KL were always higher, ranging from 66.2 to 87.6 %, than those obtained from KL_d, ranging from 61.3 to 80.9 %. Although the differences in carbon yield for Kl and KL_d are of the same order of magnitude, their evolution with temperature is not the same.

Increasing temperature from 400 to 500 °C makes the carbon yield decrease by 2.6% and 7.6 % for KL and KL_d, respectively. On the contrary, within the range 500– 600 °C, the carbon yield decreases much more for KL (19.3 %) than for KL_d (12.0 %).

PA promotes dehydration, producing an important reordering of the structure [29], decreasing the volatile compounds emitted during decomposition and hence increasing the carbon yield. Our previous works also [30-31] showed that the PA-impregnated lignin follows during decomposition a reaction path, which is different from that observed with pure lignin, and that the carbon yield is higher. PA promotes bond cleavage in the biopolymers and dehydration at low temperatures [32] followed by extensive cross-linking that binds volatile matter into the carbon product and so increase the carbon yield. Consequently, activated carbons may be prepared with good yields and high surface areas using chemical activation with PA. As demineralisation decreases the hydroxyl content of lignin, the reaction of PA with lignin, hence the subsequent cross-linking are clearly lowered, and consequently the aromatisation of the activated carbons and the carbon yield would be also reduced.

Figure 3 shows the Van Krevelen diagram plotting H/C vs O/C ratios, for activated carbons derived from KL and KL_d within the temperature range of this study. The ACs become increasingly more aromatic when the temperature increases, but the variation of H/C vs O/C ratios depends on the precursor. At constant pyrolysis temperature, ACs derived from KL have lower H/C and O/C ratios than those from KL_d, suggesting a higher aromatic nature that increases with temperature. The Van Krevelen diagram confirms the lower aromaticity of the ACs prepared from KL_d. Furthermore,

it is not excluded that the acid pretreatment could form new polymeric structures that would be thermally less resistant, resulting in a decrease of the carbon yield.

3.2.2 *Surface area and porosity*

Table III shows the apparent surface area and porosity of the carbons produced from KL and KL_d at 400, 500 and 600 °C. The apparent surface areas determined by the BET method are always higher than 800 m²/g, but the observed temperature dependences are very different for carbons prepared from KL and KL_d. The data obtained by the application of the BET, DR and α_s methods to the isotherms at high N₂ relative pressures confirm the trends already observed in the micropore region. The surface areas increase with temperature for KL-based carbons while the opposite is observed for those prepared from KL_d. The maximum surface area determined in this work, 1189 m²/g, corresponds to the carbon prepared from KL at 600 °C. The trend observed for the evolution with temperature of the surface areas of both kinds of carbons is also that of the variation of V_{DR} and $V_{\alpha_{micro}}$. However, the volume of pores smaller than 0.7 nm determined by the α_s method, $V_{\alpha_{ultra}}$, decreases with increasing temperatures for all the carbons prepared. $V_{\alpha_{ultra}}$ is always the highest for carbons prepared from KL, and its decrease with temperature (from 0.18 to 0.11 cm³/g) is less than that observed for carbons prepared from KL_d (from 0.12 to 0.04 cm³/g) when increasing temperatures from 400 to 600 °C. Finally, the average micropore width derived from the DR method, L_o , increases with the temperature, whatever the material, although higher values were found with KL_d.

Figure 4 shows the micropore size distribution of the 6 active carbons, for pores narrower than 0.9 nm, obtained by the application of the HK method. The maximum of the micropore size distribution is always found for a pore diameter lower than 0.4 nm whatever the precursor and the activation temperature. Carbons prepared from KL always showed the highest amount of pores smaller than 0.4 nm. Carbons prepared from KL_d showed wider pore diameters and a dramatic decrease of the pores smaller than 0.4 nm was observed for carbons prepared at 600 °C. These results are in good agreement with those obtained by application of the α_s method.

The results of the present study show that, on average, the adsorbents made from KL have better characteristics (higher areas and pore volumes) than those derived from KL_d. Such differences between KL and KL_d may be explained by the ability of PA to react with lignin. KL can react more extensively with PA due to its higher phenolic content. Moreover, the deashed lignin is less reactive (much more compact, as revealed by SEM, and with much less hydroxyl groups with which PA can react, as revealed by IR spectra), due to an acid-induced cross-linking of the macromolecules. PA can penetrate easily the texture of KL, producing an increasingly high number of small micropores when the temperature increases. Additionally, phosphate and polyphosphate bridges connect cross-linked biopolymer fragments, avoiding pore collapse. On the contrary, PA hardly penetrates KL_d, and cannot prevent pore collapse; hence, the activation mainly occurs at the surface of the grains, producing wider pores (higher L_0 and lower E_0 than for KL). Finally, a catalytic effect of cations improving the activation at constant temperature is also possible.

3.2.3 *Surface chemistry of the activated carbons*

Figure 5 shows the IR spectra of the ACs-derived from KL and KL_d prepared in this study. Bands between 3200 and 3600 cm⁻¹ are typically ascribed to hydroxyl groups; the bands around 2900–2800 and 1500–1400 cm⁻¹ are caused by -CH₂- groups; the band around 1300–1000 cm⁻¹ is attributed to C=O stretch. The band around 1700 cm⁻¹ is usually caused by the stretching vibration of C=O in ketones, aldehydes, lactones, and carboxyl groups; and the band around 1600 cm⁻¹ is ascribed to aromatic ring stretching vibration. The intensities of these two bands show that the aromatization extent and the content of carbonyl-containing groups. The band around 1230 cm⁻¹ is usually attributed to a C-O bond; while, for carbons activated by H₃PO₄, the bands at 1300–900 cm⁻¹ could be caused by phosphorus-containing groups [33].

Spectra of ACs prepared from KL_d were much smoother than those of ACs prepared from KL, which pointed up a lesser amount of functional groups that were present in these carbons. It can be also observed the reduction in the intensity of the bands characteristic of the different functional groups with increasing temperature for both types of carbons. In a recent study [18], it has been demonstrated that the acidic surface groups on carbons prepared from Kraft lignin consist of temperature-sensitive and temperature-insensitive. The temperature-sensitive groups consist of primarily carbonyl-containing groups of varying acidic strength; while the temperature-insensitive groups are mainly phosphorus-containing. Thus, the functional groups of the ACs prepared from KL would be essentially temperature sensitive whereas those prepared from KL_d would include temperature-sensitive and temperature-insensitive groups, phosphorus-containing, due to

the more extensive reaction of PA with KL. These findings are in good agreement with the hypothesis of lower reaction extent of PA with KL_d.

4. Conclusions

The objective of this work was to study the effect of the ash content of Kraft lignin on the physicochemical properties of the activated carbons produced by activation with H₃PO₄ (PA). SEM observations and IR studies suggested that the demineralisation process produces lignin polymerisation and reduces its ability to react with PA.

The results have shown that carbon yield, surface area, porosity and surface chemistry are affected by the removal of the mineral matter. The carbon yield and the aromaticity are the highest for activated carbons derived from the raw Kraft lignin (KL). The activated carbons prepared by activation of KL and KL_d, were essentially microporous with surface areas higher than 800 m²/g, the highest one being close to 1200 m²/g and corresponding to the AC prepared from KL at 600 °C. The surface area increased with temperature for ACs prepared from KL but the opposite evolution was observed for those prepared from KL_d. The functional groups decreased with increasing temperature and their concentration was much more significant in ACs prepared from KL probably because there are more phosphorus-containing groups, which have been recently described as temperature-insensitive groups.

In other words, it may be concluded that the very different characteristics of the ACs obtained may clearly be attributed to the demineralisation process itself. However, a favourable catalytic effect of the ashes on the activation process could not be discarded. The main conclusion of this work is then the following: since better active carbons are produced from raw lignin, the demineralisation – if required – should be carried out on the products and not on the precursors.

Acknowledgements

This research was partly made possible by financial support from MCYT (project PPQ2002-04201-CO02), DURSI (2001SGR00323) and the European Commission through the ALFA program (project LIGNOCARB-ALFA II 0412 FA FI). V. Fierro acknowledges the MCYT and the Universitat Rovira i Virgili (URV) for the financial support of her 'Ramón y Cajal' research contract. V. Torné-Fernández acknowledges the URV for her PhD grant.

References

- [1] J. Rodríguez-Mirasol, T. Cordero and J. J. Rodríguez Carbon 31 1 (1993) 87-95.
- [2] E. González-Serrano, T. Cordero, J. Rodríguez-Mirasol and J.J. Rodríguez, Development of porosity upon chemical activation of kraft lignin with $ZnCl_2$. Ind Eng Chem Res 36 (1997) 4832–4838.
- [3] J. Hayashi, A. Kazehaya, K. Muroyama, A. Paul Watkinson Carbon 38 (2000) 1873-1878.
- [4] V. Fierro, V. Torné-Fernández, A. Celzard, D. Montané, microporous and mesoporous materials 92 (2006) 243-250.
- [5] M.V. Rivera-Utrilla, López-Ramón, F. Carrasco-Marín, F.J. Maldonado-Hódar, C. Moreno-Castilla, Carbon 34 (1996) 917–921.
- [6] C. Bansal, J.B. Donnet and H.F. Stoeckli. Active carbon Marcel Dekker, New York (1988).
- [7] F. Kapteijn, H. Porre, J. A. Moulijn AIChE J. (1986) 691-695.
- [8] D. Fengel and G. Wegener. Wood: chemistry ultrastructure, reactions, Walter de Gruyter, New York (1984) 132–181.
- [9] J.G. Spreigh. Chemistry and technology of coal Marcel Dekker, New York (1994)
- [10] D.W. van Krevelen. Coal Elsevier, Amsterdam (1993)
- [11] M. Kleen, G. Gellerstedt, J Anal Appl Pyrol 35 (1995) 15-41.
- [12] E. Jakab, O. Faix, F. Till. J Anal Appl Pyrol 40 (1997) 171-186.
- [13] J.C. Rio, A. Gutierrez, J. Romero, M.J. Martinez, T. Martinez. J Anal Appl Pyrol 58–59 (2001) 425-439.

- [14] R. K. Sharma, J. B. Wooten, V. L. Baliga, X. Lin, W. G. Chan, M. R. Hajaligol *Fuel* 83 (2004) 1469-1482.
- [15] W.F. DeGroot, F.J. Shafizadeh. *J Anal Appl Pyrol* 6 (1984) 217-232.
- [16] L. Khezami, A. Chetouani, B. Taouk and R. Capart *Powder Technology* 157, (2005) 48-56.
- [17] E. Gonzalez-Serrano, T. Cordero, J. Rodriguez-Mirasol, L. Cotoruelo and J. J. Rodriguez; ; *Water Research* 3 (2004) 3043-3050.
- [18] Y. Guo, D. A. Rockstraw *Carbon*, Volume 44 (2006) 1464-1475.
- [19] J. Rodriguez-Mirasol, J. Bedia, T. Cordero, J. J. Rodriguez. *Sep. Sci. & Tech.* 40 (2005) 3113-3135.
- [20] F. Rouquerol, J. Rouquerol, K.S.W. Sing *Adsorption by Powders and Porous Solids. Principles, Methods and Applications*, Academic Press, San Diego, CA (1999).
- [21] N. Setoyama, T. Suzuki, K. Kaneko *Carbon* 36 (1998) 1459–1467.
- [22] C.H. Hoyt, D.W. Goheen, in: K.V Sarkanen, C.H. Ludwig (Eds.), *Lignins*, Wiley-Interscience, New York, 1971, Chapter 20 833.
- [23] E. Papirer, E. Guyon, N. Perol. *Carbon* 16 (1978) 133-140.
- [24] D. Fengeland, G. Wegener, Wood. *Chemistry ultrastructure reactions*. De Gruyter (Eds.), 1989: 143-164.
- [25] Socrates, G. *Infrared characteristic group frequencies*, ed. L. John Wiley & Sons. (Eds.), 1980.
- [26] C. G. Boeriu, D. Bravo, R. J. A. Gosselink, J. E. G. van Dam *Industrial Crops and Products*, 20 (2004) 205-218.
- [27] S. Yasuda, N. Terashima, T. Ito, *Mokuzai Gakkaishi* 26 (1980) 552–557.

- [28] S. Yasuda, K. Hayashi, T. Ito, N. Terashima, *Mokuzai Gakkaishi* 27 (1991) 478–483.
- [29] Y.Z. Lai, in *Wood and Cellulosic Chemistry*, Vol. 10, Eds. D.N.S. Hon and N. Shirashi. Marcel Dekker, New York, 1991, 455
- [30] D. Montané, V. Torné-Fernández, V. Fierro *Chem. Eng. JI*, 106 (2005) 1-12.
- [31] V. Fierro, V. Torné-Fernández, D. Montané, A. Celzard. *Thermo. Acta* 433 (2005) 142-148.
- [32] M. Jagtoyen, F. Derbyshire, *Carbon* 31(1993) 1185-1192.
- [33] M. Puizy, O.I. Poddubnaya, A. Martínez-Alonso, F. Suárez-García and J.M.D. Tascón, *Carbon* 40 (2002) 1493–1505.

Captions of the figures

- Figure 1** IR spectra of KL (grey line) and KL_d (black line).
- Figure 2** SEM images of KL (a, c and e) and KL_d (b, d and f) at different magnifications.
- Figure 3** Van Krevelen diagram for ACs prepared from KL (full symbols) and KL_d (open symbols) at 400, 500 and 600 °C.
- Figure 4** Micropore size distribution of ACs prepared from KL (black line) and KL_d (grey line) at 400, 500 and 600 °C (a, b and c respectively) from the application of the HK method.
- Figure 5** IR spectra of ACs prepared from KL and KL_d at 400, 500 and 600 °C.

Influence of the demineralisation on the chemical activation of Kraft lignin with orthophosphoric acid

V. Fierro, V. Torné-Fernández, A. Celzard and D.Montané

Table I

Proximate and ultimate analyses of KL and KL_d (wt.%)

	Proximate Analysis (wt %, dry basis)			Ultimate Analysis (wt %, daf)				
	Fixed Carbon	Volatile matter	Ash	C	H	N	S	O*
KL	36.4	52.5	11.1	59.5	5.1	0.1	2.2	33.3
KL _d	39.7	60.1	0.2	65.8	5.9	0.0	0.5	27.8

* Estimated by difference

Influence of the demineralisation on the chemical activation of Kraft lignin with orthophosphoric acid

V. Fierro, V. Torné-Fernández, A. Celzard and D.Montané

Table II

Carbon yield on daf basis, and ultimate analyses of the ACs prepared.

T (°C)	Yield ^a	Proximate Analysis (wt %, dry basis)			Ultimate Analysis (wt %, daf)				
		Volatile matter	Fixed Carbon	Ash	C	H	N	S	O
<i>KL</i>									
400	87.6	36.23	63.26	0.52	65.3	1.2	0.0	1.0	32.5
500	85.0	32.30	67.11	0.59	70.2	1.1	0.0	1.1	27.6
600	65.7	40.90	58.15	0.95	72.7	0.5	0.0	1.2	25.6
<i>KL_d</i>									
400	80.9	33.80	68.85	0.35	61.4	1.2	0.0	1.0	36.4
500	73.3	35.42	62.03	2.55	62.7	1.1	0.0	0.7	35.5
600	61.3	38.13	59.81	2.05	63.5	0.8	0.0	0.6	35.1

^a dry ash free basis.

Influence of the demineralisation on the chemical activation of Kraft lignin with orthophosphoric acid

V. Fierro, V. Torné-Fernández, A. Celzard and D.Montané

Table III

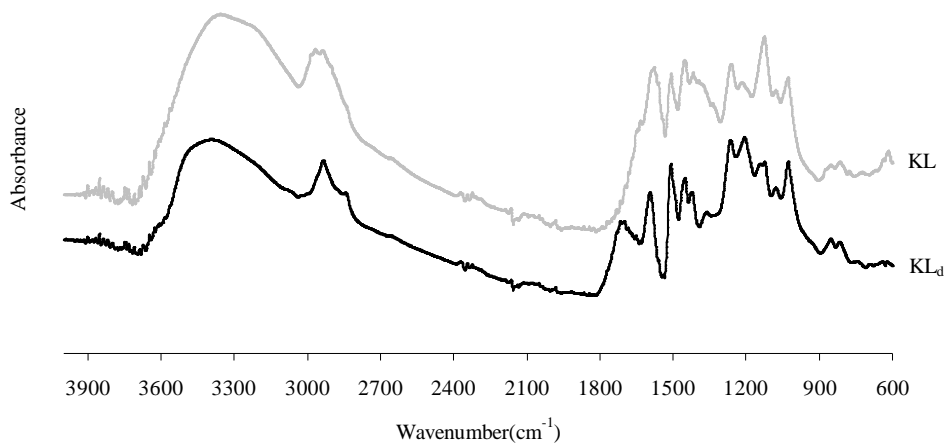
Textural parameters deduced from N₂ adsorption at 77K on activated carbons prepared from KL and KL_d

T (°C)	A _{BET} (m ² g ⁻¹)	V _{0.99} (cm ³ g ⁻¹)	DR equation			α _s method	
			V _{DR} (cm ³ g ⁻¹)	E ₀ (kJmol ⁻¹)	L ₀ (nm)	V _{α,micro} (cm ³ g ⁻¹)	V _{α,ultra} (cm ³ g ⁻¹)
<i>KL as carbon precursor</i>							
400	815	0.40	0.38	22.2	1.0	0.34	0.18
500	1004	0.49	0.45	19.7	1.3	0.43	0.13
600	1189	0.59	0.51	18.9	1.5	0.49	0.11
<i>KL_d as carbon precursor</i>							
400	1008	0.47	0.45	19.1	1.4	0.45	0.12
500	960	0.46	0.40	17.9	1.7	0.38	0.05
600	890	0.44	0.37	17.6	1.7	0.35	0.04

Influence of the demineralisation on the chemical activation of Kraft lignin with orthophosphoric acid

V. Fierro, V. Torné-Fernández, A. Celzard and D.Montané

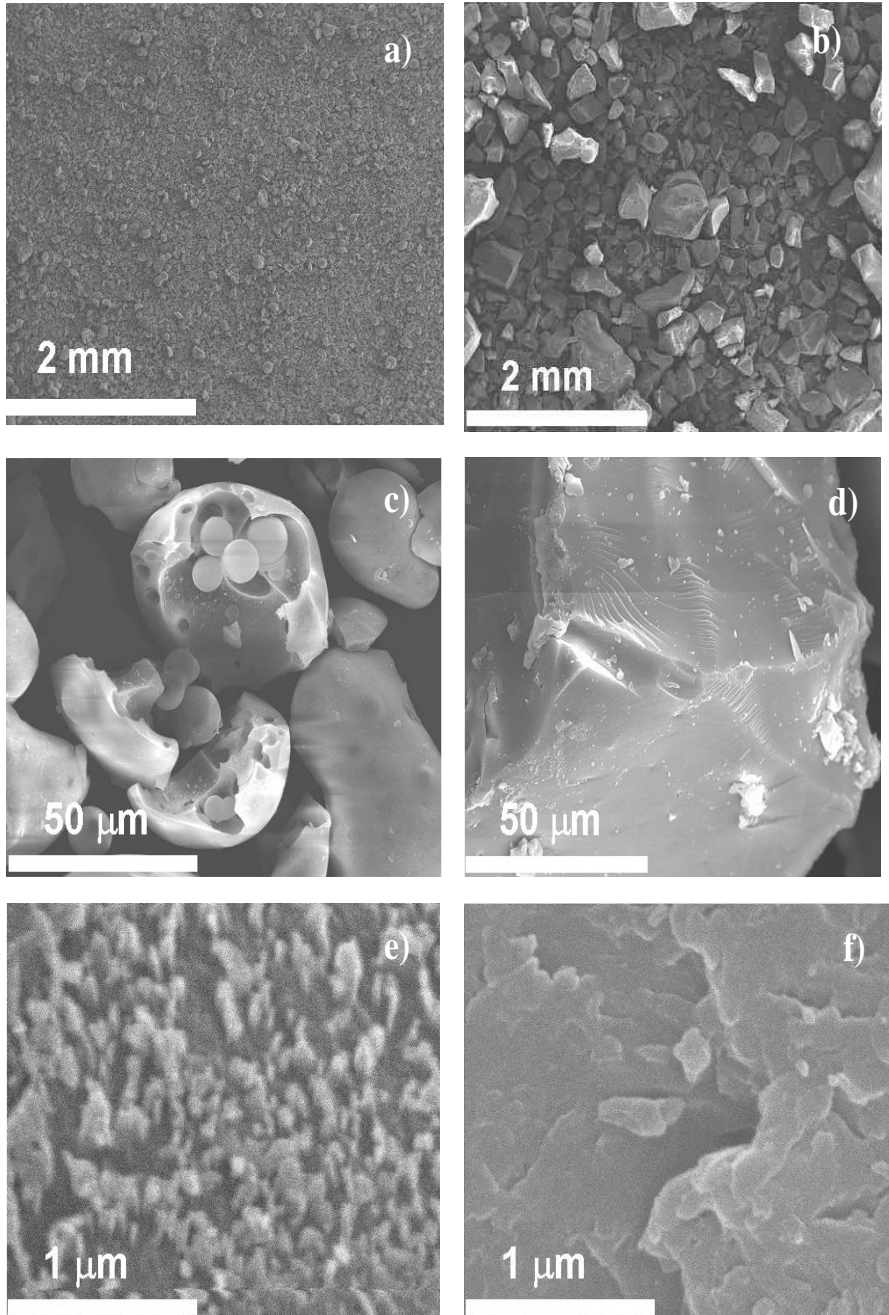
Figure 1



Influence of the demineralisation on the chemical activation of Kraft lignin with orthophosphoric acid

V. Fierro, V. Torné-Fernández, A. Celzard and D. Montané

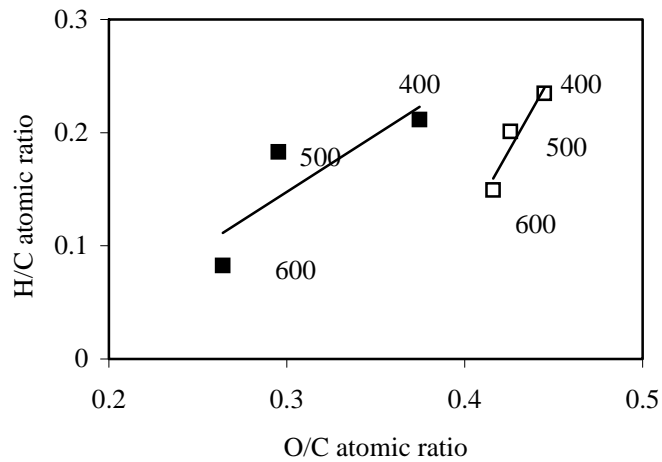
Figure 2



Influence of the demineralisation on the chemical activation of Kraft lignin with orthophosphoric acid

V. Fierro, V. Torné-Fernández, A. Celzard and D. Montané

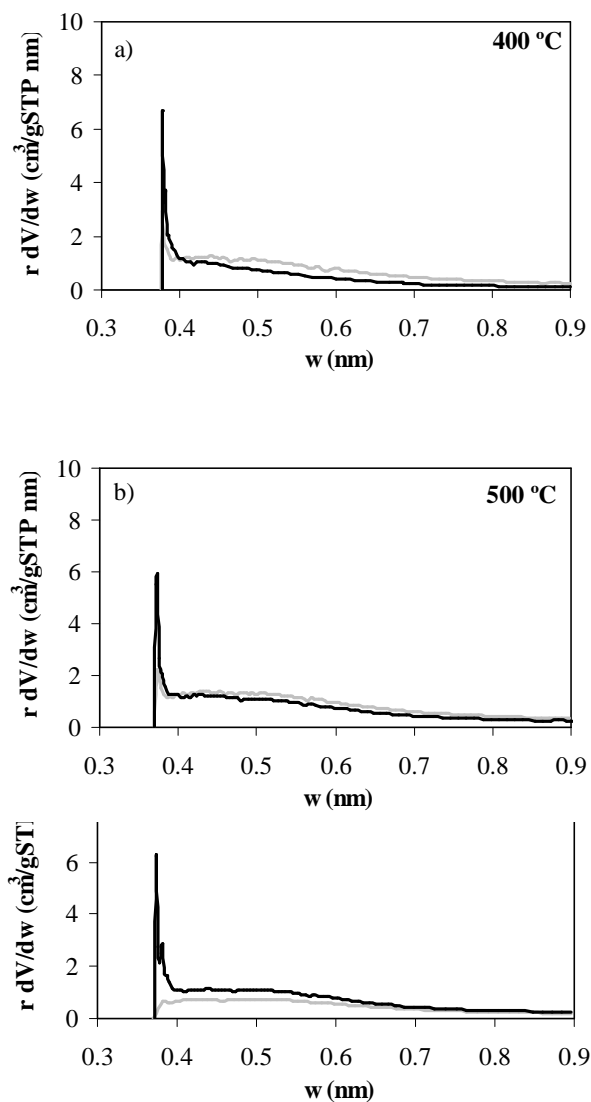
Figure 3



Influence of the demineralisation on the chemical activation of Kraft lignin with orthophosphoric acid

V. Fierro, V. Torné-Fernández, A. Celzard and D. Montané

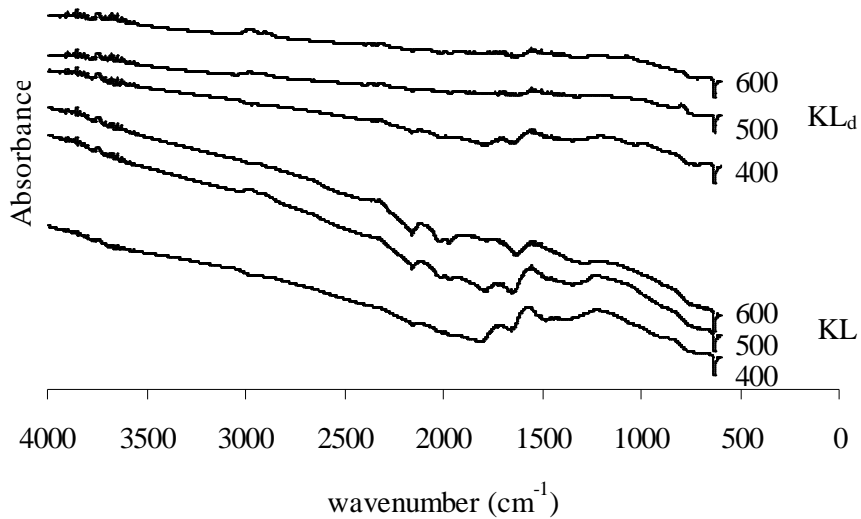
Figure 4



Influence of the demineralisation on the chemical activation of Kraft lignin with orthophosphoric acid

V. Fierro, V. Torné-Fernández, A. Celzard and D. Montané

Figure 5



5.1.5. Highly microporous carbons prepared by activation of kraft lignin with KOH

Este artículo ha sido enviado al journal *Studies in Surface Science and Catalisys* durante el año 2006.

Otros trabajos relacionados se presentan en el anexo B donde se presenta el póster “Highly microporous carbons prepared by activation of Kraft lignin with KOH” publicado en el congreso 7th Internacional symposium on the characterization of porous solids.

Highly microporous carbons prepared by activation of Kraft lignin with KOH

V. Fierro^a, V. Torné-Fernández^a and A. Celzard^b

^a Departament d'Enginyeria Química, Universitat Rovira i Virgili, Campus Sescelades, Av. dels Països Catalans 26, 43007 Tarragona, Spain.

^b Laboratoire de Chimie du Solide Minéral, UMR CNRS 7555, Université Henri Poincaré, 54506 Vandoeuvre-lès-nancy Cédex, France.

Highly microporous carbon materials with high apparent surface areas (up to $\sim 3000 \text{ m}^2 \text{ g}^{-1}$) were obtained by heat treatment of mixtures of demineralised kraft lignin (KL_d) and KOH. The effects of five parameters: temperature of activation (500-900 °C), KOH/ KL_d ratio (1-5), time of activation (0.5-2h), heating rate (5 and 10 °C min^{-1}) and nitrogen flow rate (200-800 $\text{cm}^3 \text{min}^{-1}$) on carbon yield, surface area, pore volume and pore size distribution were investigated. An increase in the activation degree of KL_d produced a gradual enhancement in the volume of total micropores. Highly activated samples also presented noteworthy mesoporosity. Too high activation temperature resulted in the burn-off of carbon structures and widening of micropores to mesopores.

1. INTRODUCTION

The term lignin refers to a group of phenolic polymers accounting for the strength and the rigidity of the vegetal cell walls. The objective of any chemical pulping process is to remove enough lignin to separate cellulosic fibres from each other, producing a suitable pulp for the manufacture of paper and other related products. In terms of industrial chemical modification of lignin, the kraft pulping process is the main one. The kraft method produces black liquor, a residue composed of lignin (30 - 40 %) and other inorganic compounds, which is used as in-house fuel for the recovery of both energy and residual inorganic matter. Several alternatives to combustion have been considered. One of the main possible applications of by-product kraft lignin (KL) consists in preparing activated carbons. Recently, the chemical activation of KL impregnated with H_3PO_4 was reported [1,2]. The activated carbons produced were essentially microporous with surface areas as high as $1300 \text{ m}^2/\text{g}$.

The literature evidences a growing interest in alkaline hydroxide activation process, and KOH has been found to be one of the most effective compounds for that purpose [3-7]. High surface areas and pore volumes are reported for lignocellulosic materials, carbons and chars activated by KOH. However, controlling the mean pore size and the pore size distribution is necessary for using such materials in a given application. The present study shows the possibility of producing highly microporous carbons by activation of KL_d with KOH. The effects of five experimental parameters: activation temperature, KOH/ KL_d ratio, time of activation, heating rate and nitrogen flow rate on surface area and pore size distribution were investigated.

2. EXPERIMENTAL

2.1. Demineralisation of KL

KL was supplied by Lignotech Iberica S.A. (Spain), and was presented in the form of a fine dark brown powder. The removal of the inorganic matter from KL was achieved as follows: batches of 100 g were introduced in 2 l of water, leading to dark brown suspensions of pH 9.5, and lignin was precipitated by adding H_2SO_4 until the pH decreased to 1. The precipitate was gently washed with distilled water until the pH of the rinse was constant, and finally dried overnight at 105 °C. The lignin prepared this way was nearly mineral-free and was termed demineralised Kraft lignin (KL_d).

2.2. Preparation of carbons

KOH lentils (Scharlau) were ground and physically mixed with KL_d according to various KOH/ KL_d mass ratios ($R = 1:1, 2:1, 3:1, 4:1$ or $5:1$). The carbonisation was carried out in a horizontal furnace and the samples were heated ($r = 5$ or 10 °C/min) from room temperature up to the final carbonization temperature ($T_{carb} = 500, 600, 700, 800$ or $900^\circ C$) in different nitrogen flows ($f_{N_2} = 200, 400, 600$ or 800 ml/min). Samples were kept at the final temperature for different carbonisation times ($t_{carb} = 0.5, 1$ or 2 h) before cooling down under nitrogen.

During the experiments, both metallic potassium (produced by the reduction of KOH by carbon at high temperature) and KOH were partly transported in the vapour phase, and could be observed at the outlet of the reactor. Metallic potassium mixed with potassium carbonate was also present inside the crucible; therefore the latter was submitted to atmospheric humidity for two days, during which the alkaline metal slowly oxidised. Finally, the

activated carbon was washed with extreme care, first with 1M HCl, and finally with distilled water until the pH of the rinse remains constant and close to 6. After drying in an oven during 24 h, a very light activated carbon was obtained.

2.3. Characterisation of lignin and carbons

Proximate and ultimate analyses. Elemental analysis of C, H, S and N content in lignins and activated carbons was done using a Carlo Erba EA-1108 instrument. Oxygen was calculated by difference. The proximate analysis was carried out by thermogravimetric analysis in a Perkin-Elmer TGA 7 microbalance equipped with a 273–1273 K programmable temperature furnace following the weight losses at 110°C/air (moisture), 900°C/non-oxidising atmosphere (volatile matter), 900°C/air (fixed carbon); ash content was obtained by difference.

SEM studies. The surface morphology of KL and KL_d was studied by scanning electron microscopy (SEM) with a JEOL JSM-6400. The microscope was equipped with an energy dispersive X-ray (EDX) microanalyser that was used for observing the dispersion of the mineral matter in KL and KL_d.

Surface area and porosity. Surface area and porosity were determined from the corresponding nitrogen adsorption–desorption isotherms obtained at 77 K with an automatic instrument (ASAP 2020, Micromeritics). The samples were previously outgassed at 523 K for several hours. N₂ adsorption data for P/P₀ from 10⁻⁵ to 0.99 (in a set of values previously fixed) were analysed according to: (i) the BET method [8] for calculating the specific surface area, S_{BET} ; and

(ii) the α_s method [9] (using Carbopack F Graphitised Carbon Black as reference material [10] for calculating the micropore volume, $V_{\alpha_{\text{micro}}}$, and the supermicropore volume, $V_{\alpha_{\text{super}}}$. The total pore volume, $V_{0.99}$, was calculated from nitrogen adsorption at a relative pressure of 0.99.

3. RESULTS AND DISCUSSION

Table 1 shows the proximate and ultimate analyses of KL and KL_d. KL has a high ash content (11.1 % on dry ash-free (daf) basis) which is nearly removed (0.2 % on daf basis) after the treatment with H₂SO₄. The high S content (2.2 %) in KL is due to both the Kraft or sulphate process, which consists in a treatment with NaOH and Na₂S to separate the cellulose from the other wood constituents, and to organically bound sulphur (up to 1.5 %) [11]. XRD analysis of lignin showed that Na is found combined with S and C inside the phase Na₂CO₃ · 2 Na₂SO₄. Lignin demineralisation produced a decrease of S content (down to 0.5 %) and of O content (from 33.3 to 27.8 %). Analysis by SEM-EDX showed that S and Na are uniformly distributed in the polymeric matrix before and after the demineralisation treatment.

Table 1. Proximate and ultimate analyses of KL and KL_d (wt. %)

	Proximate Analysis (wt %, dry basis)			Ultimate Analysis (wt %, daf)				
	Fixed Carbon	Volatile matter	Ash	C	H	N	S	O*
KL	36.4	52.5	11.1	59.5	5.1	0.1	2.2	33.3
KL _d	39.7	60.1	0.2	65.8	5.9	0.0	0.5	27.8

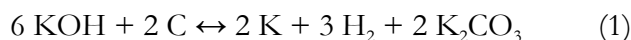
* Estimated by difference.

The effect of the experimental parameters considered in this study is discussed below.

3.1. Effect of the temperature of activation

Figure 1 a) shows the variation of carbon yield with the temperature of activation. Increasing the activation temperature produces the decrease of the carbon yield due: (i) to the pyrolysis of lignin up to 600°C; (ii) to the activation by KOH and K₂CO₃ that starts at 450-500°C. The dissociation of the two phenomena, pyrolysis and activation, is impossible because lignin have already reacted with KOH in some extent before pyrolysis finishes.

Activation with KOH involves the oxidation of C and the production of K metal, H₂ and K₂CO₃ according to the main reaction :

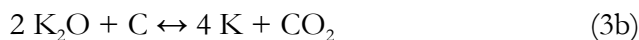
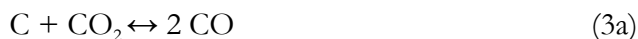


However, reaction (1) is certainly not the only one, since various molecules like CO, CO₂, H₂ and H₂O originating from the thermal decomposition of lignin are also present. Thus, K₂CO₃ produced by reaction of KOH with CO₂ also acts as an efficient activating agent. Hayashi and coworkers [12] showed that high surface areas of nearly 1700 and 2000 m²/g can be obtained by activation of KL with K₂CO₃ for R=2 at 700 and 800 °C, respectively. Moreover, carbons prepared by K₂CO₃ activation showed higher surfaces than those prepared by KOH activation at temperatures higher than 600°C. Hayashi has also worked with different raw materials: husks [13], nutshells [14] or formaldehyde resins [15] reaching very high surfaces even at 700°C. McKee [16] studied the gasification of graphite

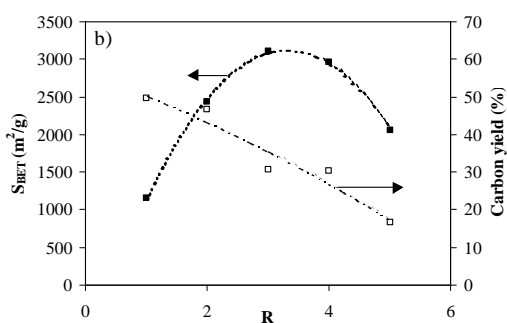
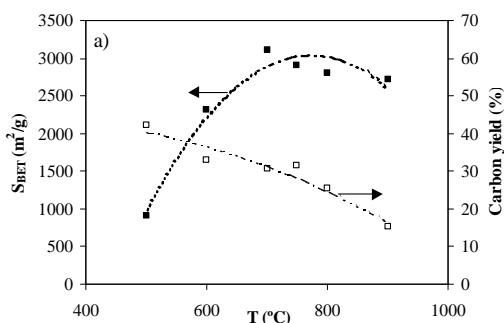
powder by a serie of alkali metal salts and found that K_2CO_3 was reduced in inert atmosphere by carbon as follows:



The decomposition of K_2CO_3 to CO_2 and K_2O could also lead to activation by the two latter products, according to:



Nevertheless, CO_2 and K_2O individually are not expected to be activating agents until high temperatures (above 800 °C) are reached. Hence, the other most efficient activant is rather the water vapour evolved from lignin pyrolysis, and giving the following reaction:



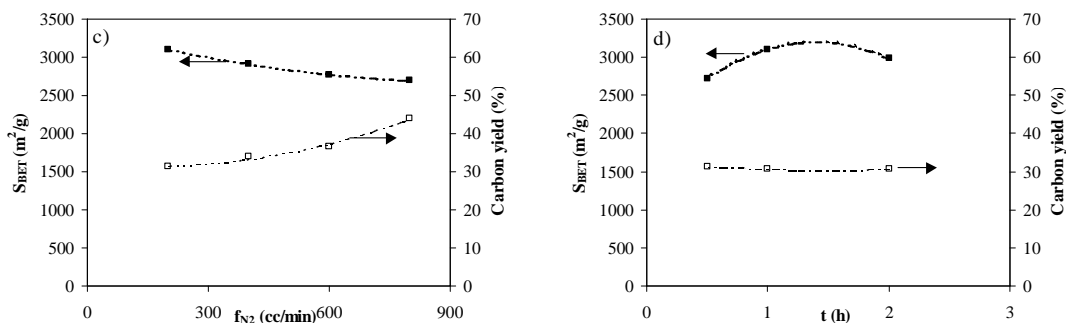


Figure 1. Variation of the S_{BET} (■) and carbon yield (□) with: a) temperature of activation ($R= 3$, $f_{N_2}= 200$ cc/min, $r= 5^\circ\text{C}/\text{min}$, $t_{carb}= 1$ h); b) R ($T= 700$ °C, $f_{N_2}= 200$ cc/min, $r= 5^\circ\text{C}/\text{min}$, $t_{carb}= 1$ h); c) N_2 flow ($T= 700$ °C, $R= 3$, $r= 5$ °C/min, $t_{carb}= 1$ h); d) activation time ($T= 700$ °C, $R= 3$, $f_{N_2}= 200$ cc/min, $r= 5$ °C/min).

Figure 2 a) shows the adsorption-desorption isotherms of N_2 at 77 K of the activated carbons prepared at 500, 600, 700, 800 and 900 °C. All the isotherms are of type I (Langmuir), characterising microporous solids. The carbon prepared at 500 °C presents an extensive plateau in the range of medium to high relative pressures, indicating an essentially microporous character. As carbonization temperature increases the knee of the isotherms widens and the width of the plateau decreases, indicating a widening of the pores. Thus, the material prepared at 900 °C shows a hysteresis loop, evidencing a well-developed mesoporosity. The decrease of carbon yield is accompanied by an increase of both surface area and microporosity up to the temperature of 750 °C, above which these properties decrease as seen in Figure 1 a).

Figure 3 a) shows the total pore, micropore and ultramicropore volumes. The total pore volume always increases with activation temperature but at temperatures higher than 750°C there is a widening of micropores to create mesopores. Figure 3 b) shows the corresponding pore size distributions calculated by application of the Horwatz-Kawazoe method; the maximum is always centered in the micropore region but, as the temperature increases the contribution of wider pores is more important, in agreement with the results of Figures 2a) and 3a).

3.2. Effect of the KOH/KLd weight ratio (R)

At constant temperature (700 °C), the value of R has a marked effect on both the carbon yield and the BET surface area S_{BET} . Figure 1b) shows that there is a linear decrease of carbon yield with R whereas a maximum of the S_{BET} can be observed at R values around 3. Figure 2 b) shows that an increase of R from 1 to 3 produces a great enhancement of N^2 adsorption capacity at 77 K but higher values of R reduce it. The micropore volumes are also reduced for $R \geq 3$ (see Figure 3 c) with the concomitant increase of the fraction of wider pores (see Figure 3 d).

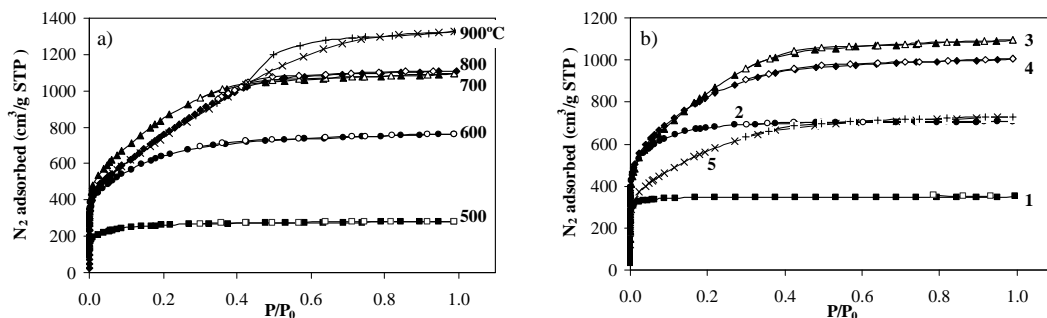


Figure 2. Adsorption-desorption isotherms of N₂ at 77 K on the activated carbons derived from KL_d: a) effect of T and b) effect of R (open symbols and x: adsorption isotherms; full symbols and +: desorption isotherms).

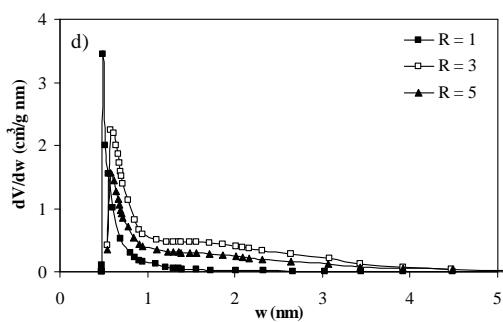
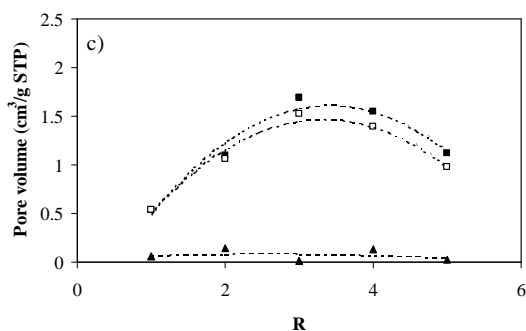
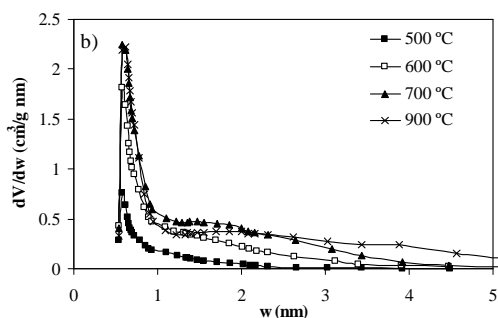
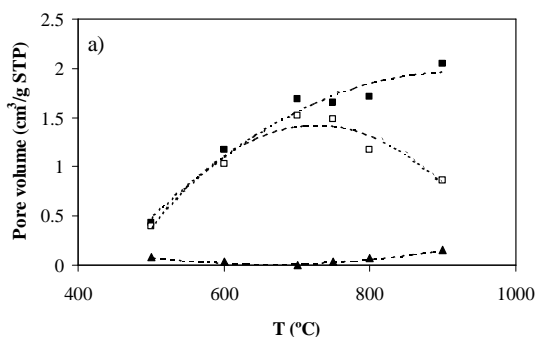
3.3. Effect of the N₂ flow

The flow of N₂ removes the gaseous reaction products but also a part of the activating agent as it was observed in this study. Figure 1 c) shows that the increase in the N₂ flow rate from 200 to 800 cc/min produces an increase of carbon yield because the activating agent is increasingly swept out.

Such a decrease of the activation efficiency may be explained both by a lower contact time of KOH vapour with the solid matter, and by the removal of other possible activating agents: CO₂ (either as such, or as K₂CO₃ after its reaction with KOH), and H₂O.

S_{BET} and the porosity, in the whole pore diameter range, decrease with increasing N₂ flow rate as it is shown in Figures 1c) and 3 e) respectively. These results are different from those found by Linares-Solano and

coworkers who found that N_2 flow enhances the activation of the carbon [6]. However, it is obvious that the different nature of the precursor has an effect on the activation process and so on the activated carbon produced. These results, apparently opposed, could not be contradictory. When pyrolysis and activation take place simultaneously, as for biomass precursors, the co-activation by water vapour evolved during pyrolysis could be important as suggested above.



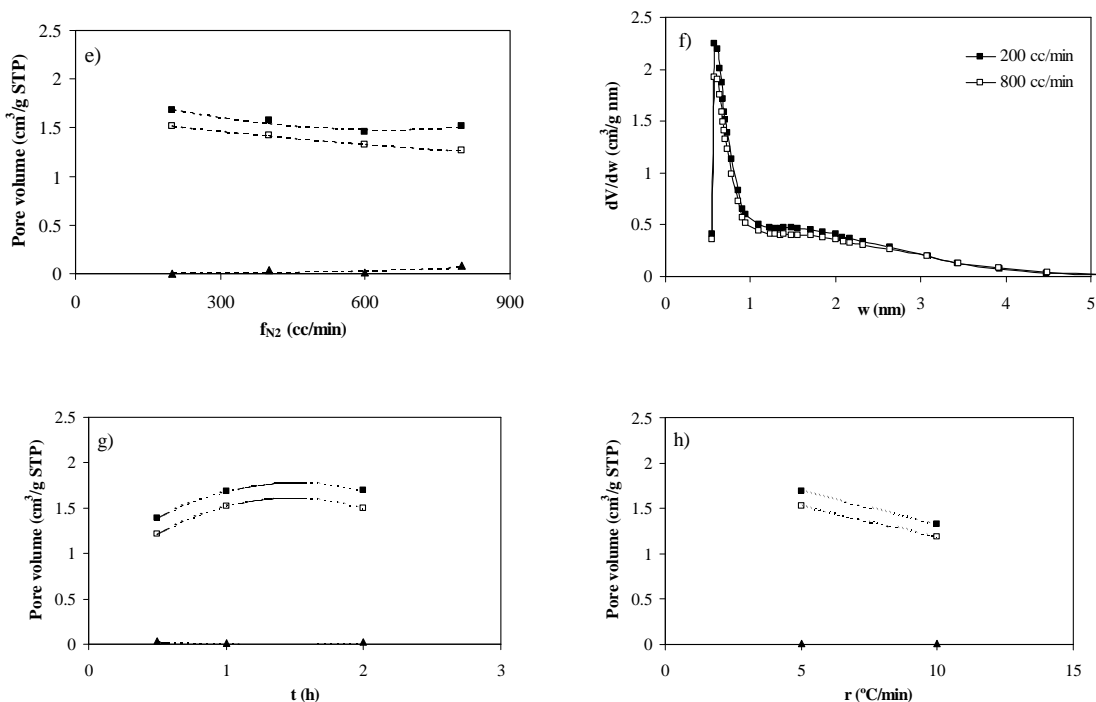


Figure 3. Variation of the $V_{0.99}$ (■), $V_{\alpha_{\text{micro}}}$ (□) and $V_{\alpha_{\text{ultra}}}$ (▲) with: a) temperature of activation ($R = 3$, $f_{\text{N}_2} = 200$ cc/min, $r = 5^\circ\text{C}/\text{min}$, $t_{\text{carb}} = 1$ h); c) R ($T = 700^\circ\text{C}$, $f_{\text{N}_2} = 200$ cc/min, $r = 5^\circ\text{C}/\text{min}$, $t_{\text{carb}} = 1$ h); e) N_2 flow rate ($T = 700^\circ\text{C}$, $R = 3$, $r = 5^\circ\text{C}/\text{min}$, $t_{\text{carb}} = 1$ h); g) activation time ($T = 700^\circ\text{C}$, $R = 3$, $f_{\text{N}_2} = 200$ cc/min, $r = 5^\circ\text{C}/\text{min}$); h) heating rate ($T = 700^\circ\text{C}$, $R = 3$, $f_{\text{N}_2} = 200$ cc/min, $t_{\text{carb}} = 1$ h). Evolution of the pore size distribution of the carbons with: b) temperature of activation (experimental conditions as in Fig. 3 a); d) R (experimental conditions as in Fig. 3 c).

Figure 3 f) shows the PSD of two activated carbons prepared with a N_2 flow of 200 or 800 cc/min. Increasing the N_2 flow does not change the PSD but decreases the pore volume (S_{BET} and $V_{0.99}$ decrease). Since the size of the

pores is the same, finding a lower pore volume should be related to a lower number of pores. Therefore, the effect of the N₂ flow is very different from that of R, even is the latter is more noticeable.

3.4. Effect of the activation time

The duration of activation at a given temperature does not seem to affect neither the carbon yield nor the elemental composition, since differences in both analyses are very small. Figure 1 d) and 3 g) show that there is an optimum in the activation time, between 1 and 2 h, to get the highest surface area and microporosity. The S_{BET} decreases from 3105 to 2990 m²/g when increasing activation time from 1 to 2h respectively.

3.5 Effect of the heating rate

An increase of the heating rate from 5 to 10 °C/min produces a lowering of the S_{BET} from 3105 to 2493 m²/g (see figure 3h). Actual technical limitations do not allow using higher heating rates but our results agree with previous findings [6]. During the heating process the hydroxide melts, then, it is reasonable that a lower heating rate allows a longer contact time between carbon and liquid hydroxide, and hence a better impregnation, before the reaction temperature is reached.

4. CONCLUSIONS

The present exploratory study evidenced the possibility of preparing highly microporous active carbons from demineralised Kraft lignin, using KOH in suitable experimental conditions. The most relevant parameters were found to be activation temperature and mass ratio KOH/lignin, while the other ones (flow of inert gas, duration time, heating rate) were found to have minor effects within the corresponding range of values investigated. Thus, the best materials (surface area $\sim 3000 \text{ m}^2/\text{g}$, micropore volumes $\sim 1.5 \text{ cm}^3/\text{g}$) were obtained at $700 \text{ }^\circ\text{C}$ and $\text{KOH}/\text{KL}_d = 3$. Such results are very close to those already reported for anthracites, which are known to lead to very good adsorbents when prepared in similar conditions [17]. Furthermore, modifying the experimental conditions easily leads to a range of active carbons, from almost purely microporous to mesoporous. Hence, even if the detailed mechanisms are still unclear, chemical activation now appears to be a valuable (rapid, simple and cheap) process for the valorization of lignin.

ACKNOWLEDGEMENTS

This research was made possible in part by financial support from MCYT (project PPQ2002-04201-CO02), DURSI (2001SGR00323 and 2002AIRE) and ALFA Program (project ALFA II 0412 FA FI). V. Fierro acknowledges the MCYT and the Universitat Rovira i Virgili (URV) for the financial support of her 'Ramón y Cajal' research contract. V. Torné-Fernández acknowledges the URV for her PhD grant.

REFERENCES

- [1] V. Fierro, V. Torné-Fernández, D. Montané and J. Salvadó, 'Activated Carbons Prepared from Kraft Lignin by Phosphoric Acid Impregnation', In proceedings of Carbon'03, Oviedo (Spain) 2003.
- [2] V. Fierro, V. Torné-Fernández, D. Montané and A. Celzard, *Thermochim. Acta*, 433 (2005) 153.
- [3] A. Ahmadpour and DD. Do, *Carbon*, 34 (1996) 471.
- [4] T. Otowa, Y. Nojima, T. Miyazaki, *Carbon*, 35 (1997) 1315.
- [5] C. Liang, Z. Wei, Q. Xin and C. Li, *Appl. Catal. A*, 208 (2001) 193.
- [6] D. Lozano-Castelló, M.A. Lillo-Ródenas, D. Cazorla-Amorós and A. Linares-Solano, *Carbon*, 39 (2001) 741.
- [7] E. Frackowiak and F. Beguin, *Carbon*, 40 (2002) 1775.
- [8] F. Rouquerol, J. Rouquerol and K.S.W. Sing Adsorption by Powders and Porous Solids. Principles, Methods and Applications, Academic Press, San Diego, CA (1999).
- [9] N. Setoyama, T. Suzuki and K. Kaneko, *Carbon*, 36 (1998) 1459.
- [10] M. Kruk, Z.J. Li, M. Jaroniec, W.R. Betz, *Langmuir*, 15 (1999) 1435.
- [11] C.H. Hoyt, D.W. Goheen, in: K.V Sarkanen, C.H. Ludwig (Eds.), *Lignins*, Wiley-Interscience, New York, 1971, Chapter 20, p. 833.
- [12] J. Hayashi, A. Kazehaya, K. Muroyama, A.P. Watkinson, *Carbon*, 38 (2000) 1873.
- [13] J. Hayashi, T. Horikawa, K. Muroyama, V.G. Gomes, *Micropor. Mesopor. Mat.*, 55 (2002) 63.
- [14] J. Hayashi, T. Horikawa, I. Takeda, K. Muroyama, F.N. Ani *Carbon*, 40 (2002) 2381.
- [15] J. Hayashi, M. Uchibayashi, T. Horikawa, K. Muroyama, V.G. Gomes, *Carbon*, 40 (2002) 2747.

[16] D.W. McKee, *Carbon*, 20 (1982) 59.

[17] A. Celzard and V. Fierro, *Energy and Fuels*, 19 (2005) 573.

5.1.6. Methodical study of the chemical activation of Kraft lignin with KOH and NaOH

Este artículo ha sido enviado al journal Microporous and Mesoporous Materials durante el año 2006.

Methodical study of the chemical activation of Kraft lignin with KOH and NaOH

V. Fierro¹, V. Torné-Fernández² and A. Celzard^{3*}

¹*Laboratoire de Chimie du Solide Minéral, UMR CNRS 7555,
Nancy-Université, BP 239,
54506 Vandœuvre-lès-Nancy, France*

²*Departament de Enginyeria Química,
Universitat Rovira i Virgili,
Avda dels Països Catalans,
43007 Tarragona, Spain*

³*Laboratoire de Chimie du Solide Minéral, UMR CNRS 7555,
Nancy-Université, ENSTIB
27 rue du Merle Blanc, BP 1041, 88051 Épinal Cedex 9, France*

* Corresponding author.

postal address : ENSTIB, 27 rue du Merle Blanc, BP 1041

Laboratoire de Chimie du Solide Minéral, UMR CNRS 7555,
88051 Épinal Cedex 9, France

fax number : 33 (0) 3 29 29 61 38

e-mail : Alain.Celzard@enstib.uhp-nancy.fr

Abstract

A commercially available Kraft lignin was chemically activated with two alkaline hydroxides, viz NaOH and KOH, using different preparation conditions. The activation was made at various temperatures, mass ratios hydroxide / lignin, activation times, flow rates of inert gas, and heating rates. The resulting active carbons were characterised in terms of BET surface area, total, micro and meso-pore volumes, average pore width, carbon yield and packing density. The influence of each parameter of the synthesis on the properties of the active carbons is discussed, and the efficiencies of each activating agent are methodically compared. It is the first time that so many preparation parameters and so many pore texture characteristics are simultaneously considered for two closely related activating agents of the same lignin precursor. Whatever the preparation conditions, it is shown that KOH is the one leading to the most microporous materials, which is in agreement with some early works. However, the surface areas and the micropore volumes obtained in the present study are much higher than in previous studies. The thorough study of the way each preparation parameter influences the properties of the final materials brings insight into the activation mechanisms. Each time it was possible, the results of lignin chemically activated with hydroxides were compared with those obtained with anthracites: explanations of similarities and differences were systematically looked for.

1. Introduction

Lignin is a waste mass-produced from the paper industry and as such, is generally used for its fuel value. However, an ever-growing number of research works are carried out in order to bring added value to this material. Lignin is becoming frequently accepted as a suitable chemical reagent for formulating new adhesives [1-5], as filler in polymer mixtures [6], and as promising precursor of carbonaceous materials [7-14]. Other possible applications are reviewed in [15]. Concerning the preparation of carbons, lignin is particularly advantageous because of its high phenolic content, leading to higher carbon yields than those obtained from the two other main macromolecular compounds of biomass: cellulose and hemicellulose [16,17]. Hence, getting almost pure lignin is really interesting for preparing carbons and, especially active carbons.

In the present work, the activating efficiency of two alkaline hydroxides classically used for chemical activation of various precursors was investigated thoroughly with one kind of commercially available Kraft lignin, once the latter was demineralised. All the parameters of the active carbon synthesis which could be varied were investigated, namely activation temperature, mass ratio hydroxide / lignin, flow rate of inert gas, activation time and heating rate. The influence of each of them was systematically correlated to the pore structure of the corresponding activated carbons. From this work, the suitable preparation conditions of the material having given desired porous characteristics can be identified, while insights into the activation mechanisms may be derived.

The first section of the present paper deals with the intrinsic features of the lignin, and with the experimental conditions by which it was demineralised and activated; the way the resultant active carbons were characterised is then described. The pore volumes and the related properties: mean pore size, surface area, and also the carbon yield and the packing density obtained with both activating agents are systematically compared and discussed in section 2.

2. Experimental

2.1. Kraft lignin and activating agents

The Kraft lignin (KL) was supplied by Lignotech Iberica S.A (Spain) in the form of a fine dark brown powder. The proximate analysis was carried out according to ISO standards, following the weight losses of the material at 100 °C in air (moisture, ISO-589-1981), at 900 °C in a non-oxidising atmosphere (volatile matter, ISO-5623-1974) and at 815 °C in air (ashes, ISO-1171-1976). The ultimate analysis was carried out in an EA1108 Carlo Erba Elemental Analyser.

The removal of the inorganic matter from KL was achieved as follows: batches of 100 g were introduced in 2 L of water, leading to dark brown suspensions of pH 9.5, and lignin was precipitated by adding carefully concentrated H₂SO₄ until the pH decreased to 1. The precipitate was gently washed with distilled water until the pH of the rinse was constant, and finally dried overnight at 105 °C. The lignin prepared this way was nearly mineral-free and was termed demineralised Kraft lignin (KL_d). It should be stressed

that the activated carbons discussed in the following were all prepared from KL_d , never from the pristine commercial lignin (KL). As a remark, it can be added that such a deashed lignin is somewhat different from the original material, since the acid treatment is known to modify the physico-chemical properties and the structural features of the polymer (see [18,19] for example). Consequently, the properties of the activated carbons obtained from KL_d are different from those derived from raw KL; a paper to be published soon was devoted to this subject [20].

KOH lentils on one hand, and NaOH lentils on the other hand (Scharlau) were ground and physically mixed with KL_d according to various hydroxide / KL_d mass ratios, R. The purity of both activating agents was higher than 99 %. Activated carbons were then obtained by heat-treatment in inert atmosphere of the hydroxide – lignin mixtures (see below). It should be stressed that such an activation mode is different from the two ones generally employed. The first widely used method indeed consists in: (i) a preliminary pyrolysis of the biomass; (ii) the impregnation of the char with a concentrated aqueous solution of the activating agent; (iii) the subsequent drying at temperatures slightly above 100 °C; and finally (iv) the heat-treatment of the dry hydroxide – char mixture (see for example [21-23]). The second well known protocol consists in a direct impregnation of the biomass in aqueous solution, followed by a drying and a heat-treatment (see for example [11,24,25]). However, as shown below, the activation method proposed here is very efficient, probably because of the low melting point of KOH and NaOH (ca 360 and 318 °C, respectively) compared with the synthesis temperatures used in this work (above 400 °C).

2.2. *Active carbon synthesis*

The carbonisation of the hydroxide – KL_d mixtures was carried out in a horizontal furnace flushed with nitrogen. The samples were heated ($r = 5$ or 10 °C/min) from room temperature up to the final carbonisation temperature ($400 \leq T \leq 900^\circ\text{C}$) in different nitrogen flows ($50 \leq f \leq 800$ mL/min). Samples were kept at the final temperature for different carbonisation times ($0.5 \leq t \leq 4$ h) before cooling down under nitrogen.

Only one of the aforementioned synthesis parameters was varied while the others were kept constant. A reference sample was defined as the one prepared in the following condition: $T = 700^\circ\text{C}$; $R = 3$; $t = 1$ h; $f = 200$ mL min^{-1} ; $r = 5$ °C min^{-1} . This means that if, for example, T was varied, the values of R , t , f and r were constant and equal to 3, 1, 200 and 5, respectively.

During the experiments, both the metallic alkaline elements produced by the reduction of NaOH or KOH by carbon at high temperature, and the hydroxides themselves were partly transported in the vapour phase, and could be observed at the outlet of the reactor. Metallic sodium or potassium mixed with sodium or potassium carbonate, respectively, were also present inside the sample-holder. Such phenomena were also observed upon activating anthracites with NaOH [26,27]. Therefore, whatever the activating agent, the sample-holder was submitted to atmospheric humidity for two days, during which the alkaline metals slowly oxidised. At last, the resulting activated carbon was washed with extreme care, first with 1M HCl, and finally with distilled water until the pH of the rinse remains constant and

close to 6. After drying in an oven during 24 h, a light, pure, activated carbon was obtained.

2.3. Active carbon characterisation

Surface area and pore volumes were determined from the corresponding nitrogen adsorption–desorption isotherms obtained at 77 K with an automatic instrument (ASAP 2020, Micromeritics). The samples were previously outgassed at 523 K for several hours. N₂ adsorption data at relative pressures ranging from 10⁻⁵ to 0.99 (in a set of values previously fixed) were analysed according to: (i) the BET method [28] for calculating the apparent surface area, S_{BET}, (ii) the α_s method [29] (using Carbopack F Graphitised Carbon Black as reference material [30]) for calculating the total micropore volume, V_{micro}, and (iii) the Dubinin-Radushkevich method [31], leading to the micropore volume V_{DR}. The values of V_{micro} and V_{DR} should have been close to each others, however, as usual, discrepancies were observed, and we have preferred to present both values. The total pore volume, V_{0.99}, was calculated from nitrogen adsorption at a relative pressure of 0.99, and the mesopore volume, V_{meso}, was obtained according to V_{meso} = V_{0.99} - V_{micro}.

The average pore size, L₀, was calculated according to the widely accepted equation:

$$L_0 \text{ (nm)} = \frac{10.8 \text{ (nm kJ mol}^{-1}\text{)}}{E_0 - 11.4 \text{ (kJ mol}^{-1}\text{)}} \quad (1)$$

in which E_0 is the characteristic adsorption energy of probe molecules, see [32] and references therein. E_0 was derived from the nitrogen adsorption isotherms at 77 K, applying the Dubinin-Radushkevich method.

The carbon yield was simply defined as the weight ratio: final active carbon / initial demineralised lignin. The packing density was determined by pouring, as reproducibly as possible, the activated carbon into a plastic tube (inner diameter 1.4 cm) until a given height, and calculating the ratio: sample weight / sample volume. When KOH was used, the material obtained after the activation was in a powder form (a phenomenon also systematically observed for KOH activation of olive stones [33]), hence no milling was done before measuring the packing density. By contrast, NaOH-activated carbons were most of times aggregated, hence the packing density of such material was ill-defined. The blocks should have been crushed in order to obtain a powder, but doing this would have modified the shape of the carbon grains, and thus the packing density itself. Consequently, the latter was not measured for activated carbons derived from NaOH activation.

3. Results and discussion

3.1. *Pristine and demineralised Kraft lignin*

Table 1 shows the proximate and ultimate analyses of KL and KL_d. KL has a high ash content (11.1 % on dry ash-free (daf) basis), which is nearly removed (0.2 % on daf basis) after the treatment with H₂SO₄. The high S content (2.2 %) in KL is due to both the Kraft or sulphate process, which consists in a treatment with NaOH and Na₂S to separate the cellulose from

the other wood constituents, and to organically bound sulphur (up to 1.5 %) [34]. XRD analysis of lignin showed that Na is found combined with S and C inside the phase Na_2CO_3 , $2 \text{Na}_2\text{SO}_4$. Lignin demineralisation produced a decrease of S content (down to 0.5 %) and of O content (from 33.3 to 27.8 %). Analysis by SEM-EDX showed that S and Na are uniformly distributed in the polymeric matrix before and after the demineralisation treatment [20].

3.2. Characteristics of the activated carbons

3.2.1. BET surface area

Figure 1 presents the variations of the BET surface area when each synthesis parameter is individually varied with respect to the reference preparation condition ($T = 700 \text{ }^\circ\text{C}$; $R = 3$; $t = 1 \text{ h}$; $f = 200 \text{ mL min}^{-1}$; $r = 5 \text{ }^\circ\text{C min}^{-1}$). It can be seen that, whatever the way the preparation conditions may vary, KOH is the activating agent leading to the highest specific area, in agreement with a previous work [11]. However, to our knowledge, BET values close to $3000 \text{ m}^2 \text{ g}^{-1}$ are the highest ever published so far for a lignin-derived activated carbon. The curves show that, most of times, an optimum may be observed for the parameters corresponding to our reference, i.e., for $T = 700 \text{ }^\circ\text{C}$, $R = 3$, etc. In other words, the reference material is the one obtained from the (already optimised) conditions leading to the most microporous active carbons. This is especially true for the ones obtained using KOH, while those made from NaOH have similar but not identical optimal preparation conditions. However, the curves clearly show that NaOH can not allow obtaining surface areas as high as those derived from KOH, while the opposite was found in the activation of anthracites, as far as the activating agent and the precursor were physically mixed together (the results being

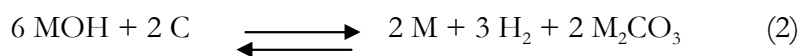
different with the more classical wet impregnation technique) [35]. This fact could be explained as follows. KOH has higher dehydrating and oxidising efficiency than NaOH, hence a higher activating activity for biomass. But anthracites are already ultramicroporous high-rank coals, with closed narrow porosity that can be open through the oxidising character of both KOH and NaOH; Na^+ being smaller than K^+ , it can penetrate more deeply the carbon structure and develop a higher number of smaller pores than K^+ can do. Anthracites activated with NaOH thus present higher surface areas than those prepared with KOH using the same protocol [35]. Thus, because the mechanisms of chemical activation of lignin and coal are different, the optimal preparation parameters are not the same.

Values of T , R and t lower than 700, 3 and 1, respectively, lead to an insufficiently activated carbon (i.e., there are a few narrow pores, hence the surface area is low), while higher values lead to materials in which the pores are too wide (i.e., there are less micropores and more mesopores, hence the surface area is also lower). Indeed, increasing the values of these parameters improve the activation phenomenon, by which the porosity is both open and widened. This effect of the activation temperature was already observed with chemically activated anthracites [26]. The existence of optimal values is thus readily explained, since the narrowest pores are those which most contribute to the surface area, provided that their number is high enough (low values of T , R and t), while these narrow pores become wider and scarcer at high values of T , R and t , leading to decreasing surface areas.

It should be emphasised that the mass ratio hydroxide / lignin, R , is the parameter having the strongest influence. This finding agrees with previous results dealing with the activation of anthracites with NaOH [36]. It is thus not surprising to find surface areas much higher than those already published

so far, for with values of R were lower than 3 [11,24]. For a given constant value of R (e.g., $R = 3$), T is the second most important parameter, while the activation time t has the lowest influence on the surface area. The heating rate r also has a low effect; for KOH, increasing r makes the BET area decrease, while the latter keeps almost constant with NaOH. This may be explained by the fact that the activation of lignin already begins during the heating step. Increasing the heating rate for a given activation time (which is defined only once the carbonisation temperature is reached) finally has a similar effect as reducing the activation time (although it will be shown below that the effects of t and r are not exactly the same in the case of NaOH). For example, assuming that the kinetics of activation is non negligible above 500 °C (which was clearly evidenced in [37]), 40 min are required for increasing the temperature from 500 up to 700 °C at 5 °C min⁻¹, while only 20 min are necessary at 10 °C min⁻¹. 40 min are indeed important when compared to an activation time of 1 h, and decreasing to 20 min logically decreases the surface area of KOH-activated carbons. Since the effect of the activation time was low on the BET area of NaOH-activated carbons, so is the effect of the heating rate.

The influence of the flow rate of inert gas is now considered. For both NaOH and KOH, an optimum is again observed. This fact is very different from what was found with anthracites activated with the same hydroxides in the same conditions, for which the higher the nitrogen flow rate, the higher was the surface area [35,38]. The behaviour of anthracites submitted to similar nitrogen flow was explained on the basis of the following chemical reaction [37,39]:



in which M is either the element K or Na. Such a reaction indeed explains how the equilibrium may be displaced towards the formation of more reaction products if dihydrogen and alkaline vapours are evacuated. However, observing completely opposite behaviour in the present work proves that Equation (2) is, as expected, not suitable to lignin. Lignin is a macromolecule which can not be compared with a coal, and whose heat-treatment produces a number of volatile matters, like CO, CO₂ and H₂O [12], among others. The presence of an optimum in the case of lignin activation may be explained by the competition between the favourable removal of gaseous reaction products and the unfavourable removal of activating agents in the gas phase. Indeed, it is expected that the volatility of both hydroxides is non negligible at the activation temperatures, and their presence at the outlet of the reactor was observed, proving that they are transported in the gas phase. However, the strongest effect might not be due to the removal of the hydroxide vapours, but to that of both water vapour and carbon dioxide necessary formed during the activation process, in which both charring and dehydration phenomena occur. CO₂ and H₂O are indeed well known activating agents of carbons, and they might induce a substantial co-activation of the char, since several hundreds of m² g⁻¹ can be easily gained or lost by simply changing the flow rate of inert gas.

It is nevertheless not clear, so far, if CO₂ should be considered or not as a possible co-activating agent, because: (i) CO₂ usually requires higher temperatures than steam to react with the char, and (ii) CO₂ causes the carbonation of the hydroxides, thus producing carbonates. On one hand, carbonation of NaOH was shown to lead to poorly microporous carbons [37] (because the activity of Na₂CO₃ is low, which was confirmed in the case of lignin activation [11]) and, on the other hand, K₂CO₃ was found to be a very effective activating agent of lignin [11]. The role of CO₂ in the co-

activation of lignin – hydroxides mixtures is thus unclear, while that of steam is more likely.

3.2.2. Pore textures

The pore volumes (total: $V_{0.99}$; micro: V_{DR} and V_{micro} ; meso: V_{meso}) are given in Figure 2. For the sake of clarity, the results concerning the carbons activated with KOH and NaOH are presented in separate plots, gathered in Figure 2(a) and 2(b), respectively. As expected, given the preceding findings about the BET surface area, the activated carbons prepared with KOH are those having the highest total pore and micropore volumes, confirming the higher activating activity of KOH on lignin.

The optima shown on the curves are nearly the same as those already observed for the surface area, as far as micropores are concerned. This finding is readily explained by the fact that the narrowest pores most contribute to the specific surface area. Thus, in the case of NaOH-activated carbons for example, the maximum of S_{BET} at $f = 400 \text{ mL min}^{-1}$ exactly coincides with that of V_{DR} and V_{micro} , while the total pore volume (hence including mesopores, with a low influence on S_{BET}) has its maximum at $f = 200 \text{ mL min}^{-1}$. In [38], it was argued that a high nitrogen flow rate could be compared to a low heating rate, since both lead to a lower concentration of the gaseous reaction products, influencing the chemical equilibria occurring during the activation process. Such arguments could not be extended to the case of lignin activation, since high flow rates of inert gas led to lower BET surface area and pore volumes, while low heating rates led to the opposite situation. These facts prove once more that the chemical reactions of lignin and anthracites are different, even if, as shown all through the present paper,

many similarities may be found between the resulting activated carbons. Concerning now the effect of the heating rate, r , the micropore volume of KOH-activated carbons decreases with r , and this may be explained as follows. A lower heating rate corresponds to a longer impregnation of the lignin with melted KOH, leading to better development of the porosity; the same is found for NaOH.

The mesopore volume, obtained as the difference $V_{0.99} - V_{\text{micro}}$ is worth studying because information about the way the chemical activation of lignin is achieved may be obtained. Concerning KOH first, it can be seen that V_{meso} increases with the activation temperature, and a stronger increase above 750 °C coincides with the drop of the micropore volume. This finding may be accounted for by the conversion of micropores into mesopores at high activation temperatures. In other words, increasing T mainly induces the widening of the pores, which is a phenomenon already clearly evidenced for the chemical activation of anthracites [26,36]. By contrast, the mesopore volume remains low and increases very slightly with the mass ratio KOH / lignin; above $R = 3$, the micropore volume decreases, however no additional mesopores are created. This means that the influences on the pore texture of T on one hand, and R on the other hand, are really different. Lignin being less and less activated at increasingly high values of R may be explained by the fact that KOH produces pores but also weakens and progressively destroys the incipient carbon structure. More and more matter is consumed when R increases, as shown by the coke yield and suggested by the packing density (see below), but no additional porosity is formed. Getting the highest amount of micropores thus really requires finding the optimum value of R , otherwise average characteristics are obtained (see the results published in [17,24] for example). The mesopore volume is the lowest at a flow rate of 200 mL min⁻¹, while the micropore volume is the highest, confirming that the

parameter f is suitably optimised for the activation of lignin with KOH. Finally, the influence of t and r on the mesopore volume is very low.

Concerning now NaOH, the mesopore volume exhibits a maximum close to 700 °C, just like does the micropore volume. The widening of the pores can thus no longer be invoked as in the case of KOH, since the total porosity decreases above 800 °C. This finding may be explained by the closure of the porosity at such high temperatures, which is a well-known mechanism in heat-treated carbon materials (see for example [12,40,41] and references therein), but also in lignin activated with H₃PO₄ [13]. This quite common phenomenon, occurring during charring and / or collapsing of the incipient carbon structure due to an excessive chemical attack, was also observed with KOH used in a different preparation condition, especially $R = 1$ in [11]. Such a low value of R indeed probably favoured charring upon activation, while an optimised value of R (3, in the present work) did not lead to the same effect (i.e., the process is rather governed by activation). The influence of the mass ratio NaOH / lignin is very similar to what was observed with KOH, hence the conclusion is identical: too much activating agent consumes the material rather than forming porosity. Concerning the flow rate of inert gas, a maximum of mesopore volume is obtained at $f = 200$, while the greatest micropore volume is obtained at 400 mL min⁻¹. This finding corroborates the fact that $f = 200$ is not the optimal value of this parameter as far as NaOH is used as activating agent. Obtaining the most microporous carbons is thus achieved at 400 mL min⁻¹, which value was also the best for activating anthracites with NaOH [36]. Activation time has, again, a low impact on the mesopore volume. Finally, increasing the heating rate produces more micropores and less mesopores. It was assumed in § 3.2.1 that a higher heating rate could be nearly equivalent to a shorter full activation process. However, Figure 2(b) evidences that a shorter activation time leads to lower

micropore volumes and higher mesopore volumes, while the opposite is observed for a higher heating rate. Consequently, a high heating rate and a short activation process are not identical. During the heating of the lignin – hydroxide mixture, charring and activation occur simultaneously; increasing the heating rate indeed probably favours the charring since it may be assumed that the dehydrating action of the hydroxide requires time, while charring is a very fast process just depending on the temperature. This is especially true with NaOH, which activating efficiency is lower than that of KOH, Na^+ being indeed less oxidising than K^+ (this fact may also explain the lower activation by NaOH in terms of surface area and pore volumes). Moreover, KOH indeed activates anthracites more rapidly than NaOH and at lower temperatures: 400 °C and 550 °C for KOH and NaOH, respectively [37]. Additionally, the reactions occur at even lower temperatures when the rank of the coal is low; it is thus expected that activation of lignin begins since 200 °C [39]. With NaOH, the charring is achieved at a much higher rate than the activation itself, leading to more char formed. A higher heating rate thus leads to a material characterised by more narrow pores and less wider pores, since the activation with NaOH of carbon structures is the one leading to the narrowest pores (compare the results given in [27] for NaOH and [42] for KOH).

3.2.3. Mean pore size

The dependence of the mean pore size, L_0 , on the process parameters is shown in Figure 3. The presented values are close to what was already calculated for a lignin and for fir wood both activated with KOH [17,23]. L_0 is an average characteristic of the pore texture closely related to both the surface area and the pore volumes. Since the data presented are either above,

or only slightly below, 2 nm, mesopores widely contribute to the values of L_0 . Thus, analogies between the dependence of L_0 and that of the total pore volume presented in Figure 2 can be evidenced. Whatever the activating agent, the same kinds of maxima are indeed recovered for nearly identical values of T , R , f and t . Increasing the heating rate decreases the average pore size, just like the total pore volume is decreased for both NaOH and KOH. It should finally be emphasised that the values of L_0 were derived only from the characteristic adsorption energy (see Equation (1)), therefore in an independent way from the pore volumes. Finding completely consistent variations of total pore volume on one hand, and of mean pore size on the other hand, supports the accuracy and the relevance of both kinds of results.

3.2.4. Carbon yield

The carbon yields of lignin activated with both hydroxides in different experimental conditions are presented in Figure 4. All the results are below 50 %; they are lower than what can be obtained with H_3PO_4 [13,25] or $ZnCl_2$ [10] activation, but only slightly below what is found for pure charring of lignin at the same temperatures [12,43], especially in the case of KOH. It can indeed be seen that, most of times and whatever the preparation conditions of the corresponding activated carbons, KOH leads to the highest carbon yields. This is a very interesting result, and also rather surprising, given that KOH was the hydroxide leading to the highest pore volumes and surface areas. This means that KOH is definitely the best activating agent, since the resulting materials are not only more microporous, but more lignin is transformed into active carbon during the process.

Examining now the effect of the individual preparation conditions, it can be observed that the carbon yield decreases with both T and R , whatever the hydroxide, in agreement with an enhanced activation when these parameters increase. However, as shown above in section 3.2.2, enhanced activation does not necessarily means higher pore volumes, and mass ratios hydroxide / lignin higher than 3 are then more prone to destroy the incipient carbon structure than to create a narrow porosity inside.

Finding that the carbon yield is an increasing function of the flow rate of inert gas confirms the assertion suggested in section 3.1.1, according to which flushing the reactor with nitrogen removes the activating agents: either the hydroxide vapour itself, or the reaction products (H_2O and also possibly CO_2) acting as co-activating agents, or both. KOH being more volatile and more oxidising (hence producing more reaction products) than NaOH, its activating efficiency is also more sensitive to the flow of inert gas removing the vapours. The materials are thus less activated with higher flow rates of nitrogen, and the carbon yield progressively tends towards that of pure charring at high flow rates. The dehydrating and hence the cross-linking activities of KOH being higher than those of NaOH, a higher coke yield is obtained.

The effect of activation time and heating rate on the carbon yield is rather small, probably within the experimental uncertainty, and hence it is better not trying to describe them.

3.2.5. *Packing density*

The packing density is a property of the material in the powder form. For this reason, it does not only depend on the density of the particles themselves, but also on the way these particles are packed (see [44] for a full description of the packing of carbon particles). Assuming that the shape of the grains does not vary from one experiment to another, and assuming that the pouring of the powder into a given vessel is fully reproducible, are the required conditions to state that the packing density is representative of the density of the constitutive grains. It reads:

$$\textit{packing density} = \textit{particle density} \times \textit{filling factor of the vessel} \quad (3)$$

The filling factor is supposed to be constant (except for the NaOH-activated materials, whose results are not worth discussing and are not given, as explained in section 2.3), the packing density therefore gives an idea on the porosity of the active carbon grains.

The packing densities shown in Figure 5 are rather low, though values with which they could be compared are few in the literature. Only packing densities of activated carbons powders made from crops, fruit stones or nut shells may be found, but such values are strongly dependent on the amount of macroscopic voids already present in the precursor and which are retained during the pyrolysis – activation process. A list of values may be found in [44] and [45], giving values ranging from 0.3 to 0.5 g cm⁻³ for typical activated carbons, suggesting that the materials made from lignin activation are light indeed.

The density of the grains decreases with the activation temperature, in agreement with the increasing total pore volume (see Figure 2(a)). By contrast, the density increases with the mass ratio hydroxide / lignin, R , and even much faster above $R = 3$. This finding corroborates the fact that less porosity is created at high values of R , because the carbon is formed as ever-smaller grains, instead of developing inner porosity. Additionally, this agrees with what was also concluded in [33], where it was assumed that for medium-to-high impregnation ratio, the KOH does not reach the interior of the char particles, remaining on the external surface. Thus, materials obtained at low R are very lights; however, their micro- and meso-porosity is poor, and large visible bubbles, inefficient for adsorption, are present inside the grains. Higher R allows obtaining higher micro- and meso-porosity, with less and less macroscopic voids. Thus, there is no contradiction between higher activation level and higher density.

The packing density increases also with the flow rate of inert gas, but for a completely different reason, i.e., because the activation level decreases, as suggested in the previous sections. The effect of the activation time is low; maybe a swallow minimum is observed at $t = 1.5$ h, i.e., coinciding with the maxima of pore volumes, L_0 , and surface area. Finally, the density increases with the heating rate, in agreement with the previously observed decrease of the activation level.

4. Conclusions

The characteristics of porous carbons made from the activation of demineralised lignin by either KOH or NaOH were described as a function of their preparation conditions. It has been shown that similar variations shall sometimes be interpreted in different ways, and this is the reason why all the characteristics presented in this work were methodically measured. Some of them are of crucial importance for the applications of the activated carbon (surface area, pore texture, average pore size), others are useful for understanding the activation mechanisms or are of practical use (carbon yield, packing density). The effect of all the synthesis parameters on the properties of the resulting activated carbons are summarised below.

Increasing the activation temperature raises the activation level; all kinds of pores are simultaneously open and widened, with subsequent increase of the total pore volumes (induced by the development of mesopores) and decrease of both carbon yield and density. Due to the widening of the micropores and their conversion into mesopores, maxima of surface area and micropore volumes are observed, showing that an optimal activation temperature exists.

Increasing the amount of activating agent has another effect; the activation level is also increased, but the resulting pore textures are different. The total pore volume presents a maximum, above which the micropores become less and less abundant. Since the carbon yield decreases while the density raises, this means that the lignin is still converted into carbon, but into a less and less porous one at high hydroxide / lignin ratios. Again, an optimum ratio exists.

The flow rate of inert gas has a lower effect, as compared with the 2 preceding parameters. The competition between the removal of useless reaction products and that of potential activating agents in the vapour phase again leads to the observation of an optimum. High flow rates decrease the efficiency of the activation, giving less micropores and a lower surface area, while a denser carbon is obtained in higher proportion (higher carbon yield and density).

Activation time and heating rates are the parameters to which the final properties are the less sensitive. Hence, only little improvement of the carbon characteristics can be achieved through their variation. Increasing these parameters may lead to higher or lower micropore volumes, depending on the hydroxide and the other preparation conditions.

The last essential conclusion is that, whatever the way the activated carbons were prepared from lignin, KOH is undoubtedly the best activating hydroxide for obtaining highly microporous adsorbents. This result is different from what can be found for the activation of carbon materials like anthracites, for which NaOH is more efficient, whatever the experimental conditions. The present work also stressed the fact that the weight ratio: activating agent / precursor is of highest importance, so poor adsorption properties may be obtained if this parameter is not optimised through a systematic investigation.

References

- [1] A. Pizzi, A. Stephanou, *Holzforschung*, 47 (1993) 439.
- [2] A. Pizzi, A. Stephanou, *Holzforschung*, 47 (1993) 501.
- [3] P. Truter, A. Pizzi, H.V. Ermaas, *J. Appl. Polymer Sci.*, 51 (1994) 1319.
- [4] N. El Mansouri, A. Pizzi, J. Salvado, *Holz. Roh. Werkstoff*, (2006) in press.
- [5] N. El Mansouri, A. Pizzi, J. Salvado, *J. Appl. Polymer Sci.*, (2006) in press.
- [6] D. Feldman, in: T.Q. Hu (Ed.), *Modification, Properties and Usage of Lignin*, Kluwer Academic, New York, 2002, p. 81.
- [7] J. Rodríguez-Mirasol, T. Cordero, J.J. Rodríguez, *Carbon*, 31 (1993) 87.
- [8] J. Rodríguez-Mirasol, T. Cordero, J.J. Rodríguez, *Carbon*, 31 (1993) 53.
- [9] J. Rodríguez-Mirasol, T. Cordero, J.J. Rodríguez, *Carbon*, 34 (1996) 43.
- [10] E. Gonzalez-Serrano, T. Cordero, J. Rodríguez-Mirasol, J.J. Rodríguez, *Ind. Eng. Chem. Res.*, 36 (1997) 4832.
- [11] J. Hayashi, A. Kazehaya, K. Muroyama, A.P. Watkinson, *Carbon*, 38 (2000) 1873.
- [12] R.K. Sharma, J.B. Wooten, V.L. Baliga, X. Lin, W.G. Chan, M.R. Hajaligol, *Fuel*, 83 (2004) 1469.
- [13] V. Fierro, V. Torné-Fernández, A. Celzard, *Micropor. Mesopor. Mater.*, 92 (2006) 243.
- [14] V. Fierro, V. Torné-Fernández, A. Celzard, *Stud. Surf. Sci. Catal.* 160 (2005) 607.
- [15] T.Q. Hu (Ed.), *Modification, Properties and Usage of Lignin*, Kluwer Academic, New York, 2002.
- [16] D.M. Mackay, P.V. Roberts, *Carbon*, 20 (1982) 87.

- [17] L. Khezami, A. Chetouani, B. Taouk, R. Capart, *Powder Technol.*, 157 (2005) 48.
- [18] R.C. Sun, J. Tomkinson, J. Bolton, *Polym. Degrad. Stab.*, 63 (1999) 195.
- [19] C. Pouteau, B. Cathala, P. Dole, B. Kurek, B. Monties, *Ind. Crops. Prod.*, 21 (2005) 101.
- [20] V. Fierro, V. Torné-Fernández, A. Celzard, D. Montané, J. *Hazardous Mater.*, submitted.
- [21] M. Olivares-Marín, C. Fernández-González, A. Macías-García, V. Gómez-Serrano, *Appl. Surf. Sci.*, 252 (2006) 5980.
- [22] R. Ubago-Pérez, F. Carrasco-Marín, D. Fairén-Jiménez, C. Moreno-Catilla, *Micropor. Mesopor. Mater.*, 92 (2006) 64.
- [23] F.C. Wu, R.L. Tseng, *J. Coll. Interf. Sci.*, 294 (2006) 21.
- [24] J. Hayashi, K. Muroyama, V.G. Gomes, A.P. Watkinson, *Carbon*, 40 (2002) 617.
- [25] Y. Guo, D.A. Rockstraw, *Carbon*, 44 (2006) 1464.
- [26] A. Perrin, A. Celzard, A. Albiniak, J. Kaczmarczyk, J.F. Marêché, G. Furdin, *Carbon*, 42 (2004) 2855.
- [27] A. Perrin, A. Celzard, A. Albiniak, M. Jasienko-Halat, J.F. Marêché, G. Furdin, *Micropor. Mesopor. Mater.*, 81 (2005) 31.
- [28] S. Brunauer, P.H. Emmett, E. Teller, *J. Am. Chem. Soc.*, 60 (1938) 309.
- [29] K.S.W. Sing, *Carbon*, 27 (1989) 5.
- [30] M. Kruk, Z.J. Li, M. Jaroniec, W.R. Betz, *Langmuir*, 15 (1999) 1435.
- [31] J.W. Patrick (Ed.), *Porosity in Carbons*, Wiley, 1995.
- [32] F. Stoeckli, A. Slasli, D. Hugi-Cleary, A. Guillot, *Micropor. Mesopor. Mater.*, 51 (2002) 197.
- [33] M. Molina-Sabio, F. Rodríguez-Reinoso, *Coll. Surf. A: Physicochem. Eng. Aspects*, 241 (2004) 15.

- [34] C.H. Hoyt, D.W. Goheen, in: K.V Sarkanen, C.H. Ludwig (Eds.), *Lignins*, Wiley-Interscience, New York, 1971, p. 833.
- [35] M.A. Lillo-Ródenas, D. Lozano-Castelló, D. Cazorla-Amorós, A. Linares-Solano, *Carbon*, 39 (2001) 751.
- [36] A. Celzard, V. Fierro, *Energy & Fuels*, 19 (2005) 573.
- [37] M.A. Lillo-Ródenas, D. Cazorla-Amorós, A. Linares-Solano, *Carbon*, 41 (2003) 267.
- [38] D. Lozano-Castelló, M.A. Lillo-Ródenas, D. Cazorla-Amorós, A. Linares-Solano, *Carbon*, 39 (2001) 741.
- [39] M.A. Lillo-Ródenas, J. Juan-Juan, D. Cazorla-Amorós, A. Linares-Solano, *Carbon*, 42 (2004) 1371.
- [40] A. Celzard, J.F. Maréché, F. Payot, D. Bégin, G. Furdin, *Carbon*, 38 (2000) 1207.
- [41] M.S. Solum, R.J. Pugmire, M. Jagtoyen, F. Derbyshire, *Carbon*, 33 (1995) 1247.
- [42] D. Lozano-Castelló, D. Cazorla-Amorós, A. Linares-Solano, D.F. Quinn, *Carbon*, 40 (2002) 989.
- [43] J. Li, B. Li, X. Zhang, *Polym. Degrad. Stab.*, 78 (2002) 279.
- [44] A. Celzard, J.F. Maréché, F. Payot, G. Furdin, *Carbon*, 40 (2002) 2801.
- [45] A. Ahmadpour, D.D. Do, *Carbon*, 35 (1997) 1723.

Table 1. Proximate and ultimate analyses of KL and KL_d (wt. %)

	Proximate Analysis			Ultimate Analysis				
	(wt %, dry basis)			(wt %, daf)				
	Fixed Carbon	Volatile matter	Ash	C	H	N	S	O*
KL	36.4	52.5	11.1	59.5	5.1	0.1	2.2	33.3
KL _d	39.7	60.1	0.2	65.8	5.9	0.0	0.5	27.8

* Estimated by difference

Figure captions

Figure 1: Dependence of the BET surface area of the activated carbons on their synthesis parameters. Empty symbols = NaOH; full symbols = KOH. Curves are just guides for the eye.

Figure 2: Dependence of the pore volumes of (a) the KOH-activated carbons (full symbols) and (b) the NaOH-activated ones (empty symbols), on their synthesis parameters. Triangles = V_{DR} ; Circles = $V_{0.99}$; Squares = V_{micro} ; Diamonds = V_{meso} . Curves are just guides for the eye.

Figure 3: Dependence of the mean pore size of the activated carbons on their synthesis parameters. Empty symbols = NaOH; full symbols = KOH. Curves are just guides for the eye.

Figure 4: Dependence of the carbon yield on the activation parameters. Empty symbols = NaOH-activated carbons; full symbols = KOH-activated carbons. Curves are just guides for the eye.

Figure 5: Dependence of the packing density of the KOH-activated carbons on their synthesis parameters. Curves are just guides for the eye.

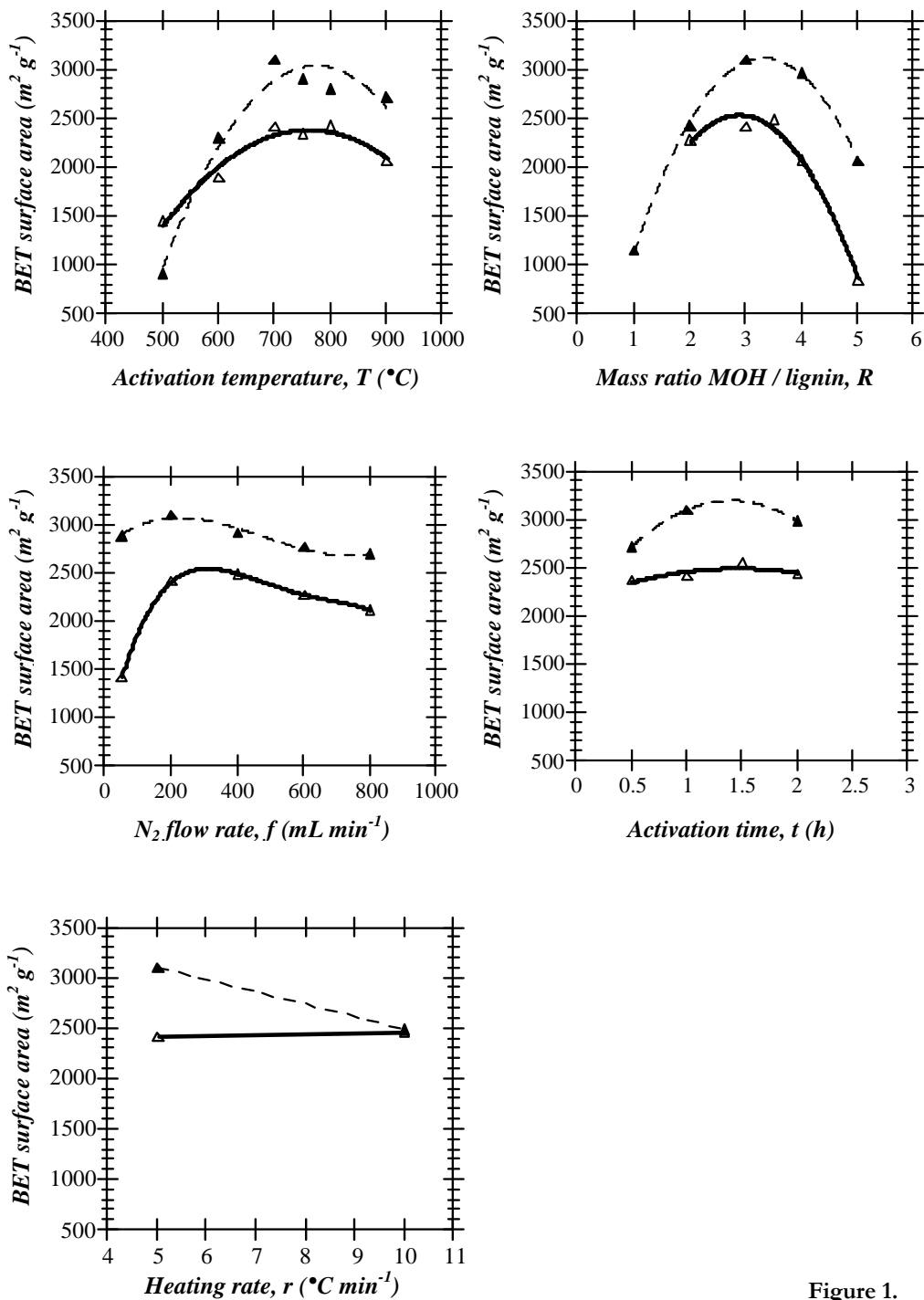


Figure 1.

V. Fierro et al.

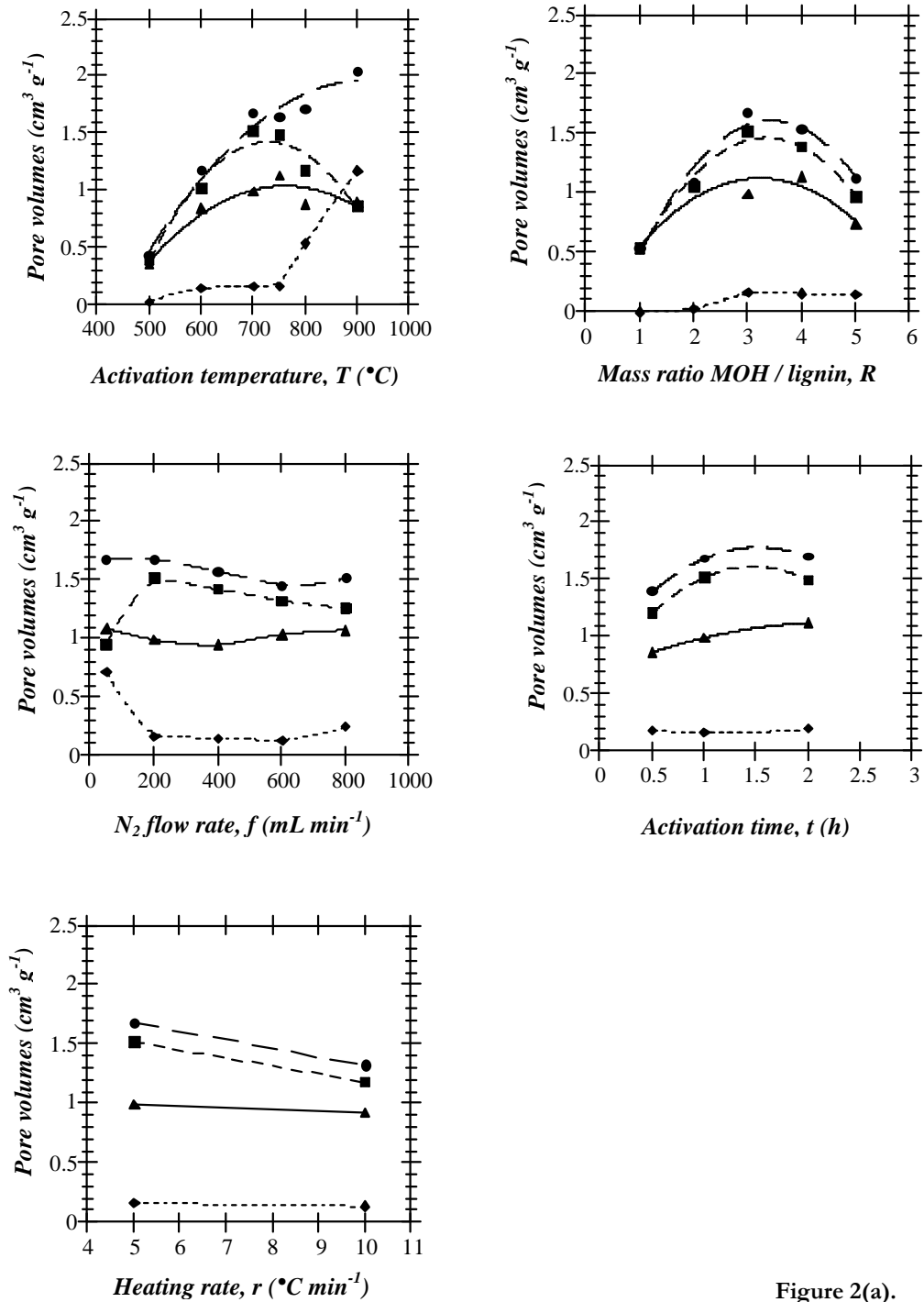


Figure 2(a).

V. Fierro et al.

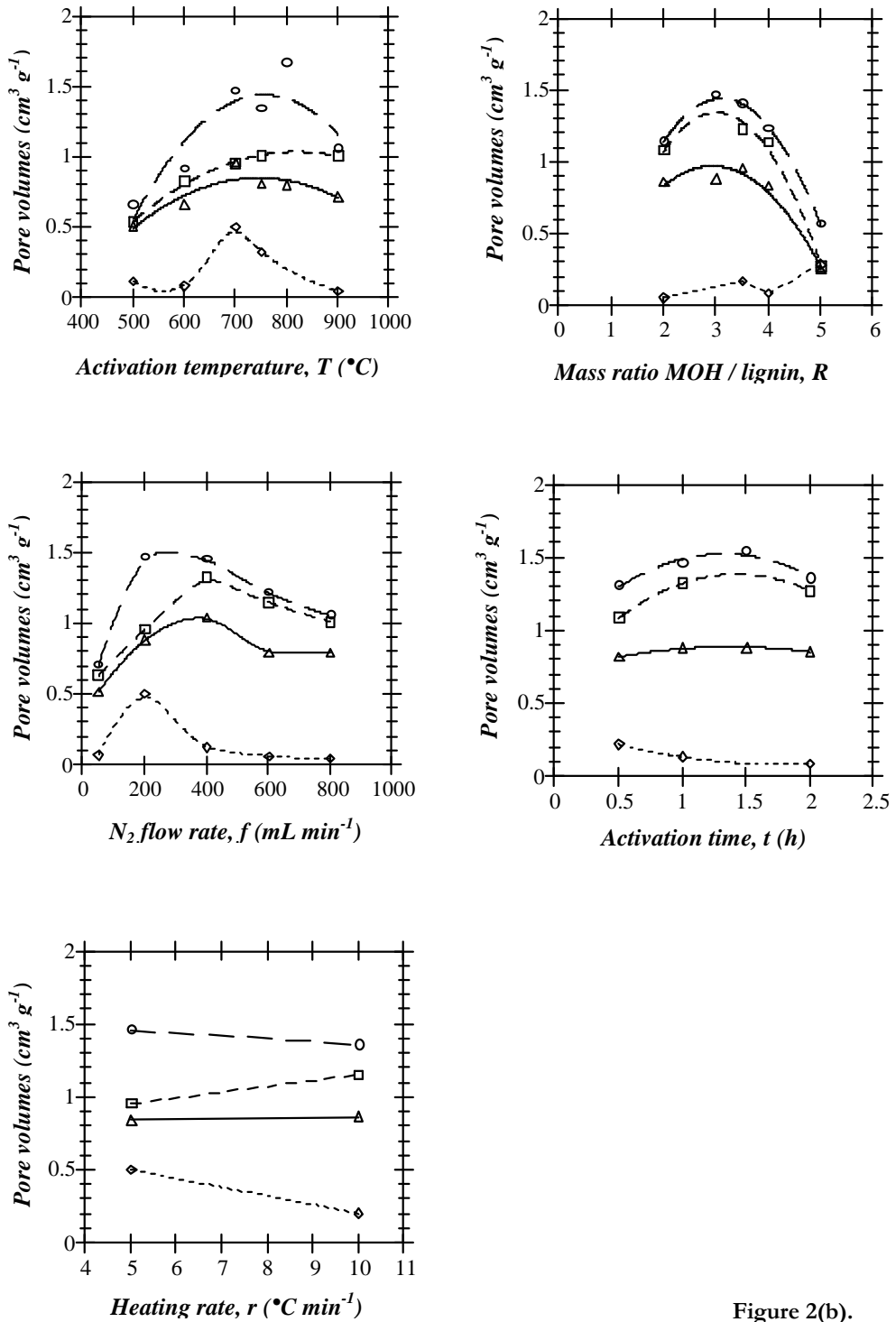


Figure 2(b).

V. Fierro et al.

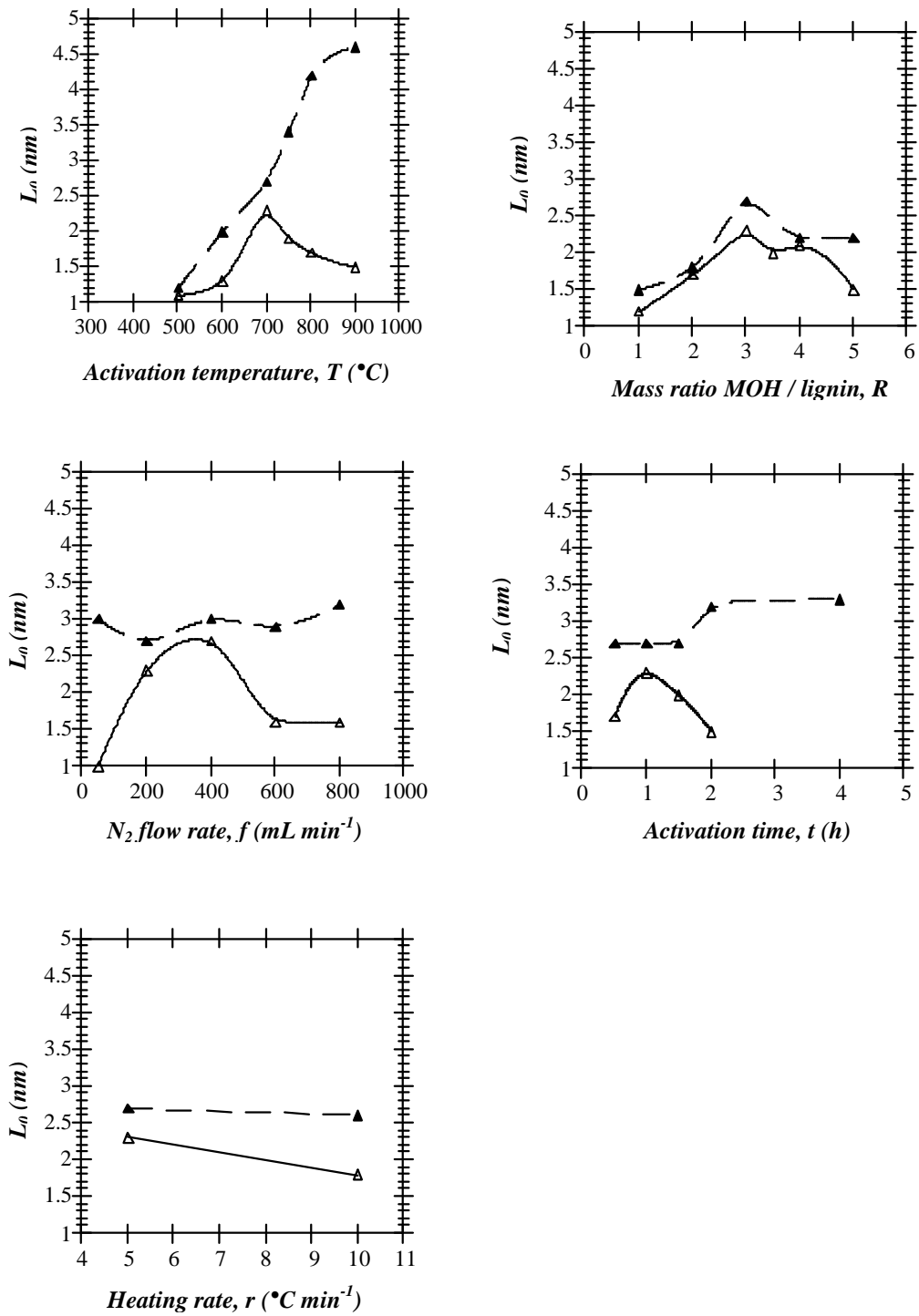


Figure 3.

V. Fierro et al.

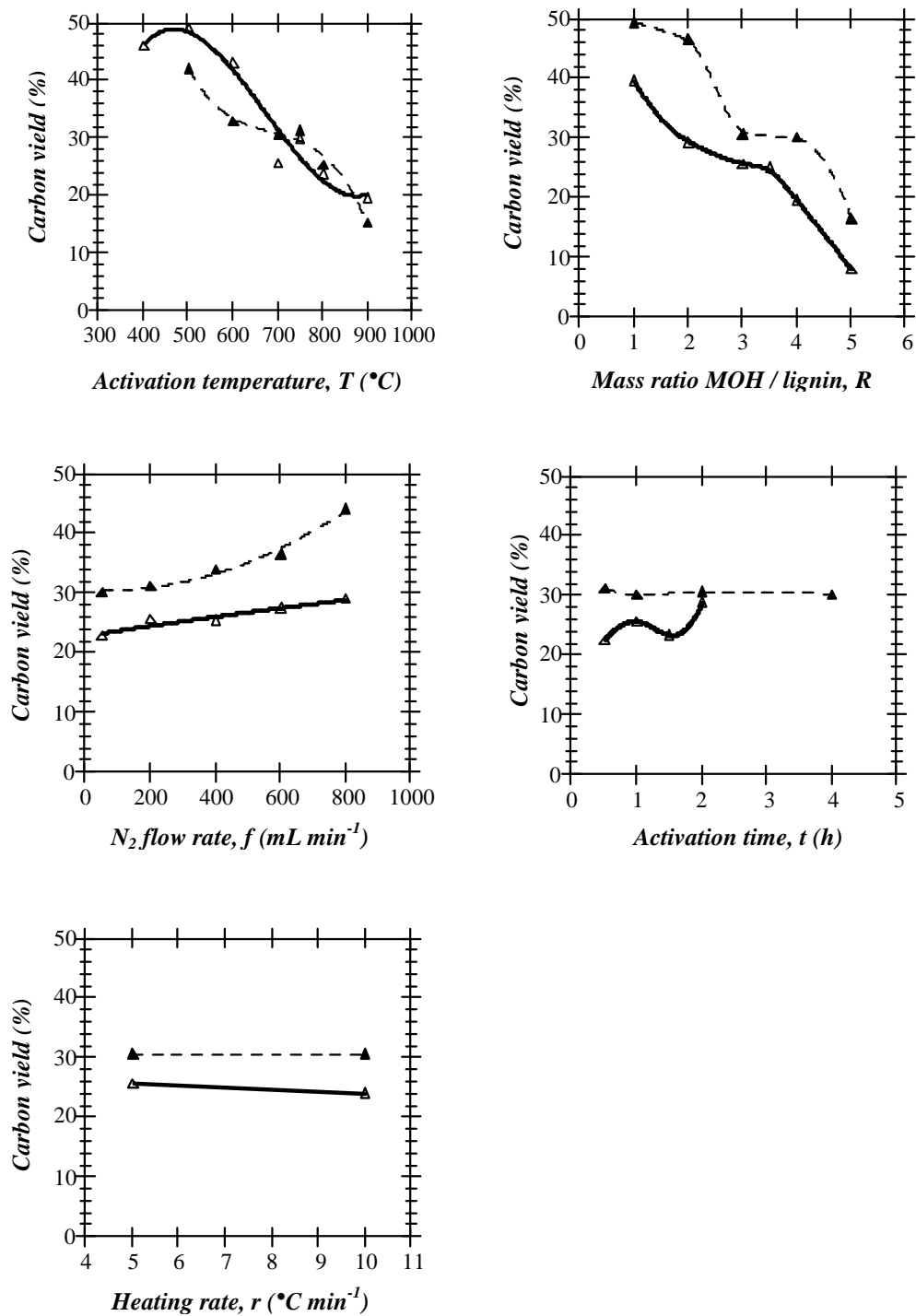


Figure 4.

V. Fierro et al.

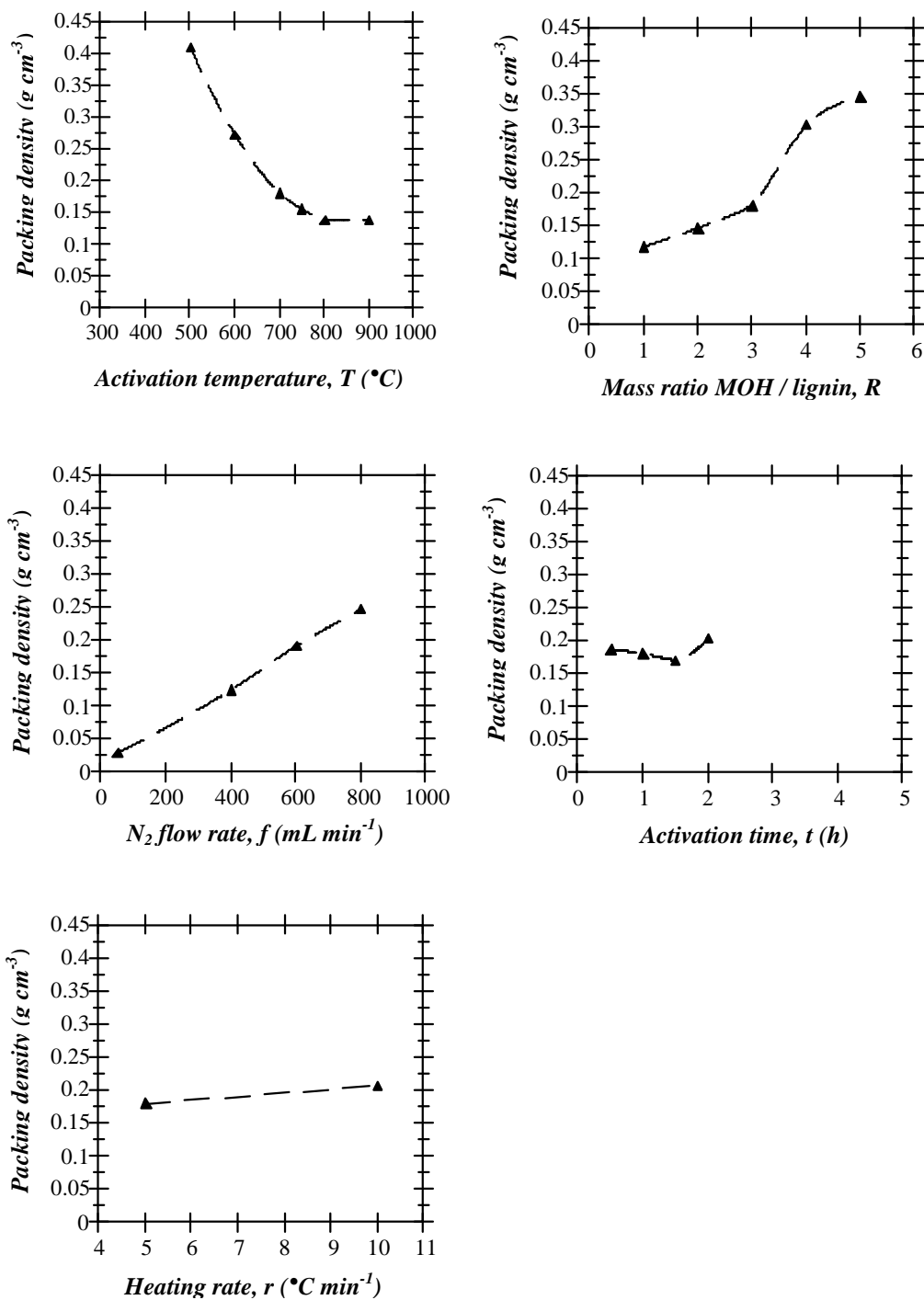


Figure 5.
V. Fierro et al.

5.2. Aplicaciones de carbones activados

Tal y como se ha mostrado, es posible obtener CA esencialmente microporosos a partir de gñina Kraft. Así pues, básicamente su aplicación se restringe a la eliminación de contaminantes en efluentes líquidos. Sin embargo, a continuación también se muestran la participación en trabajos específicos en el campo de los reactores de membrana y en la purificación de xylo-oligosacáridos.

5.2.1. Removal of Cu (II) from Aqueous Solutions by Adsorption on Activated Carbons Prepared from Kraft Lignin

Este artículo se presentó en forma de póster en el congreso internacional Carbon 2003 (consultar Anexo C).

Otros trabajos relacionados se presentan en los anexos A y D donde se presentan dos pósters: “Use of Kraft lignin for Cu (II) removal in industrial water” y “Uptake of Cu (II) and Zn from aqueous solution by Kraft lignin” publicados en los congresos 9th Mediterranean congress y 4th European Congress in Chemical Engineering, respectivamente.

Removal of Cu (II) from Aqueous Solutions by Adsorption on Activated Carbons Prepared from Kraft Lignin

V. Fierro*, V. Torne, D. Montané and R. Garcia-Valls

Departament d'Enginyeria Química, ETSEQ, Universitat Rovira i Virgili, Avinguda dels
Països Catalans 26, Campus Sescelades, Tarragona 43007, Spain

Abstract

Activated carbons were prepared by phosphoric acid activation of Kraft lignin varying carbonization temperature (400-650°C) and the weight ratio of phosphoric acid to lignin (P/L=0.7-1.75). As a result of the different pyrolysis conditions, activated carbons with various pore size distribution, surface area and surface acidic groups were obtained. The results showed the significant importance of carbonization temperature on the adsorption capacity for removal of copper. A maximum in the copper adsorption was found for carbons prepared at a carbonization temperature between 450 and 550°C. Increasing temperature acidic groups were degraded but increasing mesoporosity and surface area favored diffusion and adsorption. Increasing P/L ratio did not influence significantly on adsorption capacity of the activated carbons once lignin had completely reacted with phosphoric acid. P/L ratios higher than 1.2 did not modify the pore size distribution but it reduced the total volume of pores.

Keywords: activated carbon, phosphoric activation, porosity, surface properties, metal removal

* vfierro@etscq.urv.es

Tel: +34 977 55 85 46
Fax: +34 977 55 85 44

1. INTRODUCTION

The term lignin refers to a group of phenolic polymers that confer strength and rigidity to the woody cell wall of plants. Lignin is separated from wood during pulp and paper making operations, where it serves primarily as in-house fuel required for the recovery of chemicals. The separation of Kraft lignin could be an alternative to incineration since lignin is a bountiful and renewable resource and represents an attractive field for future industrial chemistry. One of the potential uses is the production of activated carbon.

Lignin can be used as precursor for activated carbon as it has been reported on physical activation of eucalyptus Kraft lignin by CO₂ partial gasification¹ and on chemical activation of this precursor by using zinc chloride². However, the use of ZnCl₂ has declined due to the environmental problems³ and phosphoric acid is preferred as activating-dehydrating agent.

Activated carbons are high porosity, high surface area materials used in industry for environmental remediation, purification and chemical recovery operations. While most activated carbons are used for adsorption of organic compounds, previous studies have shown that many activated carbons can uptake metal ions from solutions.

This work was undertaken to study the feasibility of the utilization of activated carbon produced from Kraft lignin by chemical activation with phosphoric acid for the removal of heavy metal cations from water solutions. For this study, we chose copper as monitor of metal uptake, since copper is a ubiquitous metal in plating and jewelry manufacturing wastewaters. The influence of carbonization temperature and phosphoric acid to lignin weight ratio on Cu adsorption are analyzed.

2. EXPERIMENTAL

2.1 Materials

Kraft lignin was provided by Lignotech Iberica S.A. Table 1 shows the ultimate and elemental analyses of lignin. Elemental analysis was carried out in a EA1108 Carlo Erba Elemental Analyzer. The proximate analysis was carried out following ISO standards following the weight losses at 100°C/air (moisture), 900°C/non-oxidizing atmosphere (volatile matter) and 815°C/air (ash).

A 85% H₃PO₄ solution (Panreac, Spain) was used as activating agent.

2.2 Preparation and characterization of the activated carbons

Lignin was mixed with varying amounts of H₃PO₄ in the range of 0.7 to 1.75 phosphoric acid to lignin weight ratio (P/L) in wet basis. The slurry was left for 1h at room temperature and under air atmosphere, then transferred to a furnace DUM Model 10CAF where carbonization was carried out under air atmosphere. The oven was heated at 10°C min⁻¹, up to 150°C where temperature was hold to allow free evolution of water. Afterwards the oven was heated at 10°C min⁻¹ to the final carbonization temperature (from 400 to 650°C) it was hold for 2h. In order to remove the excess of H₃PO₄ after carbonization, the cooled mass was extensively washed with distilled water until a neutral pH was attained (a CyberScan PC 510 pH-meter with a Hamilton-electrode 'Flushtrode', special for deionized water, was used). Then, the samples were dried in an oven at 110°C overnight.

Surface area and pore size characterization were performed using a Micromeritics ASAP2000 gas adsorption surface area analyzer. The specific

surface area of the samples was determined from the nitrogen isotherms at -196°C and by using the BET equation. Micropore volume was determined using t-plot, mesopore volume using the BJH equation and total volume of pores was calculated at a relative pressure (p/p^0) of 0.99.

2.4 *Cation-exchange capacity (CEC)*

A weighed amount of adsorbent was placed into an Erlenmeyer flask. A volume of 50ml of 0.1M NaOH was added. To attain equilibrium the flasks were shaken for 24h. After equilibration the NaOH concentration was measured by titration with HCl. The quantity of NaOH consumed was converted to CEC and expressed in meq g⁻¹.

2.5 *Copper uptake from aqueous solutions*

Experiments were done in batches with 18 Erlenmeyer flasks containing 150 mg of activated carbon and 150 ml of deionized water. Varying amounts of Cu(II) chloride (p.a. quality from Aldrich) were added to each flask. The initial pH of the solution was adjusted at pH=5 by adding 0.1N NaOH solution. The flasks were sealed to avoid evaporation and stirred for 24h at 25°C. The resulting Cu(II) concentration was analyzed by atomic absorption spectrophotometry (AAS) with a Perkin Elmer 3110 model. The amounts of adsorbed copper were obtained by calculating the difference of each concentration before and after adsorption. Several activated carbons prepared at different carbonization temperature and acid phosphoric to lignin ratio (P/L) were tested.

3. RESULTS AND DISCUSSION

3.1 Surface area and porosity

Table 2 shows BET surface area and pore volume distribution of the activated carbons prepared from Kraft lignin by phosphoric acid impregnation at different temperatures and P/L ratios.

The surface areas increased between the temperature of 400 and 600°C and the maximum surfaces of more than 1200 m²g⁻¹ was observed at 600°C. At temperatures higher than 600°C, the surface areas were considerably reduced. The isotherms approached type I (Langmuir), indicating an essentially microporous character with some contribution of wider pores (meso- and macropores) depending on the carbonization temperature. At 400°C, the activated carbon showed the highest value of microposity. Increasing the carbonization temperature produced the development of porosity in the mesoporous region. The activated carbons prepared at 550°C exhibited a high contribution of the mesoporous region with a considerably reduced microposity. At these temperatures there is a reduction in the total volume of pores due to shrinkage of the material.

The highest BET surface area was attained at P/L=1.2 and further increases in the P/L ratio produced a decrease in the BET surface area. The highest micropore to total volume ratio was found for the carbon prepared with the lowest P/L ratio. As P/L ratio increased up to P/L=1.2, the micropore volume also increased but in a lower extent than the mesoporous volume. Higher values of the P/L ratio reduced the total pore volume and affected to the micro and mesopore volume in a similar extent. Moreover, the relative importance of the volume of macropores increases with the P/L ratio. The

use of a P/L ratio of 1.2 yields a carbon with the highest surface area at 450°C ($S_{\text{BET}}=1036 \text{ m}^2\text{g}^{-1}$) and total pore volume ($V_p = 0.6 \text{ cm}^3\text{g}^{-1}$).

Detailed discussion of these results and on the effect of phosphoric acid on surface area and pore size distribution is given elsewhere⁴.

3.2 Cation-exchange capacity

The acidic groups covering the carbon surface are usually quantified by using the Boehm's method⁵. NaHCO_3 can detect only strong acids as the carboxylic group. Na_2CO_3 can detect the carboxylic groups, lactones and lactoles. NaOH , in addition of the aforementioned groups, is capable of detecting phenols.

Benadi et al.⁶ analyzed phosphoric acid activated carbons produced from wood precursors using potentiometric titration and identified peaks corresponding to phosphonic acids ($-\text{PO}_3\text{H}_2$; pK_a 7-9), phosphonous acids ($-\text{PO}_2\text{H}_2$; pK_a 3-4.5), and phosphines ($-\text{PR}_3$; pK_a 3-6.5, 8-9).

In this work, we used modified method based on Bohem's method to measure the cation-exchange capacity (CEC) of the carbons⁷. Using NaOH , the total amount of acidic groups is quantified: carboxylic groups, lactones, lactoles, phenol and phosphorous-containing acids.

Figure 1 shows that CEC decreases with carbonization temperature. The decrease in the functional groups determined by NaOH titration is possibly due to degradation of phosphorous compounds. As temperature increases phosphate and polyphosphate bridges acting as crosslinking parts of the carbon structure decompose^{8,9} and it also could affect to surface phosphorous compounds that are degraded. Dastgheib and Rockstraw¹⁰ working on pecan shell activated carbons found a linear decrease in the

functional groups detected by NaOH. These authors quantified functional groups by Boehm's method and concluded that temperature mainly affected to phenolic and/or phosphonic groups.

Figure 2 shows CEC for carbons prepared at different P/L ratio between 0.7 and 1.75. CEC increases with P/L ratio but the value remains proximately from P/L=1.0. As H₃PO₄ reacts with the hydroxyl groups of lignin it would exist a maximum in the P/L ratio and so a maximum in the phosphorous-containing acids attached to the surface. In a previous work¹¹ carried out in a thermogravimetric device, we have shown that phosphoric acid is in excess at P/L ratios higher than 1.0.

3.3 Copper adsorption isotherms

Langmuir isotherm was applied for adsorption equilibrium.

$$C_e/q_e = 1/(Q_0 b) + C_e/Q_0$$

where C_e is the equilibrium concentration (mg l⁻¹), q_e is the amount absorbed at equilibrium (mg g⁻¹), Q_0 and b are the Langmuir constants related to adsorption capacity and energy of adsorption. The linear plot of C_e/q_e versus C_e showed that the adsorption obeyed the Langmuir model. Here we study the variation of Q_0 with carbonization temperature and P/L ratio taking into account CEC, surface area and pore size distribution of the activated carbons.

Figure 3 shows the variation of the Cu adsorption capacity with the carbonization temperature. Comparing this plotting with the data showed in Figure 1 it can be clearly seen that the adsorption capacity of the activated carbons can not be directly correlated with the CEC. Although the lower the

temperature of preparation the higher the determined CEC, it must be taken into account the surface area and the pore size distribution.

Figure 3 also shows the evolution of BET surface area with temperature. The highest CEC was determined at 400°C but also the surface area was low and most of the pore size distribution (75%) are micropores (with diameters less than 2nm). Considering the diameter of copper ion in aqueous solutions as 1.2 nm¹², a portion of micropores is not accessible to the hydrated copper ion. On the one hand, as temperature of carbonization increased up to 600°C the surface area and the ratio of meso- and macropore volumes to total volume ratio also increased. On the other hand, CEC decreased with temperature as seen above. These two factors could explain the existence of a maximum in Cu adsorption for activated carbons prepared at temperatures between 450 and 550°C. At temperatures higher than 600°C, the shrinkage of the structure together with the decreasing tendency of CEC with temperature would explain the Cu adsorption observed.

Figure 4 shows the evolution of the Cu adsorption capacity and the BET surface area with the P/L ratio. Cu adsorption increased with P/L ratio according with the higher CEC determined. However, the differences observed in Cu adsorption at low P/L ratios can not only be explained by the moderate variation of CEC for P/L values between 0.7 and 1.75. There was also a strong variation of the surface area and pore size distribution with the P/L ratio. At P/L=0.7, the activated carbon had a surface area of 603 m²g⁻¹ and 75% of the total pore volume corresponded to microporosity, therefore diffusional limitations could be expected. Increasing the P/L ratio microporosity decreased and remained proximately constant at 66% of the total pore volume even at the highest P/L=1.75 where surface decreased considerably. We think that the high CEC together with the no existence of diffusional limitations in carbons at P/L=1.75 could be the reason of the

slight decrease in copper adsorption even if the surface area decreased greatly from $959 \text{ m}^2\text{g}^{-1}$ at $P/L=1.4$ to $704 \text{ m}^2\text{g}^{-1}$ at $P/L=1.75$.

4. CONCLUSIONS

This study showed that activated carbons produced from Kraft lignin can be tailored to have a high surface concentration of acidic groups and a pore size distribution favorable for adsorption of metallic ions from solutions.

Carbonization temperature strongly affects to metal adsorption by changing porosity distribution and degrading phosphorous-acidic groups. The P/L ratio does not influence the amount of copper adsorbed if the added phosphoric acid is enough to allow the complete reaction of lignin.

Thus, pyrolysis of lignin with phosphoric at temperatures about 500°C and P/L ratio of 1.0 produces activated carbons with a favorable pore size distribution and enough surface acidic groups for removal of copper ions.

ACKNOWLEDGEMENTS

V. Fierro acknowledges the “Ministerio de Ciencia y Tecnología” and the “Universitat Rovira i Virgili” for the financial support of her “Ramón y Cajal” contract. V. Torné acknowledges the “Universitat Rovira i Virgili” for her PhD grant.

REFERENCES

- [1] J. Rodríguez-Mirasol, T. Cordero, J.J. Rodríguez Carbon 31 (1993) 87-95.
- [2] E. Gonzalez Serrano et al. Ind Eng. Chem. Res., 36 (1997) 4832-4838.
- [3] H. Teng, T.S. Yeh, L.Y. Hsu, Carbon 36 (1998) 1387-1395
- [4] V. Fierro, V. Torné, D. Montané, J. Salvadó in proceedings of Carbon'03. Oviedo (Spain) 2003.
- [5] H.P. Boehm Advances in catalysis, New York: Academic Press, 1966, 179-274.
- [6] H. Benadi, T.J. Bandosz, J.Jagiello, J.A. Schwarz, J.N. Rouzaud, D. Legras, F. Beguin Carbon 38 (2000) 669-674.
- [7] F. Suárez-García, A. Martínez-Alonso, J. M. D. Tascón J. Anal. Appl. Pyrolysis 63 (2002) 283-301.
- [8] M. Jagtoyen, F. Derbyshire, Carbon 31(1993) 1185-1192.
- [9] M. Molina-Sabio, F. Rodríguez-Reinoso, F. Caturla, M. J. Sellés Carbon, 33 (1995) 1105-1113.
- [10] S. A. Dastgheib, D. A. Rockstraw, Carbon 39 (2001) 1849-1855.
- [11] V. Fierro, D. Montané submitted for publication
- [12] J. Laine, A. Calafat, M. Labady Carbon 27 (1987) 191-195.

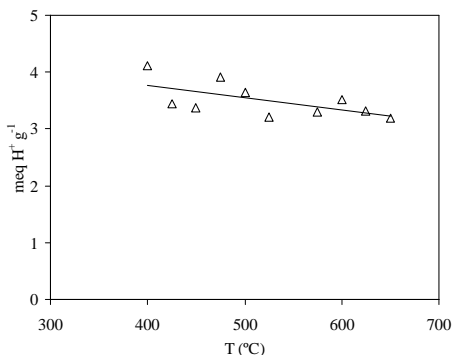


Fig. 1. Variation of the CEC of the activated carbons with the carbonization temperature. (P/L=1.4)

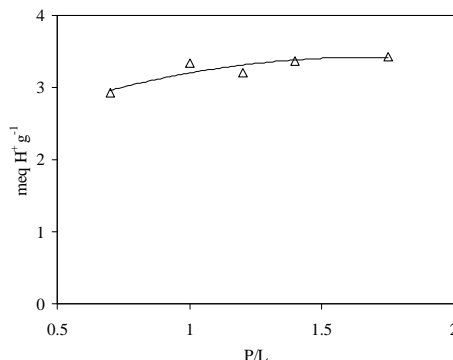


Fig. 2. Variation of the CEC of the activated carbons with the P/L ratio. (T=450°C)

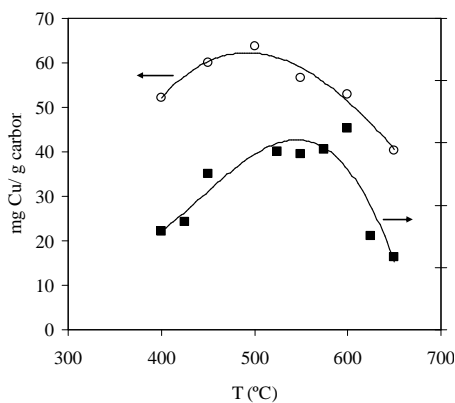


Fig. 3. Variation of the Cu adsorbed and of the BET surface area with the carbonization temperature. (P/L=1.4)

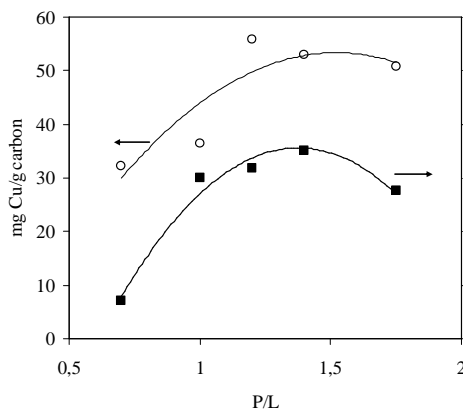


Fig. 4. Variation of the Cu adsorbed and of the BET surface area with the P/L ratio. (T=450°C)

Table 1 Lignin Analyses (wt.%)

	Proximate (wt.%, humid basis)		Elemental (wt.%, ash and moisture free)
Moisture	14.45	Carbon	59.46
Ash	9.50	Hydrogen	5.07
Volatile matter	44.93	Nitrogen	0.05
Fixed carbon ^a	31.12	Sulfur	2.15
		Oxygen ^a	33.27

^a Estimated by difference

Table 2 Surface area and porosity of the activated carbons

T (°C)	P/L	S _{BET} (m ² /g)	V _{total} (cm ³ /g)	V _{micro} (cm ³ /g)	V _{meso} (cm ³ /g)	V _{macro} (cm ³ /g)
400	1.4	917	0.48	0.34	0.11	0.03
425	1.4	944	0.50	0.27	0.18	0.05
450	1.4	1101	0.54	0.33	0.01	0.20
525	1.4	1173	0.60	0.29	0.08	0.22
550	1.4	1163	0.58	0.31	0.14	0.13
575	1.4	1178	0.59	0.30	0.05	0.25
600	1.4	1245	0.67	0.24	0.10	0.33
625	1.4	901	0.51	0.15	0.08	0.28
650	1.4	834	0.46	0.10	0.09	0.27
450	0.7	541	0.30	0.20	0.02	0.09
450	1.0	998	0.50	0.30	0.10	0.10
450	1.2	1036	0.51	0.31	0.10	0.10
450	1.8	950	0.46	0.28	0.07	0.12

5.2.2. Optimization of the synthesis of highly microporous carbons by chemical activation of Kraft lignin with NaOH

Este artículo ha sido enviado al Chemical Engineering Journal durante el año 2006.

OPTIMIZATION OF THE SYNTHESIS OF HIGHLY MICROPOROUS CARBONS BY CHEMICAL ACTIVATION OF KRAFT LIGNIN WITH NAOH

V. Torné-Fernández^{1*}, J.M. Mateo¹, D. Montané¹, V. Fierro^{1,2}

¹Departament d'Enginyeria Química, Universitat Rovira i Virgili, Campus
Sescelades, Av. dels Països Catalans 26, 43007 Tarragona, Spain.

²Laboratoire de Chimie du Solide Minéral. Université Henri Poincaré –Nancy I.
UMR CNRS 7555, BP 239, F 54506 Vandoeuvre-lés-Nancy, France.

*Corresponding author: vanessa.torne@urv.cat. FAX: +00 34 977 559667

Abstract

Highly microporous carbon materials with high apparent surface areas (up to 2400 m²/g) were obtained by heat treatment of mixtures of demineralised kraft lignin (KL_d) and NaOH. Application of a statistical tool, the response surface methodology, was used to determine the optimum operation conditions for preparing activated carbons able to adsorb phenol. For that purpose, three parameters were varied: temperature of activation, NaOH/KL_d percent mass ratio and nitrogen flow rate. This carbon was tested for the adsorption of methylene blue, obtaining adsorptions of 93.9 g/100 g AC. It has a high microporosity (0.997 cm³/g that corresponds with more than 74% of the total porosity) and specific surface area of 2400 m²/g. This best activated carbon was prepared at 783°C, 26.4% of Kraft lignin and 200 cm³ N₂/min.

Key words: activated carbon, methylene blue, phenol, adsorption capacity, response surface methodology.

1. INTRODUCTION

Lignin is an abundant bio-polymer that is obtained in large quantities during chemical pulping of wood and annual plants for the production of cellulose pulps. Several kinds of technical lignins are identified depending on the pulping process, such as Kraft lignin, lingsulfonates, and organosolv lignin, the first being the most extended. The established use of lignin in the Kraft process is as in-house fuel to supply energy to the process, which also allows the simultaneous regeneration of the pulping chemicals. However, the enormous amount of lignin that is processed through the Kraft pulping-plants yearly has prompted interest on finding higher value applications for this material. Some uses that have been explored are as binder for animal fodder, to prepare lubricants for oil well drilling, in soil stabilization, as substitute for phenol in adhesives, and as precursor for the manufacture of activated carbon. The latter is currently a favored application, since the demand of carbonaceous adsorbents is growing worldwide driven by stricter environmental regulations, which force improvement in separation techniques and intensive processing of waste streams to reduce the emissions of gas and liquid contaminants. Activated carbons and carbon molecular sieves are used in several industrial processes such as gas separation, gas storage, purification or catalyzed reactions [1-3]. The properties of the carbonaceous adsorbent depend on the pore volume distribution, the kind of pores present, and on the surface chemistry. All those factors are direct consequence of the nature of the precursor material and, most important, on the activation agent and reaction conditions [4-9].

In recent studies on the chemical activation of Kraft lignin with H_3PO_4 [10, 11], we obtained microporous activated carbons with surface areas as high as

1300 m²/g, although higher specific surfaces may be obtained with other activating agents. There is a growing interest in alkaline hydroxide activation process, and KOH has been found to be one of the most effective compounds for that purpose [9, 12-15]. High surface areas and pore volumes are reported for lignocellulosic materials, carbons and chars activated by KOH with surface areas up to 3000 m²/g [16]. Exploratory studies evidenced the possibility of preparing highly microporous carbons from Kraft lignin using NaOH and KOH as activating agent in suitable experimental conditions [16].

There are several parameters that influence the activation process [4-9]. Make a complete study of each one to observe its effect entails a large number of experiments. Conventional and classical methods of studying a process by maintaining other factors involved at an unspecified constant level does not depict the combined effect of all the factors involved. Thus, a parameter alone has not a significant effect but it can affect to others parameters. To study all this interactions and the effect of each parameter separately a statistical tool can be used, the response surface methodology [17-25]. In this case, this method also requires time, depending on the number of parameters studied, but this optimization tool studies the effect of the parameters in a collectively way reducing the number of experiments.

The aim of the present work was to develop a systematic study to optimize the manufacture of carbons activated from Kraft lignin by activation with NaOH. A statistical study based on the surface-response method [17-25] has been developed using the adsorption of methylene blue as dependent variable, since it serves as a model compound for the most usual organic

pollutants [16, 25-39]. We have used the methylene blue adsorption capacity as response variable to choose the best AC.

Methylene blue can serve as a model for the adsorption of organic pollutants [25], as several works has demonstrated [16, 26-39]. These compounds destroy the ozone stratospheric layer, are the precursors of photochemical oxidants, produce acid rain, affect to the nervous system and are carcinogenic and mutagenic agents [40]. For this reason, a big number of studies about the elimination of these compounds have been published [40-42] using different methods for treating them.

2. EXPERIMENTAL

2.1. Materials

KL was supplied by Lignotech Ibérica S.A. (Spain), and was presented in the form of a fine dark brown powder. Ash content of the lignin was 9.5% on reception, and lignin was demineralised prior to the preparation of the carbons. To remove the inorganic matter from KL, batches of 100 g were introduced in 2 l of water leading to dark brown suspensions of pH 9.5, and lignin was then precipitated by adding H₂SO₄ until the pH decreased to 1. The precipitate was gently washed with distilled water until constant pH and it was dried overnight at 105 °C. The lignin prepared this way was nearly mineral-free and was labelled demineralised Kraft lignin (KL_d).

Extra pure methylene blue chloride (MB) powder was supplied by Scharlau. It was diluted in distilled water to obtain a solution of 3.2 mM of

concentration. Sodium hydroxide (NaOH) of 99% purity was purchased in the form of lentils from Scharlau.

2.2. Preparation of carbons

Sodium hydroxides lentils were ground and physically mixed with KL_d at KL_d to total mix mass ratios between 18% and 32%. The carbonisation was carried out in a horizontal tubular furnace, where the samples were heated in a crucible at $5^\circ\text{C}/\text{min}$ from room temperature to a nominal carbonisation temperature (T_{carb}) of between 700°C and 869°C . Flows of N_2 (f) of between 200 and $500\text{ cm}^3/\text{min}$ were used, and the samples were kept at the nominal carbonization temperature for one hour before cooling them down under nitrogen atmosphere.

During the experiments, both metallic sodium and NaOH were transported by the vapours and could be observed at the outlet of the reactor. Metallic sodium mixed with sodium carbonate was also present inside the crucible. Therefore, the latter was submitted to atmospheric humidity for two days to oxidise sodium metal slowly. Finally, the activated carbon was washed with extreme care, first with 1 M HCl, and finally with distilled water until a constant pH of around 6. After drying in an oven during 24 h, a very light activated carbon was obtained.

The effectiveness of the carbons prepared from Kraft lignin for methylene blue adsorption was compared with that of three commercial AC (CAC1, CAC2 and CAC3), which were kindly provided by Norit Americas Inc. These carbons are prepared by physical activation with steam [37] and their main properties are shown in Table 1. CAC1 and CAC3 are mainly microporous

with high surface areas of more than 1000 m²/g. CAC2 has a lower surface area and less than 30% of microporous (0.185 cm³/g in microporous volume respect a total volume of 0.637 cm³/g). All of them have an acidic surface character.

2.3. Response surface methodology (RSM)

The experiments were planned using a response surface methodology, which was based on a central factorial design established around a central point located in the expected optimal zone [43, 44]. Methylene blue adsorption was the dependent variable, and the independent variables were the proportion of NaOH, the carbonisation temperature and the flow-rate of nitrogen inside the carbonization tube [16].

This technique develops a two or three dimension surface obtained from several experimental data [43, 44]. As we can see in Figure 1, this methodology is based on a central factorial design established in a central point that is determined in a theoretical optimum zone. From this point, some deviations of a controlled size are made and if it is necessary, more equidistant axial points from the central one can be added to complete the experimental table, called the compost central factorial design. Figure 2 shows the algorithm followed in the RSM.

The analysis of the surface response determined the significance of the effect of the independent variables and their interactions. The design was expanded with a second set of experiments into a compost central factorial design (see Figure 2) to locate the optimum more precisely.

In the presented work, the central point was established at a carbonisation temperature of 770°C, a mass ratio of 25% of KL₄, and a nitrogen flow of 350 cm³/min, according to the available literature [45-50]. The variations performed were ±70°C in the temperature, ±5% in the mass ratio, and ±150 cm³/min in the nitrogen flow.

2.4. Characterisation of the activated carbons

2.4.1. Surface area and porosity

Surface area and porosity were determined from the nitrogen adsorption–desorption isotherms obtained at 77 K with an automatic instrument (ASAP 2020, Micromeritics). The samples were previously degassed at 523 K for several hours. N₂ adsorption data for P/P₀ from 10⁻⁵ to 0.99 (in a set of values previously fixed) were analysed according to: (i) the BET method [51] for calculating the specific surface area, S_{BET} ; and (ii) the α_s method [52] for calculating the micropore volume, $V_{\alpha,\text{micro}}$, and the ultramicropore volume, $V_{\alpha,\text{ultra}}$, using Carbopack F Graphitised Carbon Black as reference material [53]. The total pore volume, $V_{0.99}$, was calculated from nitrogen adsorption at a relative pressure of 0.99.

2.4.2. Methylene blue (MB) adsorption tests

MB serves as a model compound for adsorption of organic contaminants from aqueous solution and is used as a primary indicator of the adsorption capacity of activated carbons [25]. The adsorption test of MB is based on a

one point adsorption isotherm. The analysis was performed mixing 33.7 mg of AC in a topped plastic bottle with 50 ml of a solution of 3.2 mM of MB. This suspension remained under mechanical agitation for 24 hours. Afterwards, a sample of the solution was extracted and analysed in a UV-VIS in an 8500 Dinko Instruments spectrophotometer, equipped with a tungsten lamp operated at 664.8 nm. The MB adsorption capacity (q_{AM}) was calculated by the difference between the initial and the final concentrations, and expressed as grams of MB per 100g of AC (g MB/100g AC).

2.4.3. Surface functionality

Modified Boehm titration [54] was used to identify and quantify the acid and basic surface functionality of the AC. For this, 25 mg of dry sample were mixed with 25 ml of NaOH 0.1 N, Na₂CO₃ 0.1 N, NaHCO₃ 0.1 N, sodium ethoxide 0.1 N and HCl 0.05 N. The first four solutions determine the acidic surface sites whereas the latter is used to measure the total basic sites. NaOH is used to quantify carboxylic, lactone and phenol groups, Na₂CO₃ for carboxylics and lactones; NaHCO₃ determines carboxylics and sodium ethoxide for the total acidic sites. By difference between them, it is possible to calculate the quantity of each surface group. The suspensions of AC were stirred for 48 hours to complete contact between the surface groups and the reagent in the solution. Afterwards, the suspension was filtered and samples of 5 ml were titrated with HCl or NaOH depending on the solution. The adsorbed quantity was calculated by the difference between the initial and the final valours and expressed in terms of miliequivalents per gram of AC (meq/g AC).

3. RESULTS AND DISCUSSION

3.1. Application of RSM to optimize adsorption capacity

A preliminary study with activated carbons prepared with LK_d and potassium hydroxide [16] dealing with the effect of the experimental conditions on the characteristics of the activated carbons was carried out in order to determine the most relevant ones. The latter were found to be activation temperature T_{carb} , mass ratio of lignin R and N₂ flow rate f , while the activation time and heating rate were found to have minor effects within the corresponding range of values investigated. For this reason, activation time and heating rate were fixed at one hour and 5 °C/min, respectively.

3.1.1. First screening experiments

According to the central factorial design, seventeen AC were prepared under the conditions detailed in Table 3. The central point was: $T_{\text{carb}} = 770$ °C, $R = 25\%$ and $f = 350$ cm³/min. Table 4 shows the values of the statistical parameter, p-value, that represent the error existing in the linear and quadratic approximations for the RSM. The error level has been established in 5% so a p-value above 0.050 means that this parameter has not a significant influence on the dependent variable. Application of a linear approximation gives information about the influence of temperature, mass ratio and nitrogen flow within the MB adsorption. Table 4 shows that the three parameters have p-values above 0.050, which means that these parameters have not a significant linear effect in the adsorption of the MB, but comparing among them temperature and the mass ratio are more

significant than nitrogen flow. The quadratic approximation of the central factorial design, shows two important facts: i) first, the influence of each parameter alone and the combined effect of each pair in the adsorption of MB (for instance, the combined effect of the temperature and mass ratio in the elimination of MB); ii) second, if the experiments are well represented by the quadratic approximation or not, from the value of the parameter $T_{carb}^2+R^2+f^2$. The latter is important because the quadratic approximation gives a surface area where an optimum can be located. If we are not working in this zone, we do not find the maximum.

Table 4 shows that the quadratic approximation corroborates the results obtained from the application of the linear approximation. The influence of temperature and mass ratio is not strictly significant on the adsorption of MB at 95% probabilities but their p-values, 0.085 and 0.078 for the temperature and the mass ratio respectively, are very close to 0.05. Probably, the election of a new central point should result in a clearer determination of the true effects of temperature and mass ratio, which is supported by the p-value of the combined effect of temperature and mass ratio, which is below 0.050. In contrast, the nitrogen flow and the combination of this parameter with temperature and mass ratio give p-values bigger than 0.300, and in consequence, the nitrogen flow was determined not to be a significant parameter for the study. Finally, the value of $T^2+R^2+f^2$ was 0.039 which shows that we are working with a quadratic surface that with a better central point should give us the optimum conditions for the preparation of ACs, with adsorption of MB. It was necessary to expand the study with a maximum a compost central factorial design by adding experiments 12 to 17.

From these results, we can conclude that we are working near the optimum zone but the central point must be improved. In summary, the effect of the

nitrogen flow and its interaction with T_{carb} and R were not significant. Therefore, a constant value of $f = 200 \text{ cm}^3 \text{ N}_2/\text{min}$, that is a typical value [49, 50, 55], was maintained for the remaining experiments. On the other hand, when the temperature was below 750°C , the MB adsorption capacity decreased with the mass ratio, but above that temperature the dependence with the mass ratio was the opposite. The mass ratio increased the MB adsorption capacity, and it also increased with the temperature for all the mass ratios studied until 777°C , where a maximum exists, and from where the adsorption decreases. This phenomenon occurs because at higher temperatures and mass ratios, the structure of the AC begins to collapse caused by an excessive effect of the activation [16] producing the reduction of the specific surface area that is the main responsible for the MB adsorption.

3.1.2. Experiments with the refined central point

The results of the first screening experiments demonstrated that nitrogen flow-rate was not significant, but the significance of temperature and mass ratio was not clearly established, nor was the optimum located. Therefore a second set of experiments was conducted according to a new design around a new central point, which used smaller variations. The central point was fixed at 777°C with a content of lignin of 23% within variations of $\pm 30^\circ\text{C}$ and $\pm 2\%$. Fourteen new samples of AC were prepared at the conditions detailed in Table 5.

The experiments realised in this second zone gave the p-values for the quadratic approximation of the temperature and mass ratio shown in Table 6. In this case, it is not necessary to study the linear approximation since we are

working with only two parameters, temperature and mass ratio. The significant influence of both parameters was clear, since the p-values were below 0.050. The combined effect of temperature and mass ratio had also significance. Values for T^2 and R^2 , 0.002 and 0.017 respectively, show that the quadratic surface should give the optimum conditions to prepare an AC with maximum adsorption of MB.

3.1.3. Integration of the first-step experiments

Figure 3 shows the response surface modelled from all the experimental data, the first and the second sets of experiments. A maximum MB adsorption of 96.4 g MB/100g AC was predicted at 783°C, 26.4% in KL_d content and 200 $\text{cm}^3 \text{N}_2/\text{min}$. The activated carbon prepared at those conditions gave a MB adsorption of 93.9 g MB/100g AC. Table 7 shows the characterisation of the AC prepared at the optimum conditions. The carbon had a specific surface of 2400 m^2/g , and it was highly microporous (more than 65% of the total porosity), and its surface was predominantly basic, with 15.8 meq/g of basic groups and only 10.5 meq/g of acidic groups.

3.2. Other characteristics of the activated carbons

In general, the MB adsorption capacity of an activated carbon is closely related to the specific surface area, as shown in Figure 4 for activated carbons prepared by chemical and physical activation. Carbons obtained by chemical activation include our own results on ACs from Kraft lignin activated with H_3PO_4 [35], KOH [16] and NaOH, and bibliographic data on carbons prepared by activation with H_3PO_4 [32], KOH [26-31, 33] and steam [38, 39].

Three commercial carbons are also included [37]. MB adsorption capacity for the activated carbons prepared in this study range from 38.7 g MB/100g AC to 98.2 g MB/100g AC, in good agreement with the results reported by several authors [26-31, 33] for carbons prepared from different types of raw materials (olive stone, petroleum coke, pistachio shells, wood, etc.) by KOH activation, which ranged from 26.3 g MB/100g AC to 110.0 g MB/100g AC which lay in the same range of values than for NaOH carbons. The very large porosities and surface areas of the activated carbons prepared with NaOH and KOH facilitates the adsorption of large quantities of adsorbates and thus carbons can find application in removing organic and inorganic molecules from contaminated streams, efficiently [26, 27, 29, 32, 34]. In contrast, activated carbons prepared from Kraft lignin by phosphoric acid activation have more limited MB adsorption capacities, about 38.9 g MB/100g AC [32], which is caused by the lower specific surfaces. Finally, carbons activated with steam [38, 39] and the three commercial activated carbons tested in this study have adsorption capacities similar to those of phosphoric acid carbons.

Due to the size of the MB molecule, around 15 Å, this compound is adsorbed only in the larger micropores or supermicropores (13-20 Å), and the mesopores (>20 Å) [34]. Figures 5 and 6 show the variation of the MB adsorption capacity with the micropore and the supermicropore and mesopore volumes. These figures confirm that MB is adsorbed on the supermicropores and mesopores.

On the other hand, in some cases where the surface area and the porosity is less developed, the MB adsorption capacity is greater than the expected and it is caused by the surface chemistry [31, 56]. MB is a dye with basic character and when is put in contact with a strong acid surface charge, electrostatic

interactions acts between the delocalised π electron of the carbon surface and the free electrons of the dye molecule presents in aromatic rings principally [56]. In Figures 7 and 8, the effect of the acid and basic surface chemistry is presented, respectively. In general, a better correlation between the MB adsorption capacities exists with the acidity surfaces (Figure 7). However, due to the fact that the porosity is well developed in the AC studied (Table 1 and 7), the surface chemistry does not play an important role collaborating in the adsorption phenomena.

4. CONCLUSIONS

The aim of this study was to optimize the preparation of carbons activated with NaOH for the purification of water polluted with organic compounds, and to study the interaction between the experimental variables by using a statistical method for the design of experiments.

The statistical method selected, the Response Surface Methodology, has been showed to provide the optimum conditions for prepare an AC that adsorb more MB and phenol than de commercials carbons used for comparison.

In the first step of the experimental application of the RSM, the effect of the nitrogen flow and its interaction with T_{carb} and R were not significant and does not affect the finally properties of the AC, especially the adsorption of MB. A typical constant value of $f = 200 \text{ cm}^3 \text{ N}_2/\text{min}$ was set for the remaining experiments centered in a second central point.

Integration of the first-step and the second-step experiments allowed selecting the optimum AC where the maximum MB adsorption take place is

achieved at 783°C, 26.4% in KL_d content and 200 cm³ N₂/min with a MB adsorption capacity of 93.9 mg/100g AC. These adsorption capacities are well correlated with the supermicropore and mesopore volume and also with the acidic groups of the surface due to the character of the basic dye employed.

ACKNOWLEDGEMENTS

Funding for this work was provided by the Spanish Ministry of Science and Technology (MCYT, project PPQ2002-04201-CO2-02, partially funded by the FEDER program of the European Union), and the Catalan Regional Government (Project 2005SGR-00580). This research was also partly made possible by financial support from the European Commission through the ALFA program (project LIGNOCARB-ALFA II 0412 FA FI). V. Torné-Fernández acknowledges the URV for her PhD grant. V. Fierro acknowledges the MCYT and the Universitat Rovira i Virgili (URV) for the financial support of her 'Ramón y Cajal' research contract.

REFERENCES

1. Activated carbon compendium. A collection of papers from the journal Carbon 1996-2000. 1^a ed, ed. H. Marsh. 2001, North Shields (UK): Elsevier.
2. Lin, S.Y., Jr., S.E. Lebo, and Lignotech USA, Inc., Lignin, in Kirk-Othmer Encyclopedia of Chemical Technology. 2000.
3. Lin, S. Y. and Lin, I. S., Lignin. Ullmann's Encyclopedia of industrial chemistry, ed. S.H. Barbara Elvers, Gail Schulz. Vol. A15. 1990, New York. 305-315.
4. Ahmad, A.L., Loh, M.M., and Aziz, J.A., Preparation and characterization of activated carbon from oil palm wood and its evaluation on Methylene blue adsorption. Dyes and Pigments. In Press, Corrected Proof.
5. Duran-Valle, Carlos J., Gomez-Corzo, Manuel, Gomez-Serrano, Vicente, et al., Preparation of charcoal from cherry stones. Applied Surface Science, 2006. 252(17): p. 5957-5960.
6. Ganan, J., González, J.F., González-García, C.M., et al., Air-activated carbons from almond tree pruning: Preparation and characterization. Applied Surface Science, 2006. 252(17): p. 5988-5992.
7. Lillo-Rodenas, M. A., Lozano-Castelló, D., Cazorla-Amorós, D., et al., Preparation of activated carbons from Spanish anthracite: II. Activation by NaOH. Carbon, 2001. 39(5): p. 751-759.
8. Lozano-Castello, D., Cazorla-Amoros, D., Linares-Solano, A., et al., Influence of pore size distribution on methane storage at relatively low pressure: preparation of activated carbon with optimum pore size. Carbon, 2002. 40(7): p. 989-1002.

9. Lozano-Castello, D., Lillo-Rodenas, M. A., Cazorla-Amoros, D., et al., Preparation of activated carbons from Spanish anthracite: I. Activation by KOH. *Carbon*, 2001. 39(5): p. 741-749.
10. Fierro, V., Torné-Fernández, V., Montané, D., et al. Activated Carbons Prepared from Kraft Lignin by Phosphoric Acid Impregnation. in *Carbon'03*. 2003. Oviedo (Spain).
11. Fierro, V., Torné-Fernández, V., Montané, D., et al., Study of the decomposition of kraft lignin impregnated with orthophosphoric acid. *Thermochimica Acta*, 2005. 433(1-2): p. 142-148.
12. Ahmadpour, A. and Do, D. D., The preparation of active carbons from coal by chemical and physical activation. *Carbon*, 1996. 34(4): p. 471-479.
13. Otowa, T., Nojima, Y., and Miyazaki, T., Development of KOH activated high surface area carbon and its application to drinking water purification. *Carbon*, 1997. 35(9): p. 1315-1319.
14. Liang, C., Wei, Z., Xin, Q., et al., Ammonia synthesis over Ru/C catalysts with different carbon supports promoted by barium and potassium compounds. *Applied Catalysis A: General*, 2001. 208(1-2): p. 193-201.
15. Frackowiak, Elzbieta and Beguin, Francois, Electrochemical storage of energy in carbon nanotubes and nanostructured carbons. *Carbon*, 2002. 40(10): p. 1775-1787.
16. Fierro, V., Torné-Fernández, V., and Celzard, A., Highly microporous carbons prepared by activation of Kraft lignin with KOH. *Studies in Surface Science and catalysis*, 2005: p. 607-614.
17. Veglio', F. and Beolchini, F., Removal of metals by biosorption: a review. *Hydrometallurgy*, 1997. 44(3): p. 301-316.

18. Ravikumar, K., Krishnan, S., Ramalingam, S., et al., Optimization of process variables by the application of response surface methodology for dye removal using a novel adsorbent. *Dyes and Pigments*, 2007. 72(1): p. 66-74.
19. K., Ravikumar, S., Ramalingam, S., Krishnan, et al., Application of response surface methodology to optimize the process variables for Reactive Red and Acid Brown dye removal using a novel adsorbent. *Dyes and Pigments*, 2006. 70(1): p. 18-26.
20. Karacan, F., Ozden, U., and Karacan, S., Optimization of manufacturing conditions for activated carbon from Turkish lignite by chemical activation using response surface methodology. *Applied Thermal Engineering*. In Press, Corrected Proof.
21. Azargohar, R. and Dalai, A.K., Production of activated carbon from Luscar char: Experimental and modeling studies. *Microporous and Mesoporous Materials*, 2005. 85(3): p. 219-225.
22. Ravikumar, K., Deebika, B., and Balu, K., Decolourization of aqueous dye solutions by a novel adsorbent: Application of statistical designs and surface plots for the optimization and regression analysis. *Journal of Hazardous Materials*, 2005. 122(1-2): p. 75-83.
23. Ravikumar, K., Pakshirajan, K., Swaminathan, T., et al., Optimization of batch process parameters using response surface methodology for dye removal by a novel adsorbent. *Chemical Engineering Journal*, 2005. 105(3): p. 131-138.
24. Goel, Jyotsna, Kadirvelu, K., Rajagopal, C., et al., Removal of mercury(II) from aqueous solution by adsorption on carbon aerogel: Response surface methodological approach. *Carbon*, 2005. 43(1): p. 197-200.

25. Bacaoui, A., Dahbi, A., Yaacoubi, A., et al., Experimental Design To Optimize Preparation of Activated Carbons for Use in Water Treatment. *Environ. Sci. Technol.*, 2002. 36(17): p. 3844-3849.
26. Stavropoulos, G.G. and Zabaniotou, A.A., Production and characterization of activated carbons from olive-seed waste residue. *Microporous and Mesoporous Materials*, 2005. 82(1-2): p. 79-85.
27. Stavropoulos, G.G., Precursor materials suitability for super activated carbons production. *Fuel Processing Technology*, 2005. 86(11): p. 1165-1173.
28. Tseng, Ru-Ling and Tseng, Szu-Kung, Pore structure and adsorption performance of the KOH-activated carbons prepared from corncob. *Journal of Colloid and Interface Science*, 2005. 287(2): p. 428-437.
29. Wu, Feng-Chin, Tseng, Ru-Ling, and Juang, Ruey-Shin, Comparisons of porous and adsorption properties of carbons activated by steam and KOH. *Journal of Colloid and Interface Science*, 2005. 283(1): p. 49-56.
30. Wu, Feng-Chin, Tseng, Ru-Ling, and Hu, Chi-Chang, Comparisons of pore properties and adsorption performance of KOH-activated and steam-activated carbons. *Microporous and Mesoporous Materials*, 2005. 80(1-3): p. 95-106.
31. El-Hendawy, Abdel-Nasser A., Surface and adsorptive properties of carbons prepared from biomass. *Applied Surface Science*, 2005. 252(2): p. 287-295.
32. Girgis, Badie S., Yunis, Samya S., and Soliman, Ashraf M., Characteristics of activated carbon from peanut hulls in relation to conditions of preparation. *Materials Letters*, 2002. 57(1): p. 164-172.
33. Khezami, L., Chetouani, A., Taouk, B., et al., Production and characterisation of activated carbon from wood components in powder: Cellulose, lignin, xylan. *Powder Technology*, 2005. 157(1-3): p. 48-56.

34. Lei, S., Miyamoto, J.-I., Kanoh, H., et al., Enhancement of the methylene blue adsorption rate for ultramicroporous carbon fiber by addition of mesopores. *Carbon*, 2006. In Press, Corrected Proof.
35. Fierro, V., Torné-Fernández, V., and Celzard, A., Kraft lignin as a precursor for microporous activated carbons prepared by impregnation with ortho-phosphoric acid: Synthesis and textural characterisation. *Microporous and Mesoporous Materials*, 2006. 92(1-3): p. 243-250.
36. Torné-Fernández, V., Fierro, V., Mateo, J. M., et al., Highly microporous carbons from chemical activation of lignin with hydroxides: optimization of preparation conditions., in 10th Mediterranean congress. 2005: Barcelona.
37. Inc., Norit Americas, www.norit-americas.com.
38. Warhurst, A. Michael, Mcconnachie, Gordon L., and Pollard, Simon J. T., Characterisation and applications of activated carbon produced from *Moringa oleifera* seed husks by single-step steam pyrolysis. *Water Research*, 1997. 31(4): p. 759-766.
39. Wu, Feng-Chin, Tseng, Ru-Ling, and Juang, Ruey-Shin, Pore structure and adsorption performance of the activated carbons prepared from plum kernels. *Journal of Hazardous Materials*, 1999. 69(3): p. 287-302.
40. Lillo-Rodenas, M.A., Cazorla-Amorós, D., and Linares-Solano, A., Behaviour of activated carbons with different pore size distributions and surface oxygen groups for benzene and toluene adsorption at low concentrations. *Carbon*, 2005. 43(8): p. 1758-1767.
41. Dimotakis, E. D., Cal, M. P., Economy, J., et al., Chemically Treated Activated Carbon Cloths for Removal of Volatile Organic Carbons from Gas Streams: Evidence for Enhanced Physical Adsorption. *Environmental Science and Technology*, 1995. 29(7): p. 1876-1880.

42. Benkhedda, J., Jaubert, J.-N., Barth, D., et al., Experimental and Modeled Results Describing the Adsorption of Toluene onto Activated Carbon. *J. Chem. Eng. Data*, 2000. 45(4): p. 650-653.
43. Montgomery, D. C., Design and analysis of experiments. 5th ed. 2000, New York: John Wiley & Sons cop.
44. Prat, A., Tort-Martorell, X., and Pozueta, L., Métodos estadísticos. Control y mejora de la calidad. 1997, Barcelona: UPC.
45. Guo, Y. P., Qi, J. R., Yang, S. F., et al., Adsorption of Cr(VI) on micro- and mesoporous rice husk-based active carbon. *Materials Chemistry and Physics*, 2002. 78(1): p. 132-137.
46. Guo, Y. P., Yang, S. F., Yu, K. F., et al., The preparation and mechanism studies of rice husk based porous carbon. *Materials Chemistry and Physics*, 2002. 74(3): p. 320-323.
47. Guo, Y. P., Zhang, H., Tao, N. N., et al., Adsorption of malachite green and iodine on rice husk-based porous carbon. *Materials Chemistry and Physics*, 2003. 82(1): p. 107-115.
48. Guo, Y. P., Yu, K. F., Wang, Z. C., et al., Effects of activation conditions on preparation of porous carbon from rice husk. *Carbon*, 2000. 41(8): p. 1645-1648.
49. Lillo-Rodenas, M. A., Cazorla-Amoros, D., and Linares-Solano, A., Understanding chemical reactions between carbons and NaOH and KOH. An insight into the chemical activation mechanisms. *Carbon*, 2003. 41(2): p. 267-275.
50. Lillo-Rodenas, M. A., Lozano-Castello, D., Cazorla-Amoros, D., et al., Preparation of activated carbons from Spanish anthracite II. Activation by NaOH. *Carbon*, 2001. 39(5): p. 751-759.
51. Rouquerol, F., Rouquerol, J., and Sing, K. S. W., Adsorption by Powders and Porous Solids. Principles, Methods and Applications. 1999, San Diego: Academic Press.

52. Setoyama, Norihiko, Suzuki, Takaomi, and Kaneko, Katsumi, Simulation study on the relationship between a high resolution [alpha]-plot and the pore size distribution for activated carbon. *Carbon*, 1998. 36(10): p. 1459-1467.
53. Kruk, M., Li, Z., Jaroniec, M., et al., Nitrogen Adsorption Study of Surface Properties of Graphitized Carbon Blacks. *Langmuir*, 1999. 15(4): p. 1435-1441.
54. Boehm, H. P., Chemical Identification of surface groups. *Advances in catalysis*, 1966. 16: p. 179-225.
55. Amarasekera, G., Scarlett, M.J., and Mainwaring, D.E., Development of microporosity in carbons derived from alkali digested coal. *Carbon*, 1998. 36(7-8): p. 1071-1078.
56. Pereira, Manuel Fernando R., Soares, Samanta F., Orfao, Jose J. M., et al., Adsorption of dyes on activated carbons: influence of surface chemical groups. *Carbon*, 2003. 41(4): p. 811-821.

Optimization of the synthesis of highly microporous carbons by chemical activation of kraft lignin with NaOH

V. Torné-Fernández, J.M. Mateo, D. Montané, V. Fierro

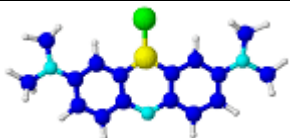
Table 1. Physical properties of the commercial AC used.

	S_{BET} (m^2/g)	$V_{\alpha,\text{micro}}$ (cm^3/g)	$V_{\alpha,\text{ultra}}$ (cm^3/g)	$V_{0.99}$ (cm^3/g)	Acidic Groups ($\text{meq H}^+/\text{gAC}$)	Basic Groups ($\text{meq OH}^-/\text{gAC}$)
CAC1	1350	0.458	0.139	0.713	2.6	0.5
CAC2	620	0.185	0.085	0.637	7.9	1.2
CAC3	1020	0.334	0.152	0.625	5.0	2.1

Optimization of the synthesis of highly microporous carbons by chemical activation of kraft lignin with NaOH

V. Torné-Fernández, J.M. Mateo, D. Montané, V. Fierro

Table 2. Properties of adsorptive molecule.

Molecule	Structure	MW ^a (g/mol)	Tb ^b (°C)	Solubility (%) w/w	Size (Å) ^a
MB		319.9	Decompose	100.0	15

MW^a. Molecular weight.

Tb^b. Normal boiling point.

Size^c. Size calculated with ACDLABS 8.0.

Optimization of the synthesis of highly microporous carbons by chemical activation of kraft lignin with NaOH

V. Torné-Fernández, J.M. Mateo, D. Montané, V. Fierro

Table 3. Points studied in the first-step experiments.

Experiment	Real Values			Statistical Values			q_{AM} (g/100 g AC)
	T_{carb} (°C)	R (%)	f (cm ³ /min)	T_{carb} (°C)	R (%)	f (cm ³ /min)	
1	700	20	200	-1	-1	-1	79.2
2	840	20	500	1	-1	1	38.7
3	770	25	350	0	0	0	86.7
4	840	30	200	1	1	-1	85.1
5	700	30	500	-1	1	1	62.6
6	770	25	350	0	0	0	98.2
7	840	30	500	1	1	1	82.2
8	700	30	200	-1	1	-1	83.6
9	770	25	350	0	0	0	91.8
10	840	20	200	1	-1	-1	49.8
11	700	20	500	-1	-1	1	87.0
Axial Points:							
12	770	32	350	0	1.4	0	91.5
13	869	25	350	-1.4	0	0	91.9
14	770	25	350	0	0	0	96.1
15	770	25	350	0	0	0	94.7
16	671	25	350	1.4	0	0	77.0
17	770	18	350	0	-1.4	0	83.4

Optimization of the synthesis of highly microporous carbons by chemical activation of kraft lignin with NaOH

V. Torné-Fernández, J.M. Mateo, D. Montané, V. Fierro

Table 4. Statistic p-value for the analysis in the first-step experiments, linear and quadratic approximations.

		T_{carb}	R	f	$T_{\text{carb}} \cdot R$	$T_{\text{carb}} \cdot f$	R · f	$T_{\text{carb}}^2 + R^2 + f^2$
Central factorial design	Linear approximation	0.298	0.282	0.606	-	-	-	-
	Quadratic approximation	0.085	0.078	0.309	0.021	0.977	0.423	0.039
Compost central factorial design	Quadratic approximation	0.822	0.230	-	0.059	-	-	0.153

Optimization of the synthesis of highly microporous carbons by chemical activation of kraft lignin with NaOH

V. Torné-Fernández, J.M. Mateo, D. Montané, V. Fierro

Table 5. Points studied in the second-step experiments.

Experiment	Real Values			Statistical Values			q_{AM} (g/100 g AC)
	T_{carb} (°C)	R (%)	f (cm ³ /min)	T_{carb} (°C)	R (%)	f (cm ³ /min)	
18	807	25	200	1	1	-	97.2
19	747	21	200	-1	-1	-	94.3
20	777	23	200	0	0	-	96.2
21	807	21	200	1	-1	-	91.9
22	747	25	200	-1	1	-	94.1
23	777	23	200	0	0	-	93.6
24	777	23	200	0	0	-	93.9
Axial Points:							
25	777	20	200	0	-1.4	-	95.1
26	777	26	200	0	1.4	-	88.0
27	777	23	200	0	0	-	97.4
28	777	23	200	0	0	-	93.2
29	777	23	200	0	0	-	95.7
30	819	23	200	1.4	0	-	90.3
31	735	23	200	-1.4	0	-	95.6

Optimization of the synthesis of highly microporous carbons by chemical activation of kraft lignin with NaOH

V. Torné-Fernández, J.M. Mateo, D. Montané, V. Fierro

Table 6. Statistic p-value for the variables, quadratic approximation.

	T_{carb}	R	$T_{\text{carb}} \cdot R$	T_{carb}^2	R^2
Quadratic approximation	0.057	0.016	0.008	0.002	0.017

Optimization of the synthesis of highly microporous carbons by chemical activation of kraft lignin with NaOH

V. Torné-Fernández, J.M. Mateo, D. Montané, V. Fierro

Table 7. Properties of the optimum AC for the adsorption of MB.

S_{BET} (m^2/g)	$V_{\alpha,\text{micro}}$ (cm^3/g)	$V_{\alpha,\text{super}}$ (cm^3/g)	$V_{0.99}$ (cm^3/g)	Acidic Groups ($\text{meq H}^+/\text{g AC}$)	Basic Groups ($\text{meq OH}^-/\text{g AC}$)
2400	0.964	0.090	1.472	10.5	15.8

Optimization of the synthesis of highly microporous carbons by chemical activation of kraft lignin with NaOH

V. Torné-Fernández, J.M. Mateo, D. Montané, V. Fierro

Table 8. MB (q_{MB}) adsorption capacity of the optimum AC and the commercial ones.

q_{MB}	AC-optimum	CAC1	CAC2	CAC3
g/100 g AC	93.9	41.5	31.5	21.7

Captions of the figures

Figure 1. Scheme of experimental points for the RSM development in two dimensions.

Figure 2. Response Surface Methodology basic steps.

Figure 3. Variation of the quantity of MB adsorbed depending on the temperature (I) and the KL_d quantity (R) a) in three dimensions and b) in two dimensions.

Figure 4. Specific surface area in front of MB adsorption capacity for AC obtained by activation with: \diamond H_3PO_4 (our AC), \blacklozenge H_3PO_4 from bibliography, \square KOH (our AC), \blacksquare KOH from bibliography, Δ NaOH, \circ commercial carbons and \bullet steam activation from bibliography. Continuous line show the general data tendency.

Figure 5. Microporous volume in front of MB adsorption capacity for AC obtained by activation with: \diamond H_3PO_4 , \square KOH, \blacksquare KOH from bibliography, Δ NaOH and \circ commercial AC. Continuous line show the general data tendency.

Figure 6. Supermicroporous and mesoporous volume in front of MB adsorption capacity for different AC obtained by activation with: \diamond H_3PO_4 (our AC), \square KOH (our AC), Δ NaOH and \circ commercial carbons. Continuous line show the general data tendency.

Figure 7. Acidic surface chemistry influence with the MB adsorption capacity for different AC obtained by activation with: \diamond H_3PO_4 (our AC), \square KOH (our AC), Δ NaOH and \circ commercial carbons. Continuous line show the general data tendency.

Figure 8. basic surface chemistry vs. MB adsorption capacity for different AC obtained by activation with: \diamond H_3PO_4 (our AC), \square KOH (our AC), Δ NaOH and \circ commercial carbons. Continuous line show the general data tendency.

Optimization of the synthesis of highly microporous carbons by chemical activation of kraft lignin with NaOH

V. Torné-Fernández, J.M. Mateo, D. Montané, V. Fierro

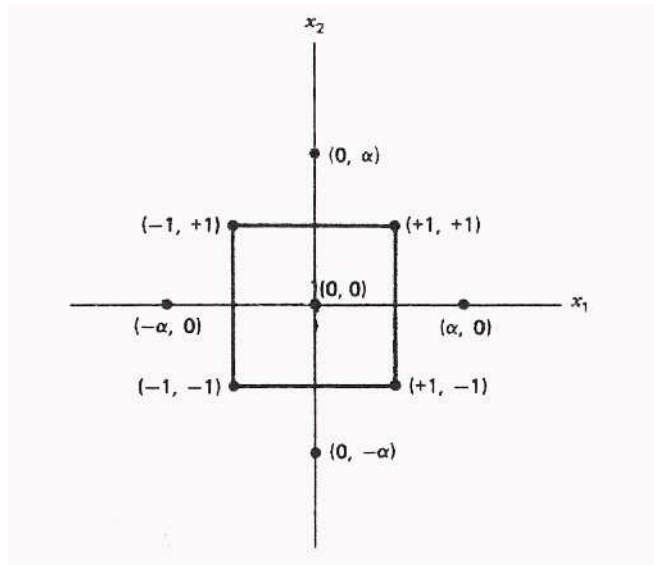


Figure 1
Torné-Fernández, V., et.al

Optimization of the synthesis of highly microporous carbons by chemical activation of kraft lignin with NaOH

V. Torné-Fernández, J.M. Mateo, D. Montané, V. Fierro

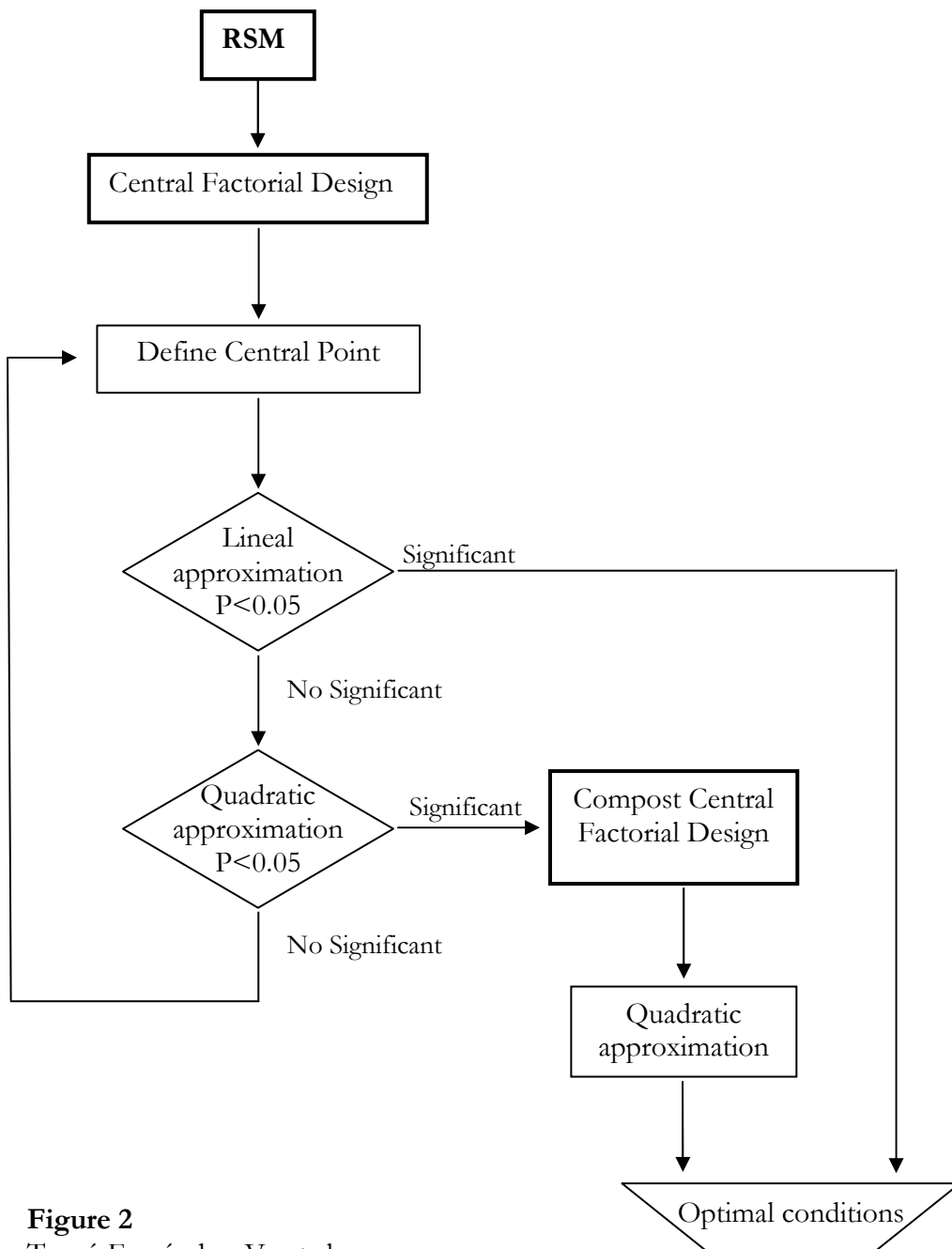


Figure 2
Torné-Fernández, V., et.al

Optimization of the synthesis of highly microporous carbons by chemical activation of kraft lignin with NaOH

V. Torné-Fernández, J.M. Mateo, D. Montané, V. Fierro

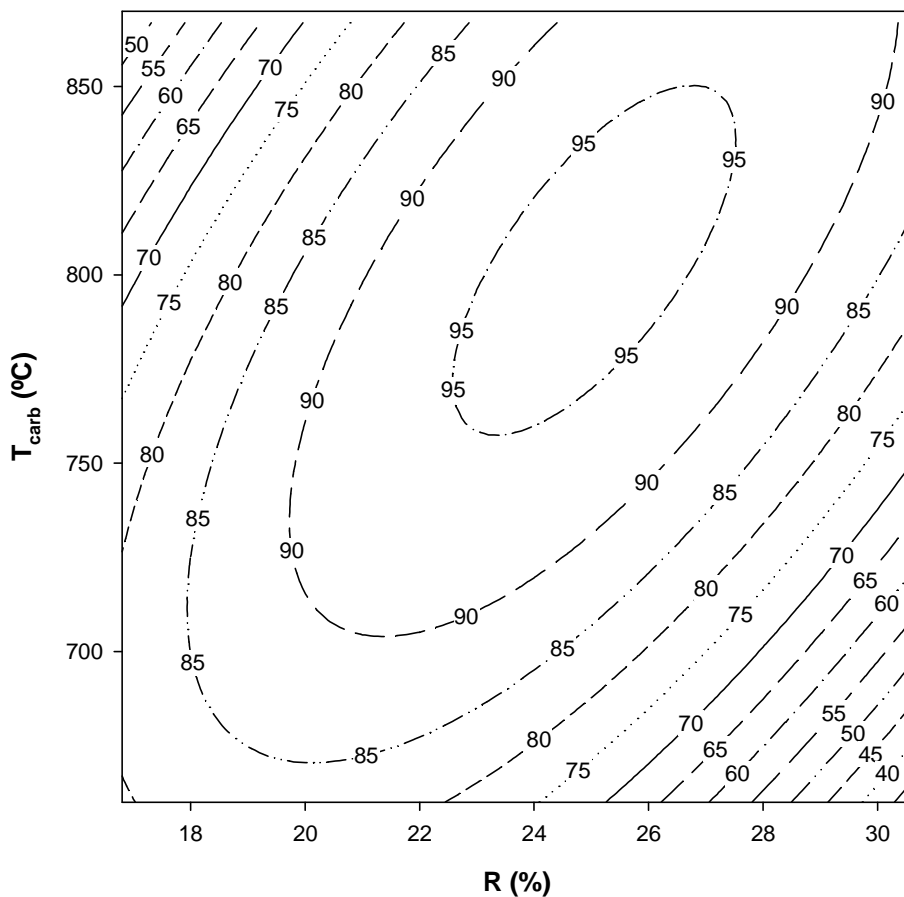


Figure 3
Torné-Fernández, V., et.al

Optimization of the synthesis of highly microporous carbons by chemical activation of kraft lignin with NaOH

V. Torné-Fernández, J.M. Mateo, D. Montané, V. Fierro

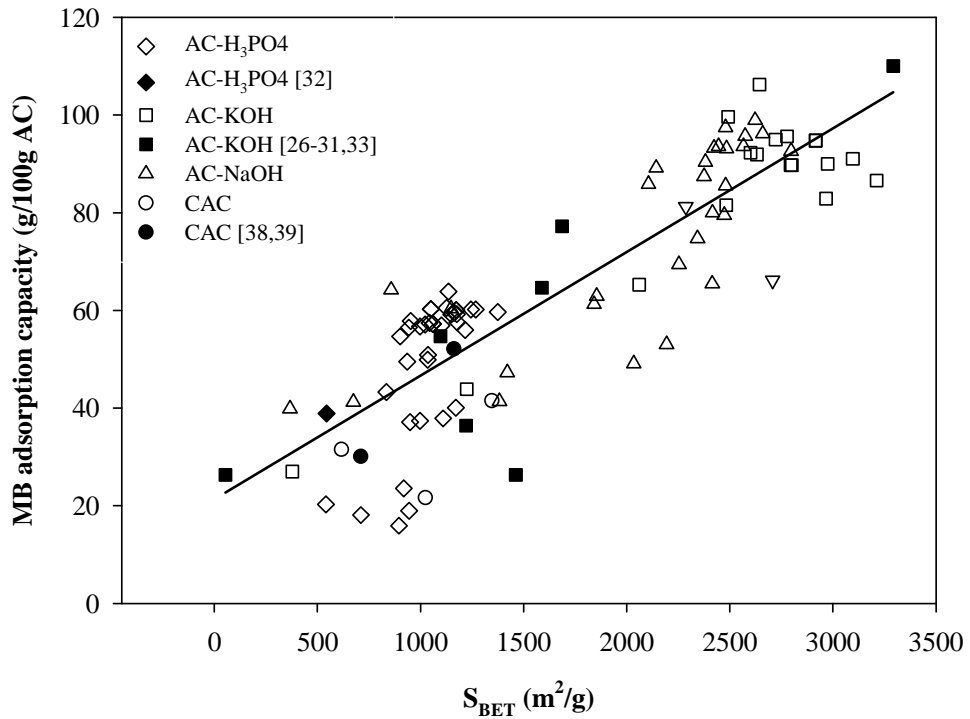


Figure 4
Torné-Fernández, V., et.al

Optimization of the synthesis of highly microporous carbons by chemical activation of kraft lignin with NaOH

V. Torné-Fernández, J.M. Mateo, D. Montané, V. Fierro

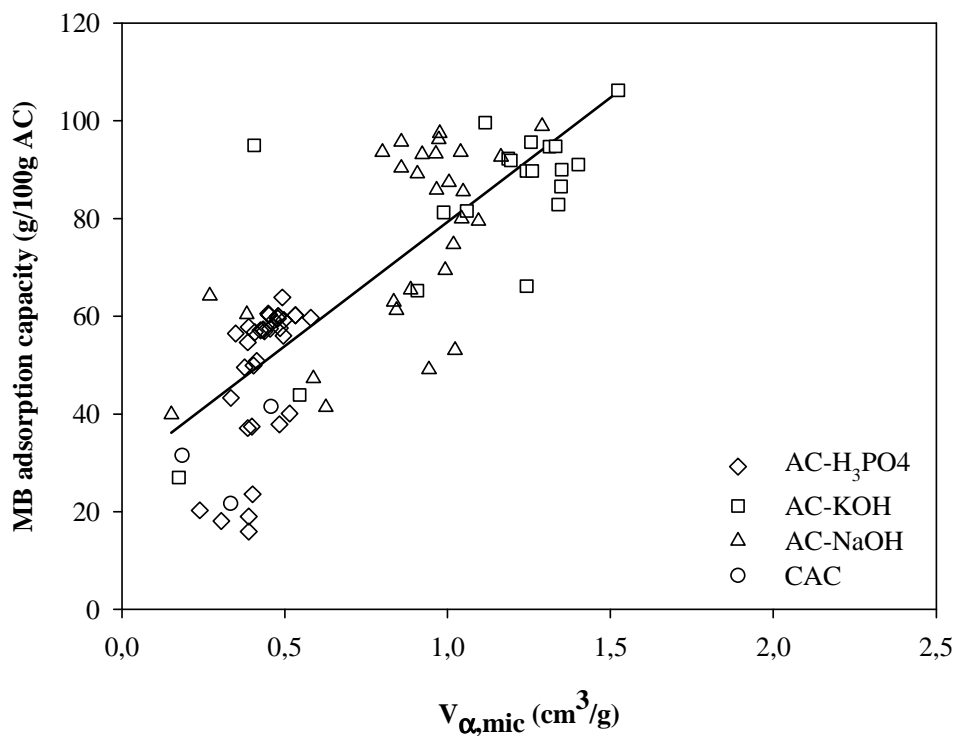


Figure 5
Torné-Fernández, V., et.al

Optimization of the synthesis of highly microporous carbons by chemical activation of kraft lignin with NaOH

V. Torné-Fernández, J.M. Mateo, D. Montané, V. Fierro

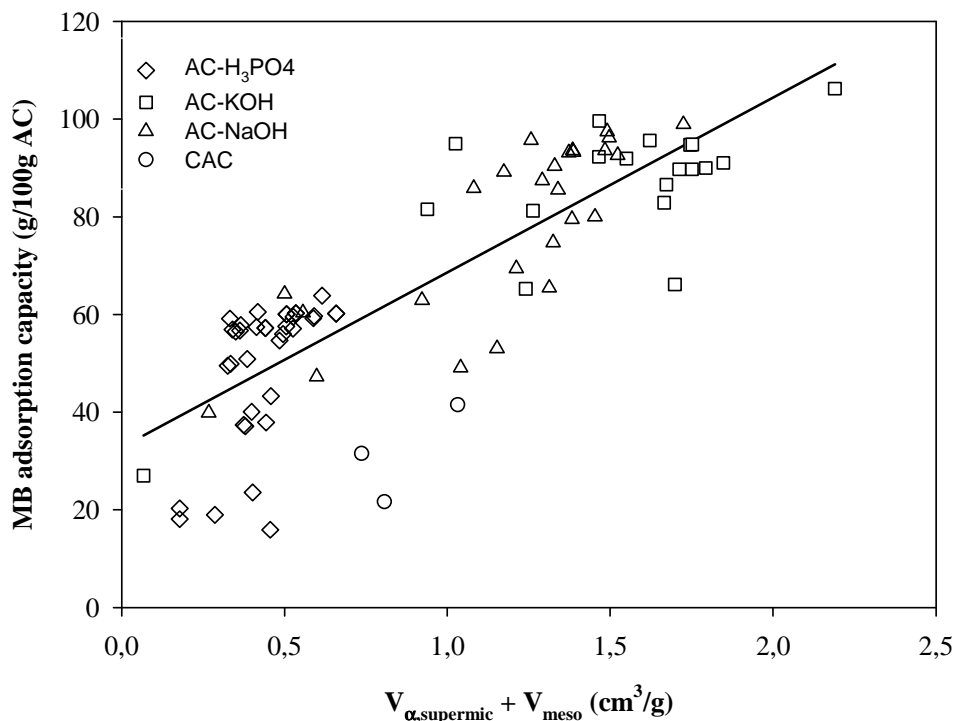


Figure 6
Torné-Fernández, V., et.al

Optimization of the synthesis of highly microporous carbons by chemical activation of kraft lignin with NaOH

V. Torné-Fernández, J.M. Mateo, D. Montané, V. Fierro

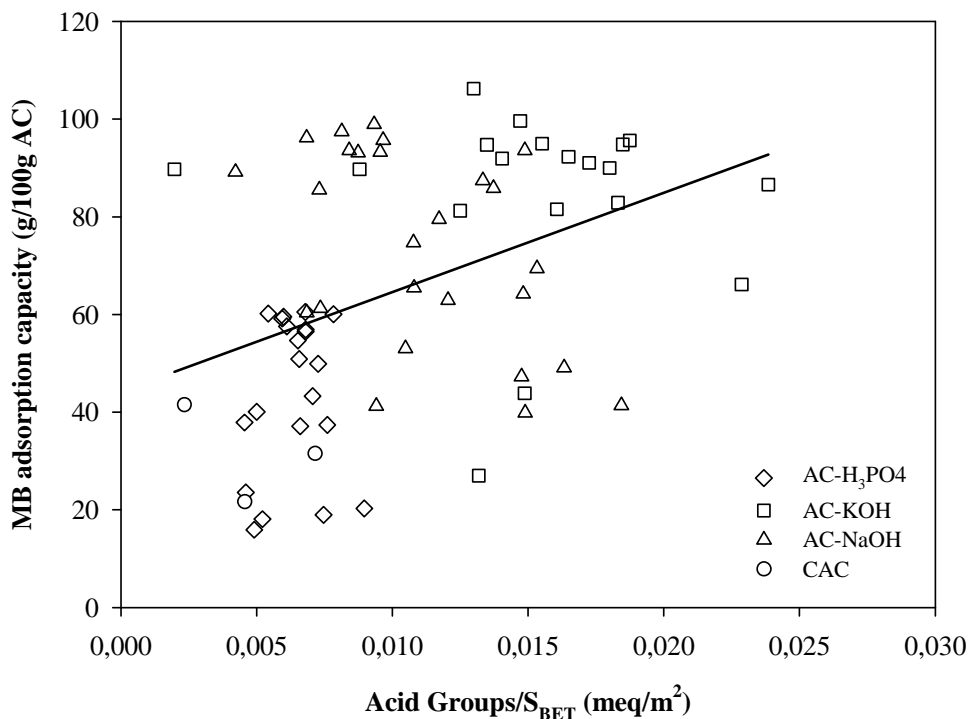


Figure 7
Torné-Fernández, V., et.al

Optimization of the synthesis of highly microporous carbons by chemical activation of kraft lignin with NaOH

V. Torné-Fernández, J.M. Mateo, D. Montané, V. Fierro

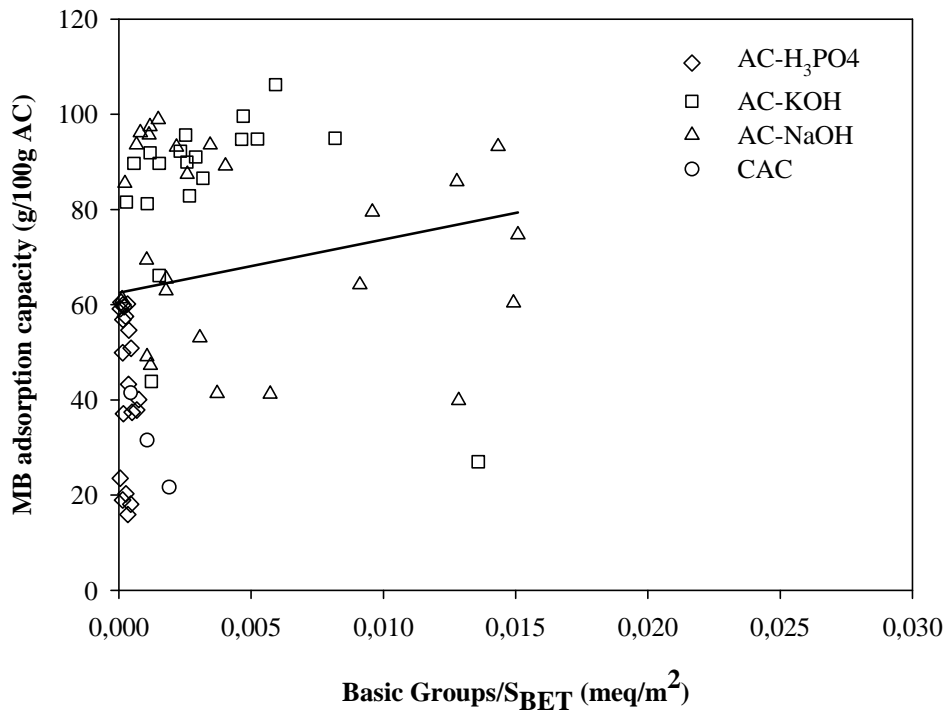


Figure 8
Torné-Fernández, V., et.al

5.2.3. Sorption study of organic compounds on highly microporous carbons prepared from Kraft lignin

Este artículo ha sido enviado al journal Adsorption Science and Technology durante el año 2006.

SORPTION STUDY OF ORGANIC COMPOUNDS ON HIGHLY MICROPOROUS CARBONS PREPARED FROM KRAFT LIGNIN

V. Torné-Fernández^{1*}, V. Fierro^{1,2}

¹ Departament d'Enginyeria Química, Universitat Rovira i Virgili, Campus
Sescelades, Av. dels Països Catalans 26, 43007 Tarragona, Spain.

² Laboratoire de Chimie du Solide Minéral. Université Henri Poincaré –
Nancy I. UMR CNRS 7555, BP 239, F 54506 Vandoeuvre-lés-Nancy,
France.

*Corresponding author: vanessa.torne@urv.cat. FAX: +00 34 977 559667

Abstract

Activated carbons obtained from Kraft lignin by chemical activation with sodium hydroxide, potassium hydroxide or phosphoric acid are highly microporous carbon materials with high apparent surface areas up to 2900 m²/g. Carbonaceous microporous adsorbates have been used for the adsorption of organic contaminants in aqueous phase. Thus, three different types of activated carbons derived from Kraft lignin are used for this purpose and large amounts of adsorbed pollutants are achieved with values between 100 and 240 mg g⁻¹ for phenol and 185 and 235 mg g⁻¹ for benzene. A kinetic study was done and phenol and benzene adsorption data obtained fit well a pseudo-second-order reaction, as it is described in the literature.

Key words: activated carbon, phenol, benzene, adsorption capacity, liquid phase.

1. INTRODUCTION

Kraft lignin is obtained from the treatment of black liquors originating of paper production. This black liquor is a residue composed principally of cellulose, hemicellulose and lignin. This last one, the second most abundant component in wood in a proportion until 24%.

The preparation of activated carbons (AC) from Kraft lignin [1-6] is a novel usage of this raw material, which is mainly used as in-house fuel for the recovery of both energy and residual inorganic matter, and also others employments [7-14] as animal feed binding, oil well drilling, soil stabilization, protein precipitation or board additives are of minor importance.

We have recently reported the chemical activation of KL impregnated with H_3PO_4 [6, 15], NaOH [5, 16] and KOH [16] obtaining AC essentially microporous with surface areas as high as 1300 m^2/g for the activation with H_3PO_4 and 2400 m^2/g for alkaline hydroxides. Activation with potassium hydroxide (KOH) has gained a growing interest as activating agent since it has been found to be one of the most effective compounds for that purpose [17-21]. High surface areas and pore volumes are reported for lignocellulosic materials, carbons and chars activated by KOH with surface areas up to 3000 m^2/g [5].

ACs are used in several industrial processes such as gas separation, gas storage, purification or catalyzed reactions [7, 22, 23]. The aim of the present study is to examine the capability of a series of AC developed from the chemical activation of Kraft lignin with phosphoric acid, sodium hydroxide and potassium hydroxide impregnation to adsorb organic compounds from

low concentration wastewater. These organic components are common contaminants in industrial waters since they are used as intermediates in the synthesis of dyes, pesticides, explosives, insecticides, and also they constitute priority pollutants [24]. These waters are generally treated with chlorine, used as disinfectant and it reacts with phenol and form chlorophenols. This derived compound from phenol is a big problem since it is one of the most toxic pollutants found in industrial wastewaters. For these reasons, benzene and phenol in dilute aqueous solution were chosen as representative model compounds for adsorption assessment.

As it is presented in Table 1, phenol is commonly used in this sense [25-92] but only few experimental aqueous-phase adsorption isotherm data are available in the literature for benzene [24, 36, 53, 93-96] and toluene [24, 36, 49, 53, 70, 93-95, 97] compared with the large quantity of tests in gas phase [98]. The importance of the study of this kind of compounds is based on the fact that they destroy the ozone stratospheric layer, are the precursors of photochemical oxidants, produce acid rain, affect to the nervous system and are carcinogenic and mutagenic agents [98]. For this reason, a big number of studies about the elimination of these compounds have been published [98-100] using different methods for treating it.

2. EXPERIMENTAL

2.1. Materials

KL was supplied by Lignotech Ibérica S.A. (Spain), and was presented in the form of a fine dark brown powder. The removal of the inorganic matter from KL was achieved as follows: batches of 100 g were introduced in 2 l of

water, leading to dark brown suspensions of pH 9.5, and lignin was precipitated by adding H_2SO_4 until the pH decreased to 1. The precipitate was gently washed with distilled water until the pH of the rinse was constant and finally dried overnight at 105 °C. The lignin prepared this way was nearly mineral-free and was termed demineralised Kraft lignin (KL_d).

Two activating agents were used with KL_d : sodium hydroxide (NaOH) with a 99% purity and potassium hydroxide (KOH) with 85% of purity, both provided by Scharlau as lentils. Another activating agent was used with KL_d , an 85% solution of phosphoric acid (H_3PO_4) supplied by Panreac Spain.

For the adsorption tests, phenol (Ph) crystals and benzene solution were supplied by Aldrich with more than 99% of purity. Both organic compounds were solved in ultrapure water from a Milli-Q Millipore equipment for preparing 100 ppm solutions that were kept in crystal bottles under a temperature of 6°C.

2.2. Preparation of carbons

For the preparation of AC with NaOH (AC-Na), sodium hydroxides lentils were ground and physically mixed with KL_d according to a NaOH/ KL_d mass ratio of 3/1. The carbonisation was carried out in a horizontal furnace and the samples were heated from room temperature to 750°C in a N_2 flow of 200 cm^3/min . This sample was kept at the final temperature for a carbonisation time of one hour before cooling down under nitrogen. The heat rate was established in 5°C/min. Afterwards, the sample was submitted to atmospheric humidity for two days, during which the alkaline metal remaining slowly oxidised. Finally, the activated carbon was washed with

extreme care, first with 1 M HCl, and finally with distilled water until the pH of the rinse remains constant and close to 6 (a CyberScan PC 510 pH-meter with a Hamilton-electrode “Flushtrode” was used). After drying in an oven during 24 hours, a very light activated carbon was obtained.

The preparation of AC with KOH (AC-K) was made following the same methodology explained before but with different activating conditions: 700°C of carbonisation temperature, a KOH/ KL_d mass ratio of 3/1 and a 400 cm³ N₂/min.

In the chemical activation with H₃PO₄ (AC-P), the procedure was different. KL was mixed with H₃PO₄ a 1.4 acid to lignin weight ratio (P/L) on a wet basis. The slurry was left for an impregnation time of 48 hours at room temperature in air, and then transferred to a furnace DUM Model 10CAF where carbonization was carried out under air atmosphere. The furnace was heated at 10 °C min⁻¹, up to 150 °C, which temperature was held for 1 h to allow free evolution of water. Afterwards the oven was heated at 10 °C min⁻¹ up to the final carbonisation temperature, 450°C, which was held for 2 h. To remove the excess of H₃PO₄ after carbonisation, the activated carbon was extensively washed with distilled water until a neutral pH was met (a CyberScan PC 510 pH-meter with a Hamilton-electrode “Flushtrode” was used). Then, the samples were dried overnight in an oven at 105 °C.

To compare with these activated carbons, three commercial AC was used, called CAC1, CAC2 and CAC3. These AC are prepared by physical activation with steam [101] and are provided from Norit Americas Inc. The properties of all these carbons are shown in Table 2. AC-Na, AC-K, AC-P, CAC1 and CAC3 are highly microporous AC with high surface area between 900 m²/g and 2900 m²/g. CAC2 has less surface area with less than 30% of

microporous ($0.185 \text{ cm}^3/\text{g}$ in microporous volume respect a total volume of $0.637 \text{ cm}^3/\text{g}$). All these AC have a high acidic surface character although AC-Na has also a large quantity of basic groups.

2.3. Characterisation of adsorbates

Surface area and porosity were determined from the corresponding nitrogen adsorption–desorption isotherms obtained at 77 K with an automatic instrument (ASAP 2020, Micromeritics). The samples were previously outgassed at 523 K for several hours. N_2 adsorption data for P/P_0 from 10^{-5} to 0.99 (in a set of values previously fixed) were analysed according to: (i) the BET method [102] for calculating the specific surface area, S_{BET} ; and (ii) the α_s method [103] (using Carbo-pack F Graphitised Carbon Black as reference material [104] for calculating the micropore volume, $V_{\alpha_{\text{micro}}}$, and the ultramicropore volume, $V_{\alpha_{\text{ultra}}}$. The total pore volume, $V_{0.99}$, was calculated from nitrogen adsorption at a relative pressure of 0.99.

2.4. Phenol (Ph) and Benzene (B) adsorption

Adsorption of phenol and benzene was studied with the six AC presented before. The properties of these organic molecules used in the adsorption tests onto the different AC are present in the table 3. As it is showed, both compounds are very similar in molecular weight and size but the presence of an OH group in the phenol structure gives different polarity compared with benzene. From this property, benzene presents a highest volatility and less

solubility in comparison with phenol. Thus, this both components represent good models for this type of tests.

2.4.1. Kinetic study

For the determination of the time needed for achieve the adsorption equilibrium, 10 mg of AC was mixed with 10 ml of a 100 ppm solution of phenol or benzene in several well topped glass flasks. The mixing step took place for a determined time until a maximum of 7 days to ensure the equilibrium state at a constant temperature of 25°C. The tubes were attached perpendicularly with clamps to a horizontal revolving shaft that had a rotating speed of 2 rpm and the temperature was controlled with an electronic digital regulator P-Selecta Digiterm-100. Afterwards, 3 ml of sample were taken and filtered in a regenerated cellulose filter of 0.45 μm of pore size to a vial topped. The concentration of the organic compound was obtained by liquid chromatography in an 1100 Series Agilent chromatograph with a Hypersil ODS 250 mm column. The dynamic phase was acetonitrile/water in a relation of 65/35. The adsorbed quantity (q) was calculated by the difference between the initial and the final valour.

2.4.2. Adsorption isotherms

For the preparation of the adsorption isotherms, different quantities of adsorbate (between 1 and 20 mg) were mixed with 10 ml of a 100 ppm solution of phenol or benzene in several well topped glass flasks. The sample granulometry was between 63 and 500 μm of diameter particle. The tubes were capped and placed in a water bath at 25°C, attached perpendicularly

with clamps to the horizontal revolving shaft for 8 hours to ensure the equilibrium. Afterwards, 3 ml of sample were taken and filtered in a regenerated cellulose filter of 0.45 μm of pore size to a vial topped. The concentration of the organic compound was obtained by HPLC, as it has been explained before.

The adsorbed quantity (q_t) was calculated by the difference between the initial and the final valour.

The acidic surface of the AC used in this report provides low pH during the tests for the AC activated with KOH and H_3PO_4 and not high variations for the rest of AC. The initial pH of the phenol adsorption test was proximally 7 but due to the acidity character of AC the final pH varies to between 4 (AC-K and AC-P) and ~ 6.7 (AC-Na, CAC1, CAC2 and CAC3) depending on the adsorbate used. In the benzene adsorption tests, the behaviour is quite similar. The initial pH is 7.7 and the free evolution of the pH goes to 4 (AC-K and AC-P) and ~ 6.5 (AC-Na, CAC1, CAC2 and CAC3).

At lows pH, the acidic compounds prevails in the nonionized form, that have higher adsorption capacity of organic species than when is present in the ionized form [24]. This phenomena occurs because the reduction of repulsions interactions that improve the organic adsorption capacity.

3. RESULTS AND DISCUSION

Experimental adsorption tests realised with phenol and benzene present similar results. Figure 1 and 2 present the experimental data obtained for ACs prepared from lignin and the commercial carbons for phenol and benzene

adsorption, respectively. As it can be appreciated, in both cases the maximum adsorption capacity is achieved in less than 2 hours. Results presented only correspond to the first 10 hours of experiments, when the stability is achieved.

3.1. Kinetic of the adsorption processes

The dependence of the reaction rate on the concentration of the species present, in form of quantity adsorbed, must be determined by experimental observation. Although, the functional dependence must be obtained from the theory and corroborated with the experimental data. One of the most common general form [105] of the dependence of organic adsorption on the adsorbate is

$$-r_t = k \cdot (q_e - q_t)^n \quad (1)$$

Where $-r_t$ is the reaction rate that can be expressed as the variation of the adsorption capacity respect to the time (dq_t/dt); k is the adsorption rate constant expressed in terms of mass phenol or benzene adsorbed per adsorbate mass unit and time ($\text{g} \cdot \text{mg}^{-1} \cdot \text{min}^{-1}$); q_e and q_t are the equilibrium and instantaneous mass amount of the organic compound adsorbed per carbon mass unit (mg/g), respectively; t is the contact time (minutes); and n is the reaction order. The reaction order refers to the powers to which the concentration is raised in the kinetic rate law and gives an idea about how fast the reaction take place.

Equation 1 can be rearranged as:

$$\frac{dq_t}{(q_e - q_t)^n} = k \cdot dt \quad (2)$$

Integrating the general form of Eq. (2) for the boundary conditions $t = 0$ to $t=t$ and $q_t = 0$ to $q_t = q_t$ gives:

$$\log(q_e - q_t) = \log(q_e) + \frac{1}{1-n} \{ \log(t) + \log[k \cdot (n-1)] \} \quad (3)$$

Linear plot of $\log(q_e - q_t)$ against $\log(t)$ gives values of the global reaction order, n , and kinetic constant, k , presented in Table 4. As it is showed, the reaction order of the adsorption process is quite similar to a second order chemical reaction with good correlations ($r^2 > 0.930$) of the data for phenol and benzene adsorptions on the AC studied. For this reason, a pseudo-second order (equation 4) can be applied for this process, as is well cited in the literature [24, 54, 64], providing very similar results for constant rates, k and k' .

$$\frac{t}{q_t} = \frac{1}{k' \cdot q_e^2} + \frac{1}{q_e} \cdot t \quad (4)$$

The adsorption rate constant points to a faster adsorption rates for phenol than for benzene in the AC derived from lignin except for CAC2 and CAC3 that are very similar. The AC derived from lignin presents better adsorptions capacities compared with the commercial carbons in both experiments, with phenol and benzene.

Phenol and benzene are small organic molecules with a size of 6 Å and 5 Å respectively and it is well known that they are adsorbed essentially in micropores, as previous studies have shown for other organic compounds [106]. The highest phenol adsorption capacity corresponds with the maximum benzene adsorption capacity that is achieved for AC-Na and AC-K. Both ACs have the maximum volume of mesopores (0.428 cm³/g and 0.384 cm³/g, respectively) and micropores (1.018 cm³/g and 1.332 cm³/g, respectively). Figure 3 shows the adsorption of phenol and benzene on each AC studied as a function of their microporosity. It can be seen that the organic adsorption capacity linearly increases with the micropore volume.

3.2. Isotherm tests

From the experimental data presented in Figures 1 and 2, it is possible to obtain the equilibrium isotherms for the adsorption of phenol or benzene on the AC studied. Adsorption isotherm is important to describe the interaction between the solute and the adsorbate and is very important to optimize the use of adsorbents.

Figure 4 shows the relation between the amounts of phenol adsorption capacity versus the equilibrium concentration at 25°C. Figure 5 shows the same data as in Figure 4 but using benzene as solute. In the experimental data, there is a general agreement that the adsorption isotherms of phenol and benzene on AC are L-shaped [63]. However, there are many attempts in the literature to fit the adsorption isotherms to some kind of model. For this data, three well-known empirical equations were proposed. The first one is the Freundlich model [38, 54, 63, 73] (Equation 5) that is normally used for

high concentrations. This method is based on adsorptions variations with the pressure and considers the decrease of the affinity with the surface saturation, giving best fit at high concentrations.

$$q_e = k_f \cdot C_e^{1/n} \quad (5)$$

where q_e is the mass amount of the organic compound adsorbed per carbon mass unit (mg/g), k_f is the Freundlich constant related with the adsorption capacity (mg g^{-1}), C_e is the concentration of adsorbate in solution at equilibrium (mg l^{-1}) and n is the empirical parameter that represents the heterogeneity of the site energies (dimensionless).

The second model is the Langmuir equation [24, 38, 54, 60, 63, 72, 90]. Generally, this model is better than the Freundlich model but not all the adsorptions fit well with this isotherm (Equation 6) due to the formation of a monomolecular layer in the adsorbate surface. The fit is better at low concentrations.

$$\frac{C_e}{q_e} = \frac{1}{Q_0 \cdot b} + \frac{C_e}{Q_0} \quad (6)$$

where C_e and q_e are the same parameters as in the Freundlich isotherm. Q_0 is maximum amount of adsorbate adsorbed per carbon mass unit (mg/g) and b is the Langmuir constant related with the adsorption energy (l mg^{-1}).

This isotherm is the relation between the recovery degree of the solute particles and the pressure and is based on the velocity of the decrease of intermolecular interactions with the increase of the distance between the

adsorptive molecules and the adsorbate. This isotherm consider several factors: the adsorption is localized, all the active sites on the surface are power equivalents, there is not interaction between adsorbed molecules and the limiting reaction step is the surface reaction as in the heterogeneous catalytic reaction.

The efficiency of adsorption process can be predicted by the dimensionless equilibrium parameter R_L , which is defined by the following equation:

$$R_L = \frac{1}{1+b \cdot C_o} \quad (7)$$

where b is the Langmuir constant ($l \cdot mg^{-1}$) and C_o the initial concentration of phenol and benzene compounds ($mg \cdot l^{-1}$). When $R_L > 1$, the isotherm is considered to be unfavourable, linear when $R_L = 1$, favourable when $0 > R_L > 1$ or irreversible when $R_L = 0$.

The last model is the Tempkin isotherm [27, 107-110]. The main difference between these three models is in the variation of the heat of adsorption with the surface coverage. Langmuir model assumes uniformity, Freundlich isotherm assumes logarithmic decrease and Tempkin model assumes linear decrease in heat of adsorption with surface coverage.

$$q_e = k_1 \cdot \ln(k_2) + k_1 \cdot \ln(C_e) \quad (8)$$

where k_1 is the Tempkin isotherm energy constant ($l \text{ mg}^{-1}$) and k_2 is the dimensionless Tempkin isotherm constant.

The results of the fitted parameters to the adsorption isotherms are summarised in Table 5. In general, the experimental data are well correlated for all the equations. According to the fits obtained, none of those two equations can be postulated as definitely better to reproduce the equilibrium data, particularly in the case of phenol. Langmuir fitted well with all the phenol and benzene data with regression coefficients higher than 0.91. Freundlich isotherm are quite well related with for all the data except for the phenol adsorption onto AC-Na ($r^2 = 0.88$) and benzene adsorption on CAC2 ($r^2 = 0.83$). Tempkin gives goods adjustments for all the data except for the phenol adsorption on CAC1 ($r^2 = 0.89$).

The maximum adsorption capacity achieve was 33.84 mg g^{-1} for phenol in CAC3 and 21.20 mg g^{-1} in AC-Na, as it is showed in Table 5. For benzene, the maximum are 38.30 mg g^{-1} in CAC3 and 17.02 mg g^{-1} in AC-Na. These values also correspond with ones of the highest energetic heterogeneity. Respect the results obtained with the Langmuir isotherm, the maximum adsorption capacity for benzene and phenol are achieved for the AC-Na (238 mg g^{-1} and 233 mg g^{-1} , respectively). These values are all quite similar with values detailed in Table 1, presented before as a summary of the liquid adsorption test realised by several authors.

4. CONCLUSIONS

AC obtained with Kraft lignin and chemical activation with sodium hydroxide, potassium hydroxide or phosphoric acid gives as result, essentially microporous AC that adsorb larger amounts of phenol and benzene, compared with the data available in the literature.

The phenol or benzene adsorption data obtained for the AC studied correspond to a pseudo-second-order reaction with good correlations. The adsorption rate constant points to faster adsorption rates for phenol than for benzene in the AC derived from lignin except for CAC2 and CAC3 that are very similar. The AC derived from lignin presents better adsorptions capacities compared with the commercial carbons in both experiments, with phenol and benzene.

The experimental data are well correlated with the three models presented, Freundlich, Langmuir and Tempkin. According to the fits obtained, none of those three equations can be postulated as definitely better to reproduce the equilibrium data, particularly in the case of phenol. Langmuir fitted well the phenol and benzene data adsorption on all the ACs. Freundlich isotherm is quite well related with for all the data except for the phenol adsorption onto AC-Na and benzene adsorption on CAC2. Tempkin gives goods adjustments for all the data except for the phenol adsorption on CAC1.

Maximum adsorption capacity for benzene and phenol are achieved for the AC-Na (238 mg g^{-1} and 233 mg g^{-1} , respectively) that are good values compared with the ones available in the literature. The AC-K and AC-P also showed high adsorption capacities with values greater than 213 mg g^{-1} and

106 mg g⁻¹, respectively, for phenol and 213 mg g⁻¹ and 185 mg g⁻¹, respectively, for benzene.

ACKNOWLEDGEMENTS

Funding for this work was provided by the Spanish Ministry of Science and Technology (MCYT, project PPQ2002-04201-CO2-02, partially funded by the FEDER program of the European Union), and the Catalan Regional Government (Project 2005SGR-00580). This research was also partly made possible by financial support from the European Commission through the ALFA program (project LIGNOCARB-ALFA II 0412 FA FI). V. Torné-Fernández acknowledges the URV for her PhD grant. V. Fierro acknowledges the MCYT and the Universitat Rovira i Virgili (URV) for the financial support of her 'Ramón y Cajal' research contract.

REFERENCES

1. Gonzalez-Serrano, E., Cordero, T., Rodríguez-Mirasol, J., et al., Development of Porosity upon Chemical Activation of Kraft Lignin with ZnCl₂. *Industrial & Engineering Chemical Research*, 1997. 36(11): p. 4832-4838.
2. Rodríguez-Mirasol, J., Cordero, T., and Rodríguez, J.J., Preparation and characterization of activated carbons from eucalyptus kraft lignin. *Carbon*, 1993. 31(1): p. 87-95.
3. Guo, Y. and Rockstraw, D.A., Physical and chemical properties of carbons synthesized from xylan, cellulose, and Kraft lignin by H₃PO₄ activation. *Carbon*, 2006. 44(8): p. 1464-1475.
4. Fierro, V., Torné-Fernández, V., and Celzard, A., Kraft lignin as a precursor for microporous activated carbons prepared by impregnation with ortho-phosphoric acid: Synthesis and textural characterisation. *Microporous and Mesoporous Materials*, 2006. 92(1-3): p. 243-250.
5. Fierro, V., Torné-Fernández, V., and Celzard, A., Highly microporous carbons prepared by activation of Kraft lignin with KOH. *Studies in Surface Science and catalysis*, 2005: p. 607-614.
6. Fierro, V., Torné-Fernández, V., Montané, D., et al. Activated Carbons Prepared from Kraft Lignin by Phosphoric Acid Impregnation. in *Carbon'03*. 2003. Oviedo (Spain).
7. Lin, S.Y. and Lin, I.S., Lignin. *Ullmann's Encyclopedia of industrial chemistry*, ed. S.H. Barbara Elvers, Gail Schulz. Vol. A15. 1990, New York. 305-315.
8. Adler, E., Lignin chemistry-Past, Present and Future. *Wood Science Technology*, 1977. 11: p. 169-218.

9. Northey, R.A. Low-Cost Uses of Lignin, Emerging Technology of Materials and Chemicals from Biomass. in ACS Symposium Series 476. 1992. Washington D.C.
10. Sarkanen, K.V. and Ludwig, C.H., Lignins: Occurrence, Formation, Structure and Reactions. 1971, New York: Wiley-Interscience.
11. Ballerini, A., Ewert, R., and Solís, M., Utilización de Ligninas en la formulación de adhesivos para tableros contrachapados. Maderas: Ciencia y Tecnología, 1998. 1(1).
12. Crawford, D.L., Pometto, A.L., and Crawford, R.L., Production of useful modified lignin polymers by bioconversion of lignocellulose with *Streptomyces*. Biotechnology Advances, 1984. 2(2): p. 217-232.
13. Goheen, D.W. and Hoyt, C.H., Lignin. Third Edition ed. Kirk-Othmer Encyclopedia of Chemical Technology, ed. I. John Wiley & Sons. Vol. 14. 1981, New York: Wiley-Interscience. 294-313.
14. Mansilla, H., Lizama, C., Gutarra, A., et al., Tratamiento de residuos líquidos de la industria de celulosa y textil.
15. Fierro, V., Torné-Fernández, V., Montané, D., et al., Study of the decomposition of kraft lignin impregnated with orthophosphoric acid. Thermochemica Acta, 2005. 433(1-2): p. 142-148.
16. Fierro, V., Torné-Fernández, V., and Celzard, A., Methodical study of the chemical activation of Kraft lignin with KOH and NaOH. Microporous and Mesoporous Materials, 2006. Submitted.
17. Ahmadpour, A. and Do, D.D., The preparation of active carbons from coal by chemical and physical activation. Carbon, 1996. 34(4): p. 471-479.
18. Otowa, T., Nojima, Y., and Miyazaki, T., Development of KOH activated high surface area carbon and its application to drinking water purification. Carbon, 1997. 35(9): p. 1315-1319.

19. Liang, C., Wei, Z., Xin, Q., et al., Ammonia synthesis over Ru/C catalysts with different carbon supports promoted by barium and potassium compounds. *Applied Catalysis A: General*, 2001. 208(1-2): p. 193-201.
20. Lozano-Castelló, D., Lillo-Rodenas, M.A., Cazorla-Amorós, D., et al., Preparation of activated carbons from Spanish anthracite: I. Activation by KOH. *Carbon*, 2001. 39(5): p. 741-749.
21. Frackowiak, E. and Beguin, F., Electrochemical storage of energy in carbon nanotubes and nanostructured carbons. *Carbon*, 2002. 40(10): p. 1775-1787.
22. Activated carbon compendium. A collection of papers from the journal *Carbon* 1996-2000. 1^a ed, ed. H. Marsh. 2001, North Shields (UK): Elsevier.
23. Lin, S.Y., Jr., S.E.L., and LignoTech USA, I., Lignin, in *Kirk-Othmer Encyclopedia of Chemical Technology*. 2000.
24. Basso, M.C. and Cukierman, A.L., Arundo donax - Based activated carbons for aqueous-phase adsorption of volatile organic compounds. *Industrial Engineering Chemical Research*, 2005. 44: p. 2091-2100.
25. Alvarez, P.M., Garcia-Araya, J.F., Beltran, F.J., et al., Ozonation of activated carbons: Effect on the adsorption of selected phenolic compounds from aqueous solutions. *Journal of Colloid and Interface Science*, 2005. 283(2): p. 503-512.
26. Ariyadejwanich, P., Tanthapanichakoon, W., Nakagawa, K., et al., Preparation and characterization of mesoporous activated carbon from waste tires. *Carbon*, 2003. 41(1): p. 157-164.
27. Ayranci, E. and Duman, O., Adsorption behaviors of some phenolic compounds onto high specific area activated carbon cloth. *Journal of Hazardous Materials*, 2005. 124(1-3): p. 125-132.

28. Bae, S.-D., Sagehashi, M., and Sakoda, A., Activated carbon membrane with filamentous carbon for water treatment. *Carbon*, 2003. 41(15): p. 2973-2979.
29. Brasquet, C., Rousseau, B., Estrade-Szwarckopf, H., et al., Observation of activated carbon fibres with SEM and AFM correlation with adsorption data in aqueous solution. *Carbon*, 2000. 38(3): p. 407-422.
30. Chen, X., Jeyaseelan, S., and Graham, N., Physical and chemical properties study of the activated carbon made from sewage sludge. *Waste Management*, 2002. 22(7): p. 755-760.
31. de Oliveira Pimenta, A.C. and Kilduff, J.E., Oxidative coupling and the irreversible adsorption of phenol by graphite. *Journal of Colloid and Interface Science*, 2005. In Press, Corrected Proof.
32. El-Hendawy, A.-N.A., Influence of HNO₃ oxidation on the structure and adsorptive properties of corncob-based activated carbon. *Carbon*, 2003. 41(4): p. 713-722.
33. El-Hendawy, A.-N.A., Surface and adsorptive properties of carbons prepared from biomass. *Applied Surface Science*, 2005. 252(2): p. 287-295.
34. Furuya, E.G., Chang, H.T., Miura, Y., et al., A fundamental analysis of the isotherm for the adsorption of phenolic compounds on activated carbon. *Separation and Purification Technology*, 1997. 11: p. 69-78.
35. Galiatsatou, P., Metaxas, M., Arapoglou, D., et al., Treatment of olive mill waste water with activated carbons from agricultural by-products. *Waste Management*, 2002. 22(7): p. 803-812.
36. Ghiaci, M., Abbaspur, A., Kia, R., et al., Equilibrium isotherm studies for the sorption of benzene, toluene, and phenol onto organo-zeolites and as-synthesized MCM-41. *Separation and Purification Technology*, 2004. 40(3): p. 217-229.

37. Girgis, B.S. and El-Hendawy, A.-N.A., Porosity development in activated carbons obtained from date pits under chemical activation with phosphoric acid. *Microporous and Mesoporous Materials*, 2002. 52(2): p. 105-117.
38. Gonzalez-Serrano, E., Cordero, T., Rodriguez-Mirasol, J., et al., Removal of water pollutants with activated carbons prepared from H₃PO₄ activation of lignin from kraft black liquors. *Water Research*, 2004. 38(13): p. 3043-3050.
39. Hsieh, C.-T. and Teng, H., Liquid-Phase Adsorption of Phenol onto Activated Carbons Prepared with Different Activation Levels. *Journal of Colloid and Interface Science*, 2000. 230(1): p. 171-175.
40. Hsieh, C.-T. and Teng, H., Influence of mesopore volume and adsorbate size on adsorption capacities of activated carbons in aqueous solutions. *Carbon*, 2000. 38(6): p. 863-869.
41. Hu, Z. and Srinivasan, M.P., Preparation of high-surface-area activated carbons from coconut shell. *Microporous and Mesoporous Materials*, 1999. 27(1): p. 11-18.
42. Hu, Z., Srinivasan, M.P., and Ni, Y., Novel activation process for preparing highly microporous and mesoporous activated carbons. *Carbon*, 2001. 39(6): p. 877-886.
43. Juang, R.-S., Lin, S.-H., and Cheng, C.-H., Liquid-phase adsorption and desorption of phenol onto activated carbons with ultrasound. *Ultrasonics Sonochemistry*, 2005. In Press, Corrected Proof.
44. Juang, R.-S., Wu, F.-C., and Tseng, R.-L., Adsorption Isotherms of Phenolic Compounds from Aqueous Solutions onto Activated Carbon Fibers. *J. Chem. Eng. Data*, 1996. 41(3): p. 487-492.

45. Juang, R.-S., Wu, F.-C., and Tseng, R.-L., Mechanism of Adsorption of Dyes and Phenols from Water Using Activated Carbons Prepared from Plum Kernels. *Journal of Colloid and Interface Science*, 2000. 227(2): p. 437-444.
46. Juang, R.-S., Wu, F.-C., and Tseng, R.-L., Characterization and use of activated carbons prepared from bagasses for liquid-phase adsorption. *Colloids and Surfaces A: Physicochemical and Engineering Aspects*, 2002. 201(1-3): p. 191-199.
47. Katoh, M., Takao, H., Abe, N., et al., Adsorption Selectivity of FSM-16 for Several Organic Compounds. *Journal of Colloid and Interface Science*, 2001. 242(2): p. 294-299.
48. Khan, A.R., Al-Bahri, T.A., and Al-Haddad, A., Adsorption of phenol based organic pollutants on activated carbon from multi-component dilute aqueous solutions. *Water Research*, 1997. 31(8): p. 2102-2112.
49. Khan, A.R., Ataullah, R., and Al-Haddad, A., Equilibrium Adsorption Studies of Some Aromatic Pollutants from Dilute Aqueous Solutions on Activated Carbon at Different Temperatures. *Journal of Colloid and Interface Science*, 1997. 194(1): p. 154-165.
50. Khezami, L., Chetouani, A., Taouk, B., et al., Production and characterisation of activated carbon from wood components in powder: Cellulose, lignin, xylan. *Powder Technology*, 2005. In Press, Corrected Proof.
51. Klimenko, N., Winther-Nielsen, M., Smolin, S., et al., Role of the physico-chemical factors in the purification process of water from surface-active matter by biosorption. *Water Research*, 2002. 36(20): p. 5132-5140.
52. Koh, M. and Nakajima, T., Adsorption of aromatic compounds on CxN-coated activated carbon. *Carbon*, 2000. 38(14): p. 1947-1954.

53. Koh, S.-M. and Dixon, J.B., Preparation and application of organo-minerals as sorbents of phenol, benzene and toluene. *Applied Clay Science*, 2001. 18(3-4): p. 111-122.
54. Kumar, A., Kumar, S., and Kumar, S., Adsorption of resorcinol and cathecol on granular activated carbon: equilibrium and kinetics. *Carbon*, 2003. 41: p. 3015-3025.
55. Laszlo, K., Bota, A., Nagy, L.G., et al., Porous carbon from polymer waste materials. *Colloids and Surfaces A: Physicochemical and Engineering Aspects*, 1999. 151(1-2): p. 311-320.
56. Laszlo, K., Bota, A., and Nagy, L.G., Characterization of activated carbons from waste materials by adsorption from aqueous solutions. *Carbon*, 1997. 35(5): p. 593-598.
57. Laszlo, K. and Szucs, A., Surface characterization of polyethyleneterephthalate (PET) based activated carbon and the effect of pH on its adsorption capacity from aqueous phenol and 2,3,4-trichlorophenol solutions. *Carbon*, 2001. 39(13): p. 1945-1953.
58. Lee, K.M. and Lim, P.E., Bioregeneration of powdered activated carbon in the treatment of alkyl-substituted phenolic compounds in simultaneous adsorption and biodegradation processes. *Chemosphere*, 2005. 58(4): p. 407-416.
59. Leng, C.-C. and Pinto, N.G., Effects of surface properties of activated carbons on adsorption behavior of selected aromatics. *Carbon*, 1997. 35(9): p. 1375-1385.
60. Moreno-Castilla, C., Rivera-Utrilla, J., López-Ramón, M.V., et al., Adsorption of some substituted phenols on activated carbons from a bituminous coal. *Carbon*, 1995. 33(6): p. 845-851.
61. Nakagawa, K., Namba, A., Mukai, S.R., et al., Adsorption of phenol and reactive dye from aqueous solution on activated carbons derived from solid wastes. *Water Research*, 2004. 38(7): p. 1791-1798.

62. Namane, A., Mekarzia, A., Benrachedi, K., et al., Determination of the adsorption capacity of activated carbon made from coffee grounds by chemical activation with $ZnCl_2$ and H_3PO_4 . *Journal of Hazardous Materials*, 2005. 119(1-3): p. 189-194.
63. Nevskaja, D.M., Castillejos-Lopez, E., Guerrero-Ruiz, A., et al., Effects of the surface chemistry of carbon materials on the adsorption of phenol-aniline mixtures from water. *Carbon*, 2004. 42(3): p. 653-665.
64. Nevskaja, D.M., Santianes, A., Munoz, V., et al., Interaction of aqueous solutions of phenol with commercial activated carbons: an adsorption and kinetic study. *Carbon*, 1999. 37(7): p. 1065-1074.
65. Nevskaja, D.M., Santianes, A., Muñoz, V., et al., Interaction of aqueous solutions of phenol with commercial activated carbons: an adsorption and kinetic study. *Carbon*, 1999. 37: p. 1065-1074.
66. Okolo, B., Park, C., and Keane, M.A., Interaction of Phenol and Chlorophenols with Activated Carbon and Synthetic Zeolites in Aqueous Media. *Journal of Colloid and Interface Science*, 2000. 226(2): p. 308-317.
67. Otero, M., Rozada, F., Calvo, L.F., et al., Elimination of organic water pollutants using adsorbents obtained from sewage sludge. *Dyes and Pigments*, 2003. 57(1): p. 55-65.
68. Otero, M., Zabkova, M., and Rodrigues, A.E., Adsorptive purification of phenol wastewaters: Experimental basis and operation of a parametric pumping unit. *Chemical Engineering Journal*, 2005. 110(1-3): p. 101-111.
69. Podkoscielny, P., Dabrowski, A., and Marijuk, O.V., Heterogeneity of active carbons in adsorption of phenol aqueous solutions. *Applied Surface Science*, 2003. 205(1-4): p. 297-303.

70. Rio, S., Faur-Brasquet, C., Coq, L.L., et al., Experimental design methodology for the preparation of carbonaceous sorbents from sewage sludge by chemical activation--application to air and water treatments. *Chemosphere*, 2005. 58(4): p. 423-437.
71. Roostaei, N. and Tezel, F.H., Removal of phenol from aqueous solutions by adsorption. *Journal of Environmental Management*, 2004. 70(2): p. 157-164.
72. Sabio, E., González-Martín, M.L., Ramiro, A., et al., Influence of the regeneration temperature on the phenols adsorption on activated carbon. *Journal of Colloid and Interface Science*, 2001. 242: p. 31-35.
73. Salame, I.I. and Bandosz, T.J., Role of surface chemistry in adsorption of phenol on activated carbons. *Journal of Colloid and Interface Science*, 2003. 264(2): p. 307-312.
74. San Miguel, Guillermo, Fowler, G.D., and Sollars, C.J., A study of the characteristics of activated carbons produced by steam and carbon dioxide activation of waste tyre rubber. *Carbon*, 2003. 41(5): p. 1009-1016.
75. Shu, H.-T., Li, D., Scala, A.A., et al., Adsorption of small organic pollutants from aqueous streams by aluminosilicate-based microporous materials. *Separation and Purification Technology*, 1997. 11(1): p. 27-36.
76. Singh, B., Madhusudhanan, S., Dubey, V., et al., Active carbon for removal of toxic chemicals from contaminated water. *Carbon*, 1996. 34(3): p. 327-330.
77. Streat, M., Patrick, J.W., and Perez, M.J.C., Sorption of phenol and para-chlorophenol from water using conventional and novel activated carbons. *Water Research*, 1995. 29(2): p. 467-472.
78. Tai, H.-S. and Jou, C.-J.G., Application of granular activated carbon packed-bed reactor in microwave radiation field to treat phenol. *Chemosphere*, 1999. 38(11): p. 2667-2680.

79. Tamon, H., Atsushi, M., and Okazaki, M., On Irreversible Adsorption of Electron-Donating Compounds in Aqueous Solution. *Journal of Colloid and Interface Science*, 1996. 177(2): p. 384-390.
80. Tancredi, N., Medero, N., Moller, F., et al., Phenol adsorption onto powdered and granular activated carbon, prepared from Eucalyptus wood. *Journal of Colloid and Interface Science*, 2004. 279(2): p. 357-363.
81. Tanthapanichakoon, W., Ariyadejwanich, P., Japthong, P., et al., Adsorption-desorption characteristics of phenol and reactive dyes from aqueous solution on mesoporous activated carbon prepared from waste tires. *Water Research*, 2005. 39(7): p. 1347-1353.
82. Terzyk, A.P., Molecular properties and intermolecular forces--factors balancing the effect of carbon surface chemistry in adsorption of organics from dilute aqueous solutions. *Journal of Colloid and Interface Science*, 2004. 275(1): p. 9-29.
83. Tryba, B., Morawski, A.W., and Inagaki, M., Application of TiO₂-mounted activated carbon to the removal of phenol from water. *Applied Catalysis B: Environmental*, 2003. 41(4): p. 427-433.
84. Tseng, R.-L., Wu, F.-C., and Juang, R.-S., Liquid-phase adsorption of dyes and phenols using pinewood-based activated carbons. *Carbon*, 2003. 41(3): p. 487-495.
85. Villacanas, F., Pereira, M.F.R., Orfao, J.J.M., et al., Adsorption of simple aromatic compounds on activated carbons. *Journal of Colloid and Interface Science*, 2005. In Press, Corrected Proof.
86. Warhurst, A.M., McConnachie, G.L., and Pollard, S.J.T., Characterisation and applications of activated carbon produced from *Moringa oleifera* seed husks by single-step steam pyrolysis. *Water Research*, 1997. 31(4): p. 759-766.

87. Wu, F.-C. and Tseng, R.-L., Preparation of highly porous carbon from fir wood by KOH etching and CO₂ gasification for adsorption of dyes and phenols from water. *Journal of Colloid and Interface Science*, 2005. In Press, Corrected Proof.
88. Wu, F.-C., Tseng, R.-L., and Hu, C.-C., Comparisons of pore properties and adsorption performance of KOH-activated and steam-activated carbons. *Microporous and Mesoporous Materials*, 2005. 80(1-3): p. 95-106.
89. Wu, F.-C., Tseng, R.-L., Hu, C.-C., et al., Physical and electrochemical characterization of activated carbons prepared from firwoods for supercapacitors. *Journal of Power Sources*, 2004. 138: p. 351-359.
90. Wu, F.-C., Tseng, R.-L., and Juang, R.-S., Pore structure and adsorption performance of the activated carbons prepared from plum kernels. *Journal of Hazardous Materials*, 1999. 69(3): p. 287-302.
91. Wu, F.-C., Tseng, R.-L., and Juang, R.-S., Preparation of highly microporous carbons from fir wood by KOH activation for adsorption of dyes and phenols from water. *Separation and Purification Technology*, 2005. In Press, Corrected Proof.
92. Wu, F.-C., Tseng, R.-L., and Juang, R.-S., Comparisons of porous and adsorption properties of carbons activated by steam and KOH. *Journal of Colloid and Interface Science*, 2005. 283(1): p. 49-56.
93. Hindarso, H., Ismadji, S., Wicaksana, F., et al., Adsorption of benzene and toluene from aqueous solution onto granular activated carbon. *Journal of Chemical and Engineering Data*, 2001. 46(4): p. 788-791.
94. Toles, C.A., Marshall, W.E., and Johns, M.M., Granular activated carbons from nutshells for the uptake of metals and organic compounds. *Carbon*, 1997. 35(9): p. 1407-1414.

95. Toles, C.A., Marshall, W.E., Johns, M.M., et al., Acid-activated carbons from almond shells: physical, chemical and adsorptive properties and estimated cost of production. *Bioresource Technology*, 2000. 71(1): p. 87-92.
96. Chiou, C.T., Porter, P.E., and Schmedding, D.W., Partition equilibriums of nonionic organic compounds between soil organic matter and water. *Environmental science and technology*, 1983. 17(4): p. 227-231.
97. Chatzopoulos, D. and Varma, A., Aqueous-phase adsorption and desorption of toluene in activated carbon fixed beds: Experiments and model. *Chemical Engineering Science*, 1995. 50(1): p. 127-141.
98. Lillo-Rodenas, M.A., Cazorla-Amorós, D., and Linares-Solano, A., Behaviour of activated carbons with different pore size distributions and surface oxygen groups for benzene and toluene adsorption at low concentrations. *Carbon*, 2005. 43(8): p. 1758-1767.
99. Lillo-Rodenas, M.A., Cazorla-Amorós, D., and Linares-Solano, A., Behaviour of activated carbons with different pore size distributions and surface oxygen groups for benzene and toluene adsorption at low concentrations. *Carbon*, 2005. 43(8): p. 1758-1767.
100. Dimotakis, E.D., Cal, M.P., Economy, J., et al., Chemically Treated Activated Carbon Cloths for Removal of Volatile Organic Carbons from Gas Streams: Evidence for Enhanced Physical Adsorption. *Environmental Science and Technology*, 1995. 29(7): p. 1876-1880.
101. Benkhedda, J., Jaubert, J.-N., Barth, D., et al., Experimental and Modeled Results Describing the Adsorption of Toluene onto Activated Carbon. *J. Chem. Eng. Data*, 2000. 45(4): p. 650-653.
102. Inc., N.A., www.norit-america.com.
103. Rouquerol, F., Rouquerol, J., and Sing, K.S.W., *Adsorption by Powders and Porous Solids. Principles, Methods and Applications*. 1999, San Diego: Academic Press.

104. Setoyama, N., Suzuki, T., and Kaneko, K., Simulation study on the relationship between a high resolution [alpha]s-plot and the pore size distribution for activated carbon. *Carbon*, 1998. 36(10): p. 1459-1467.
105. Kruk, M., Li, Z., Jaroniec, M., et al., Nitrogen Adsorption Study of Surface Properties of Graphitized Carbon Blacks. *Langmuir*, 1999. 15(4): p. 1435-1441.
106. Fogler, H.S., Elements of chemical reaction engineering. 2nd edition ed. 1992, New Jersey: Prentice-Hall, Inc.
107. Lei, S., Miyamoto, J.-I., Kanoh, H., et al., Enhancement of the methylene blue adsorption rate for ultramicroporous carbon fiber by addition of mesopores. *Carbon*, 2006. In Press, Corrected Proof.
108. Sathishkumar, M., Binupriya, A.R., Kavitha, D., et al., Kinetic and isothermal studies on liquid-phase adsorption of 2,4-dichlorophenol by palm pith carbon. *Bioresource Technology*, 2006. In Press, Corrected Proof.
109. Bridelli, M.G., Ciati, A., and Crippa, P.R., Binding of chemicals to melanins re-examined: Adsorption of some drugs to the surface of melanin particles. *Biophysical Chemistry*, 2006. 119(2): p. 137-145.
110. Chen, B., Hui, C.W., and McKay, G., Film-Pore Diffusion Modeling for the Sorption of Metal Ions from Aqueous Effluents onto Peat. *Water Research*, 2001. 35(14): p. 3345-3356.
111. Bartholomew, C.H., Mechanisms of catalyst deactivation. *Applied Catalysis A: General*, 2001. 212(1-2): p. 17-60.

Sorption study of organic compounds on highly microporous carbons prepared from Kraft lignin.

V. Torné-Fernández, V. Fierro.

Table 1. State of the art in the phenol and benzene adsorptions on different materials in liquid systems.

Type of AC	Activating agent	Co (ppm)	m _{AC} (mg)	S _{BET} (m ² /g)	V _{microp} (cm ³ /g)	q _{Ph} q _B		Ref.
						(mg/g)		
AC with microorganism		1000	1000			188.2		[24]
AC		800				75.8		[25]
		100	100	803	-	24.0	39.0	[26]
ACF		100	500			160.0		[27]
Almond shells	H ₃ PO ₄	80	100	1416	-		9.0	[28]
Arundo-donax	H ₃ PO ₄	78	200	1194	0.660		22.7	[23]
Bagasses	Vapour		600			308.0		[29]
Bitumen			100	1114	0.130	218.0		[30]
	CO ₂	500	1200			240.0		[31]
Charsorb CP-1300			200	-	-	156.0		[32]
Coffee grain		20				3.5		[33]
Comercial	-					10.6		[34]
Carbon		>300	50			197.6		[35]
		500	800			221.5		[36]
						451.7		[37]
			100	982	0.304	291.7		[38]
		250		1790	0.773	300.0		[39]
		200				309.0		[40]
		50	300			74.2		[41]
		500	1200			131.8		[42]
		100	50			190.0		[43]
		2000	500			142.9		[44]
		5 · 10 ⁶				301.2		[45]
		998	2500			188.2		[46]
			50			258.8		[47]
		400	50000			220.0		[48]
		235	100			207.4		[49]
			100			80.0		[50]
		250				205.0		[51]
			2000			188.2		[52]
		1505	100	1654	0.651	131.8		[53]

		941	50	-	-	117.6		[54]
		550	800	900	-		221.5	[55]
Coconut shell		498.8	1000			141.2		[56]
		998	1000			178.8		[56]
		47	50			45.7		[57]
	ZnCl ₂	200	50			210.0		[58]
	Vapour	1600	100			571.0		[59]
Corn cobs	KOH		50			153.0		[60]
	Vapour	1000	50			178.2		[61]
Date pits	H ₃ PO ₄	100	200			166.0		[62]
Eucalyptus wood		200	100			148.0		[63]
Filtratorb F400		500				169.1		[65]
Firwood		94110	100			240.6		[66]
	Vapour	94110	100	1131	0.056	831.0		[67]
	KOH	200	600			23.1		[68]
	KOH	94	100			257.9		[69]
	Vapour		100			255.9		[69]
	KOH+CO ₂	200	600			274.8		[70]
Garbage waste	Vapour			700	0.280	300.0		[71]
Grain shells			100			209.2		[72]
Graphite			100	310	0.057	85.6		[38]
		1000				4.0		[73]
Hydro-Anthrasit H		1000		1090	-	112.9	258.0	[74]
Lignin	H ₃ PO ₄		10	1459	0.820	170.0		[75]
Molecular sieves		110	100	-	-	59.4	112.9	[76]
Moringa oleifera seed husks		4706	500			235.3		[77]
Olive mill	Vapour+N ₂	1500	200			91.7		[78]
Pecan shell	H ₃ PO ₄	80	100	1267	-		7.8	[79]
PET	Vapour		100			263.5		[80]
	N ₂	470	50			225.9		[81]
Pistachio	KOH	94	100			285.2		[69]
	Vapour	94	100			242.8		[69]
		94110	100			728.3		[82]
Plum kernels		376				257.0		[83]
			100	1160	-	257.4		[84]
Pneumatics						180.0		[85]
			60			200.0		[86]
Rubber	Vapor/CO ₂ +N ₂	235	600			106.0		[87]
Sludge	H ₂ SO ₄	100	500	3	-	54.0		[88]
	H ₂ SO ₄	100				42.0		[89]
Soil		1600		-	-	0.5		[90]
Straw		100	500			197.6		[91]
Wood		100	30			320.0		[92]

Sorption study of organic compounds on highly microporous carbons prepared from Kraft lignin.

V. Torné-Fernández, V. Fierro.

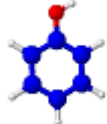
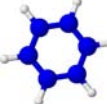
Table 2. Physical properties of the AC used.

	S_{BET}	$V_{0.99}$	$V_{\alpha,\text{micro}}$	$V_{\alpha,\text{super}}$	V_{meso}	Acidic Groups (meq H ⁺ /gAC)	Basic Groups (meq OH ⁻ /gAC)
	(m ² /g)	(cm ³ /g)					
AC-Na	2340	1.338	1.018	0.941	0.428	11.9	16.6
AC-K	2920	1.583	1.332	1.324	0.384	20.4	5.8
AC-P	940	0.442	0.377	0.261	0.118	7.5	0.2
CAC1	1350	0.713	0.458	0.319	0.235	2.6	0.5
CAC2	620	0.637	0.185	0.100	0.407	7.9	1.2
CAC3	1020	0.625	0.334	0.182	0.246	5.0	2.1

Sorption study of organic compounds on highly microporous carbons prepared from Kraft lignin.

V. Torné-Fernández, V. Fierro.

Table 3. Properties of adsorptive molecules.

Molecule	Structure	MW ^a (g/mol)	P _v ^b (mmHg)	T _b ^c (°C)	Solubility (%)	Size ^d (Å)
Ph		94.1	0.4	182	8.3	6
B		78.1	100.8	80.1	0.2	5

MW^a. Molecular weight.

P_v^b. Vapour pressure at 25°C.

T_b^c. Normal boiling point.

Size^a. Size calculated with ACDLABS 8.0.

Sorption study of organic compounds on highly microporous carbons prepared from Kraft lignin.

V. Torné-Fernández, V. Fierro.

Table 4. Kinetic parameters estimated in the adsorption of phenol or benzene on different adsorbates for an initial concentration of 100 ppm.

Adsorbate	General order n (equation 3)				Pseudo-second order (equation 4)
	n	k (g mg ⁻¹ min ⁻¹)	r ²	q _{e,max} (mg g ⁻¹)	k' (g mg ⁻¹ min ⁻¹)
Solute: Phenol					
AC-Na	2.4	7.24	0.98	169.2	5.16
AC-K	2.4	1.30	0.96	165.0	1.54
AC-P	2.1	1.19	0.96	60.6	1.24
CAC1	2.5	2.78	0.97	95.7	3.15
CAC2	2.0	0.11	0.99	74.4	0.46
CAC3	2.2	0.02	0.95	95.3	0.42
Solute: Benzene					
AC-Na	2.1	0.65	0.95	20.1	0.72
AC-K	1.7	0.34	0.98	19.7	0.13
AC-P	2.2	0.40	0.99	7.9	0.56
CAC1	2.3	0.20	0.94	10.6	0.37
CAC2	2.5	0.17	0.96	8.2	0.39
CAC3	2.5	0.07	0.96	9.5	0.49

Sorption study of organic compounds on highly microporous carbons prepared from Kraft lignin.

V. Torné-Fernández, V. Fierro.

Table 5. Isotherms constants for phenol and benzene sorption onto different AC.

	Freundlich			Langmuir				Tempkin		
	k_f	n	r^2	Q_0	b	R_L	r^2	k_1	k_2	r^2
Phenol										
AC-Na	21.20	2.08	0.99	238.10	0.004	0.7	0.97	37.93	0.57	0.97
AC-K	12.96	1.46	0.96	212.77	0.005	0.7	0.97	48.25	0.39	0.98
AC-P	11.73	2.26	0.95	106.38	0.009	0.5	0.97	24.69	0.30	0.96
CAC1	32.48	3.60	0.91	105.26	0.009	0.5	0.98	19.58	2.62	0.89
CAC2	24.58	4.38	0.97	73.53	0.014	0.4	0.98	12.27	2.75	0.98
CAC3	33.84	3.09	0.94	135.14	0.007	0.6	0.98	26.44	1.76	0.97
Benzene										
AC-Na	17.02	1.83	0.99	232.558	0.004	0.7	0.99	48.845	0.37	0.98
AC-K	11.63	1.51	0.99	212.77	0.005	0.7	0.97	45.36	0.33	0.98
AC-P	5.70	1.59	0.97	185.19	0.005	0.7	0.85	39.00	0.12	0.93
CAC1	32.90	2.25	0.93	212.77	0.005	0.7	0.93	39.81	1.45	0.98
CAC2	17.40	2.34	0.99	76.92	0.013	0.4	0.97	22.94	0.78	0.96
CAC3	38.30	2.44	0.93	175.44	0.006	0.6	0.99	36.85	1.82	0.93

Captions of the figures

Figure 1. Experimental data for phenol adsorption kinetic on different AC obtained at 25°C with a initial 100 ppm solution.

Figure 2. Experimental data for benzene adsorption kinetic on different AC obtained at 25°C with a initial 100 ppm solution.

Figure 3. Adsorption capacities for phenol and benzene on different AC related with the supermicropore and mesoporo volume.

Figure 4. Adsorption isotherm for phenol on different ACs at 25°C and its fitted Langmuir isotherm.

Figure 5. Adsorption isotherm for benzene on different ACs at 25°C and its fitted Langmuir isotherm.

Sorption study of organic compounds on highly microporous carbons prepared from Kraft lignin.

V. Torné-Fernández, V. Fierro.

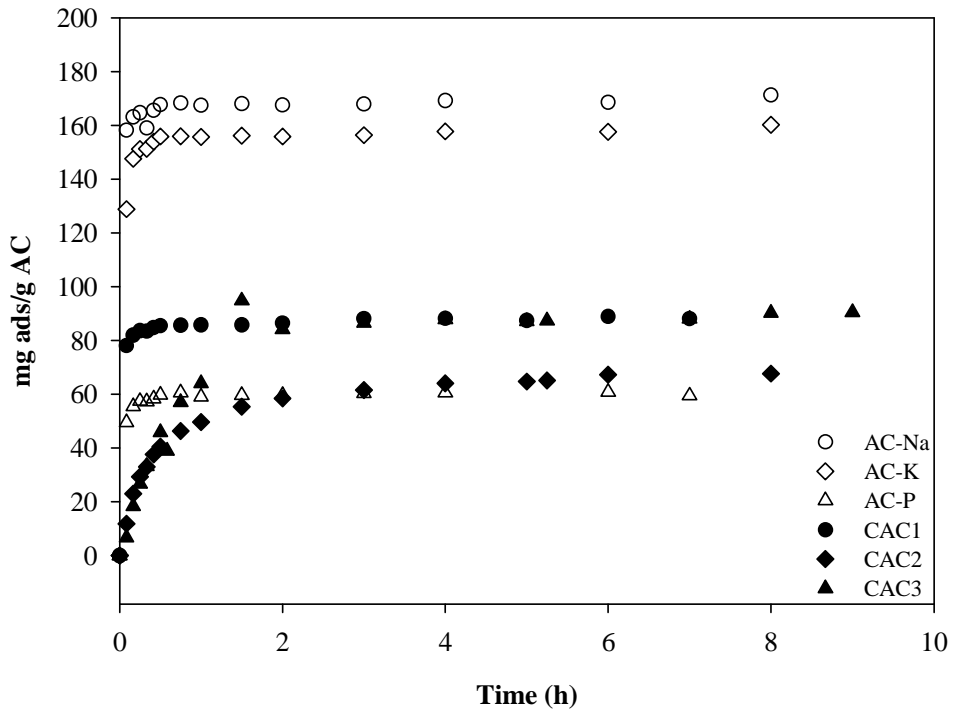


Figure 1
Torné-Fernández, V.; et.al

Sorption study of organic compounds on highly microporous carbons prepared from Kraft lignin.

V. Torné-Fernández, V. Fierro.

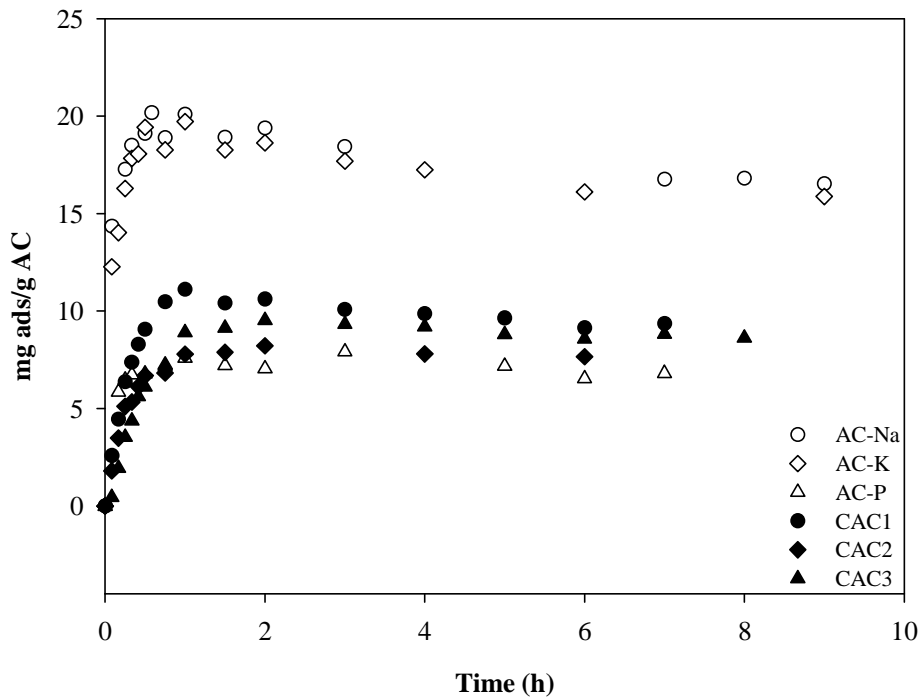


Figure 2
Torné-Fernández, V.; et.al

Sorption study of organic compounds on highly microporous carbons prepared from Kraft lignin.

V. Torné-Fernández, V. Fierro.

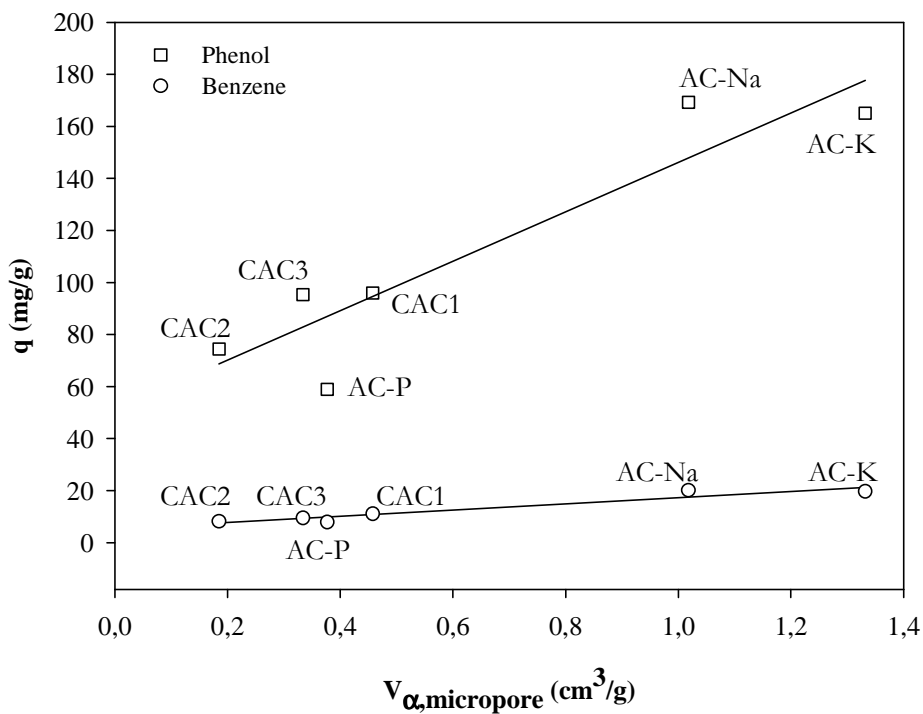


Figure 3
Torné-Fernández, V.; et.al

Sorption study of organic compounds on highly microporous carbons prepared from Kraft lignin.

V. Torné-Fernández, V. Fierro.

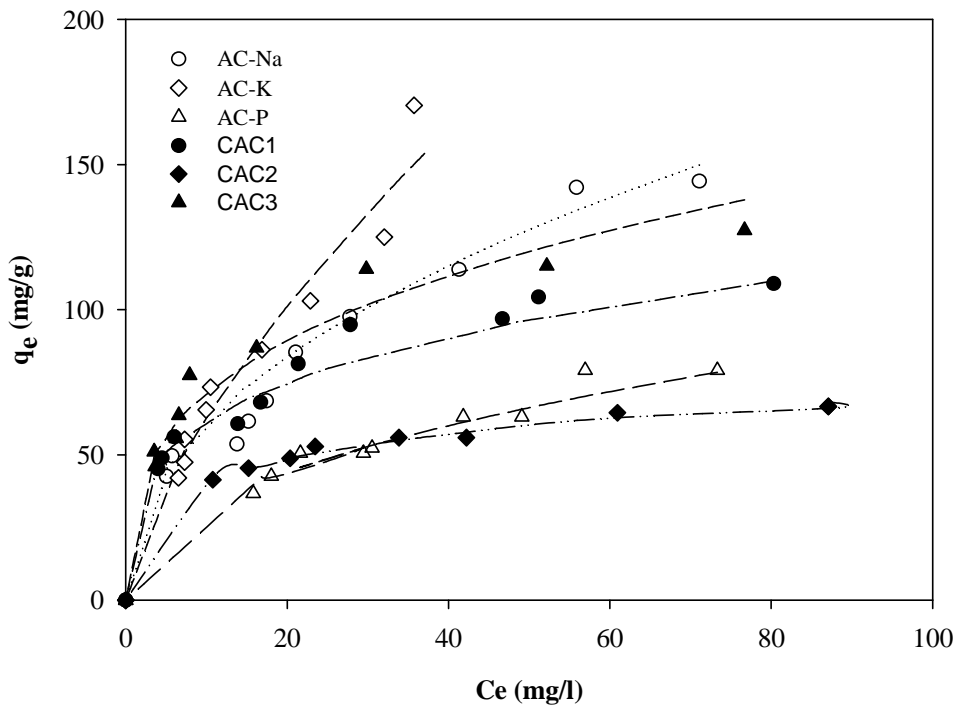


Figure 4
Torné-Fernández, V.; et.al

Sorption study of organic compounds on highly microporous carbons prepared from Kraft lignin.

V. Torné-Fernández, V. Fierro.

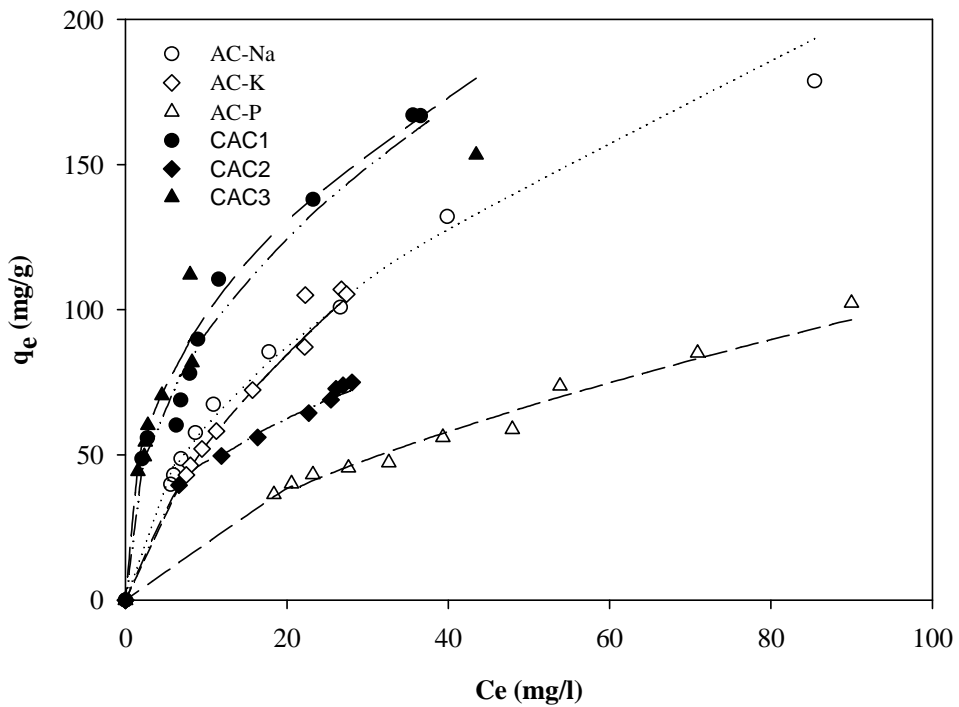


Figure 5
Torné-Fernández, V.; et.al

5.2.4. Polymeric composite membranes based on carbon/PSf

Este artículo se ha publicado en Journal of Membrana Science en 2006 en el volumen 273, páginas 38 a 46.

Otros trabajos relacionados se presentan en el Anexo F donde se presenta el póster “Enzymatic composite membranes based on carbon/polysulfone” publicado en el congreso Engineering with membranes: medical and biological applications.



Available online at www.sciencedirect.com



Journal of Membrane Science 273 (2006) 38–46

Journal of
MEMBRANE
SCIENCE

www.elsevier.com/locate/memsci

Polymeric composite membranes based on carbon/PSf

C. Torras, V. Torné, V. Fierro, D. Montané, R. Garcia-Valls*

*Grup de Biopolímers Vegetals, Departament d'Enginyeria Química, Universitat Rovira i Virgili,
Av. Països Catalans 26, 43007 Tarragona, Catalonia, Spain*

Received 30 June 2005; received in revised form 30 September 2005; accepted 6 October 2005
Available online 29 November 2005

Abstract

Enzymatic membrane reactors were obtained from polymeric membranes and activated carbon, and used for oligosaccharide purification. The activated carbon was used to adsorb the enzyme, directly or via a metal ion as intermediate. We studied the adsorption capacity of two activated carbons (a commercial carbon and a home-made one) and the formation of the complex. In a second step, we studied the activity of the enzymes in batch experiments, and analyzed the synthesis and performance of the membrane reactors. Different kinds of enzymatic membrane reactors were obtained with immobilized solid enzymes. Our results show good agreement between the kinetics of the reactions and the velocity of the flux across the membrane, since both reaction and separation were properly achieved. We also determined optimum amounts of enzyme for obtaining the desired products with a low degree of polymerization and low concentrations of monomer.
© 2005 Elsevier B.V. All rights reserved.

Keywords: Enzymatic membrane reactor; Activated carbon; Oligosaccharides

1. Introduction

Process intensification, in which two unit operations are combined in a single step, is one of the most promising lines of research in chemical engineering. In the area of membrane research, this concept means that the reaction and separation/purification steps are combined in a new single unit. Thanks to their expected selectivity, enzymatic membrane reactors (EMR) offer great potential in this area. In addition to the intrinsic advantages of these systems, the process is continuous, the catalyst component can be re-used and a permeate free of this compound is obtained [1,2].

EMRs include a membrane that holds an active enzyme either by light or by strong bonding. In this project we have used a carbon/PSf composite membrane. The carbon acts as the base surface on which the enzyme bonds [3]. The carbon can hold the enzyme by one of two methods: by holding a metal ion as an intermediate (as IMACS [4]) or by adsorbing the enzyme directly onto the carbon surface. When the metal is used, activated carbons, whose structure is highly microporous, are able

to complexate Cu(II) ions that will act as the intermediate component in an IMAC-like structure.

Several publications related to protein binding due to adsorption processes can be found in the literature. Salins et al. [5] published an interesting application of this technique to a biological process. This technique has also been applied to membranes [6,7].

2. Experimental

Three types of enzyme membrane reactors were obtained. One contained solid enzyme, which was trapped between two membrane layers (without chemical bonds). The other two were prepared with an enzymatic liquid solution, and the enzyme was bound to the activated carbon or to the pair-activated carbon–metal system (to obtain a complex). The difference between these last two reactors was the number of layers of the composite membrane. The monolayer EMR was obtained by adding the complex to the polymeric solution, thus obtaining a homogeneous layer. The two-layer EMR was obtained by adding the complex over the top of the surface of the polymeric film (after casting) before precipitation in the coagulation bath and before the membrane is obtained. Fig. 1 shows schematically these three configurations.

* Corresponding author. Tel.: +34 977 55 96 11.

E-mail address: ricard.garcia@urv.net (R. Garcia-Valls).

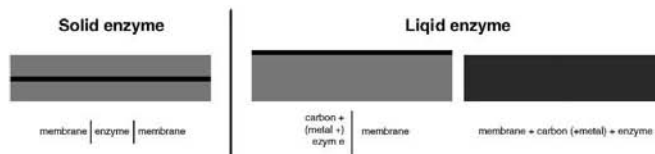


Fig. 1. Scheme of the three types of enzymatic membrane reactor synthesized.

2.1. Membrane synthesis

Membranes were obtained by immersion precipitation (phase inversion) from a polymeric mixture comprising 20% weight of polysulfone (Sigma–Aldrich, Spain) in di-methyl formamide (DMF, Panreac, Spain) as solvent [8]. The polymer was dissolved after 24 h of controlled atmosphere and agitation. The coagulation bath comprised 50% v demineralised water and 50% v DMF. When composite monolayer membranes were obtained, the complex was also added to the polymeric solution with a composition of 0.9%.

The polymeric film was obtained using a casting knife with a thickness of 200 μm applied over a glass support with a controlled and constant velocity using a K-Paint Applicator (R.K. Print Coat Instruments Ltd., United Kingdom).

2.2. Activated carbon

Two kinds of activated carbons were used. One of these was prepared in our laboratories and the other was a Norit Darco 12X40 from Norit Americas Inc. In our laboratories the activated carbon was prepared by phosphoric acid activation (an 85% H_3PO_4 solution from Panreac, Spain) of Kraft lignin (provided by Lignotech Iberica S.A.) by varying the carbonization temperature (400–650 $^\circ\text{C}$) and with a weight ratio of phosphoric acid to lignin of P/L = 0.7–1.75 [9]. Surface area and pore size characterization were performed using a Micromeritics ASAP2020 gas adsorption surface area analyzer. The specific surface area of the samples was determined from the nitrogen isotherms at $-196\text{ }^\circ\text{C}$ and the BET equation. Micropore volume was determined from the t-plot, mesopore volume from the BJH equation and total volume of pores was calculated with a relative pressure (p/p_0) of 0.99.

2.3. Metal

The metal ion used as intermediate in the IMAC-like structures was copper from a solution of $\text{CuCl}_2 \cdot 2\text{H}_2\text{O}$ (Sigma–Aldrich, Spain) with a purity of 99.9% ACS. To study the adsorption capacity of the activated carbon to the metal, an atomic adsorption spectrophotometer (Perkin-Elmer, Spectrometer 3110) was used to determine the copper concentration in solutions. The experiments were carried out by preparing several solutions containing the activated carbon and the metal solution in stirred agitation, and by keeping the temperature and pH constant and controlled. A water bath was used at 25 $^\circ\text{C}$ and the pH

was kept constant at 5 using a basic solution of NaOH 0.5 M (Panreac, Spain).

2.4. Enzymes

We used two kinds of enzymes: a solid enzyme made up of 1,4-beta-xylanase from Sigma–Aldrich (2500 U/g) and a liquid solution made up of a mixture of enzymes (including arabanase, cellulase, β -glucanase, hemi-cellulase and xylanase) from Sigma–Aldrich. To obtain the complex with the liquid enzyme, solutions containing the activated carbon or the activated carbon–metal system, and the enzyme solution were agitated for controlled periods.

2.5. Experimental device

Enzymatic membrane reactors were tested in an experimental system containing a pump piston, a surge suppressor, a back-pressure controller (to keep the pressure constant) and a circular flat membrane module with an effective membrane area of 15 cm^2 . The pressure was fixed at 9 bars. Fig. 2 shows the experimental device (Fig. 2a) and the membrane module (Fig. 2b).

Two different oligosaccharides solutions were tested. A real sample mixture of oligosaccharides obtained in the laboratory by acid hydrolysis from nutshells for the EMR containing the solid enzyme, and a commercial dextrane (Leuconostec, Fluka) of 200 kDa with a concentration of 1 g/L approximate for the EMR containing the liquid enzyme. Oligosaccharides and dextran analysis were performed by gel permeation chromatography (Agilent). A PWXL SS, 12 μm precolumn (Teknokroma, Spain) and a G3000PwXL, SS, 6 μm column (Teknokroma, Spain) were used at 25 $^\circ\text{C}$. A refractive index detector was used at 30 $^\circ\text{C}$ and the mobile phase was a 0.05 M KNO_3 (Panreac, Spain) solution.

In this paper, the results are presented in chromatographic formats related to the logarithm of mass. Table 1 shows the

Table 1
 Relation between the size of several compounds and their logarithm of mass

Compound	Logarithm of mass	Compound (kDa)	Logarithm of mass
Monomer	2.256	Dextrane 12	4.064
Polymer DP=3	2.703	Dextrane 50	4.687
Polymer DP=6	2.996	Dextrane 150	5.169
Dextrane 1 kDa	3.104		

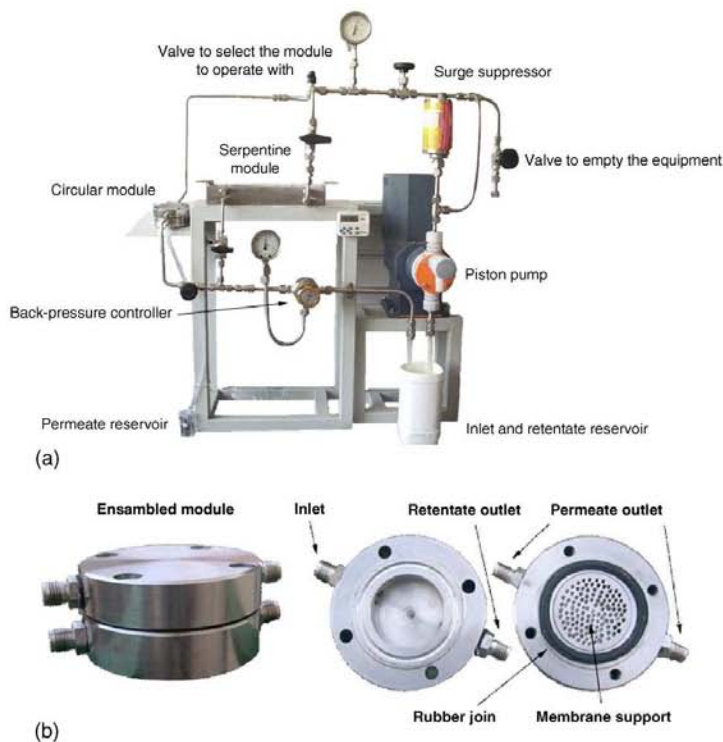


Fig. 2. (a) Experimental device. (b) Membrane module.

equivalence between this number and the size of several compounds.

3. Results and discussion

3.1. Enzymatic activity

3.1.1. Activity of the solid enzyme

The test fluid used to determine the activity of the xylanases (solid enzyme) was a mixture of oligosaccharides obtained by acid hydrolysis from nutshells. Two enzyme concentrations were tested in batch experiments and for each concentration the kinetics were studied. The concentrations considered were 80, 40, 10, 2 and 0.5 g/L. Fig. 3 shows the results for each concentration, as well as the GPC signal of oligosaccharides at several times. We can see that when the enzyme concentration decreases, the activity also decreases. When the activity is high, the main product obtained corresponds to the monomer saccharide. This is the least interesting compound since there are easier ways to obtain it, e.g. hydrolysis at high temperature. The most interesting compounds, which are the most difficult ones to obtain, are those with a low and controlled degree of polymerization, such as the dimer and trimer, etc. These compounds are obtained when the enzyme activity is low.

When checking the kinetics of the reaction (Fig. 4), we found that a high percentage of monomer production was carried out in the first few minutes of the reaction. This is interesting because, ideally, the velocity of the reaction should agree with the velocity of the flux across the membrane.

3.1.2. Activity of the liquid enzyme

The test fluid used to evaluate the activity of the liquid enzyme contained a 200 kDa commercial dextrane. As in the previous case, several enzyme concentrations were tested in batch experiments: 100, 10, 2 and 0.44 mL/L. Fig. 5 shows the chromatographic results related to the enzyme and to the dextrans at several times, for the lowest concentrations.

From the reaction we can see that the signals corresponding to the products of the reaction increase with time. This indicates that the reaction occurs, though at a slow rate. Also, our results indicate that the concentration of the enzyme in this case is not a critical factor since the reaction rate is similar in all cases.

3.2. Adsorption capability of the activated carbons

The optimal conditions for the home-made activated carbon were already determined in a previous study [10]. In that study, the adsorption results were best with activated carbon produced

at a carbonization temperature of 450 °C and a phosphoric acid to lignin ratio of P/L = 1.4. We studied how three variables influenced the commercial carbon: the concentration of the metal in solution, the agitation time (24 and 48 h) and the particle size. The particle size of the home-made activated carbon was between 30 and 100 μm. The particles of the commercial carbon were therefore ground and sieved in order to also obtain particles of similar size to those produced in the lab.

Before the activated carbons were tested and their surface characteristics were determined (see Table 2).

These results show that there are small discrepancies between the results provided by the manufacturer and those obtained with the BET. These discrepancies could be due to differences in measurement conditions and type of analyzer, etc. With regard to the differences in particle size, similar results were obtained for all properties, although the smaller particles have a larger surface area. There are clear differences between the commercial and the home-made activated carbon. Our results show that the home-made activated carbon has a larger surface area and a larger micro pore volume, which indicates that the adsorption capability is higher.

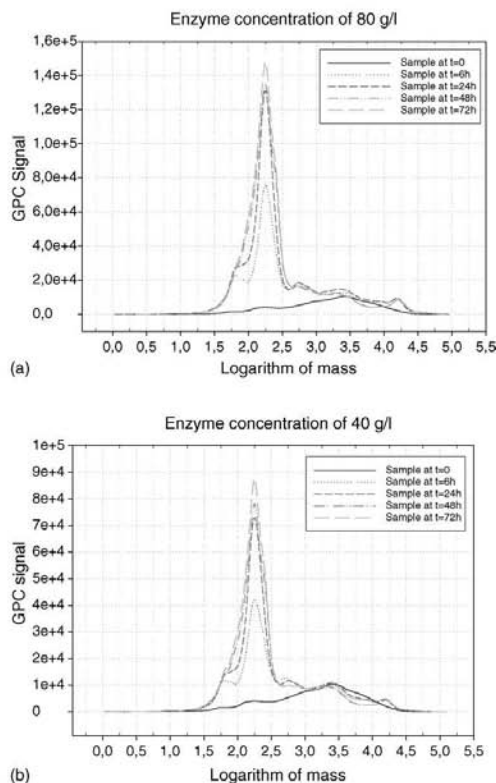


Fig. 3. Chromatographic results of oligosaccharides corresponding to the study of the solid enzyme activity at several concentrations: (a) 80 g/L, (b) 40 g/L, (c) 10 g/L, (d) 2 g/L and (e) 0.5 g/L.

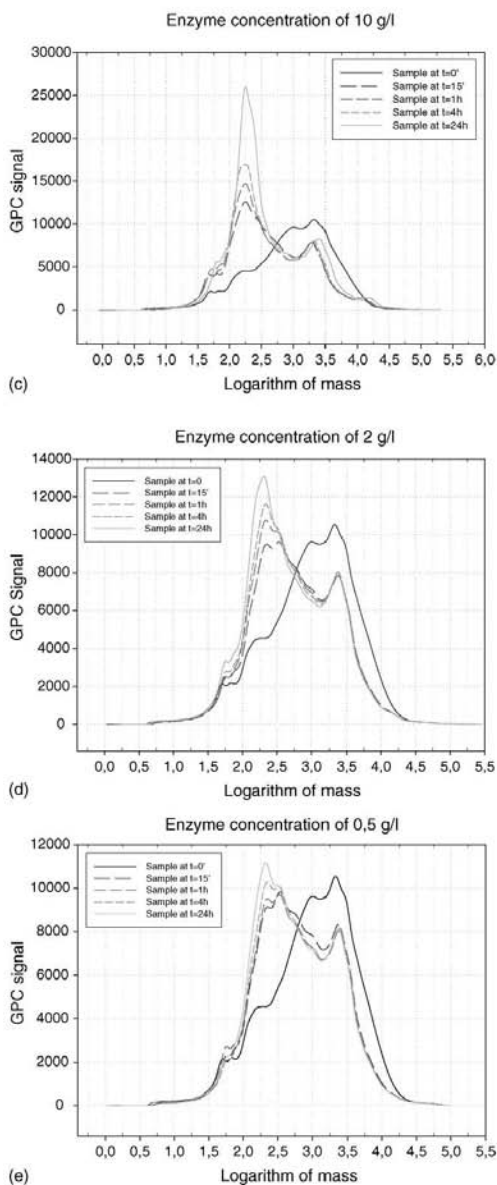


Fig. 3. (Continued).

The results obtained by keeping the metal solution in contact with the activated carbon in batch experiments and using the same variables as before confirmed that there was no variation with time, since the copper adsorbed by the carbon was almost the same for both times. With regard to the concentration of the metal solution, the best results in terms of loading were obtained

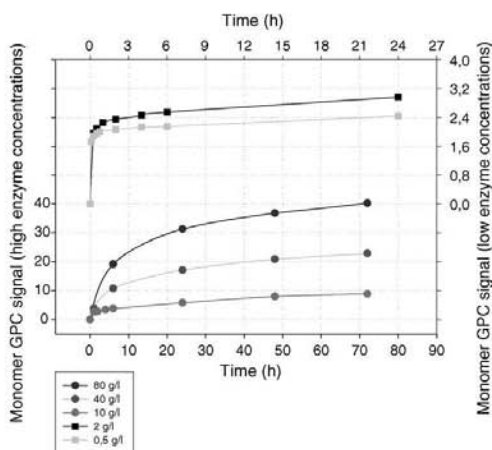


Fig. 4. Kinetics corresponding to the production of the monomer in the reactions carried out with the solid enzyme.

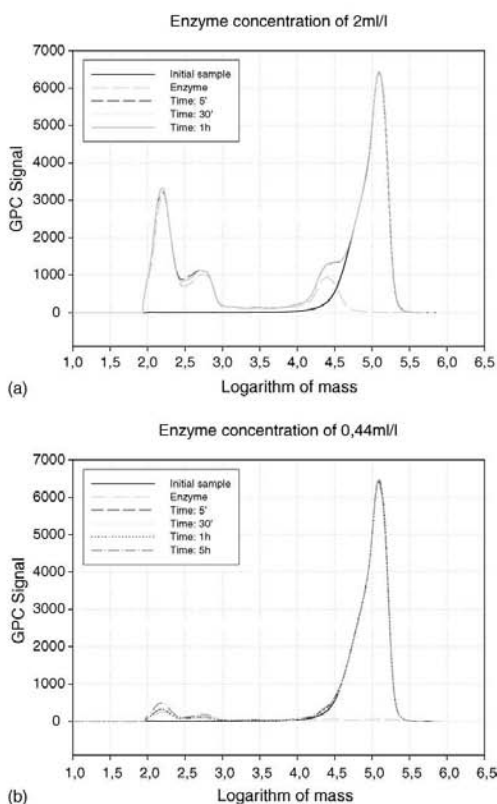


Fig. 5. Chromatographic results of dextrans and enzyme corresponding to the study of the liquid enzyme activity at several enzyme concentrations: (a) 2 mL/L and (b) 0.44 mL/L.

Table 2
 Results of the characterization of the activated carbons with the gas adsorption surface area analyzer

	Surface area	Total pore volume (ml/g)	Micro pore volume (ml/g)
Commercial AC (manufacturer's data)	650	0.93	N/A
Commercial AC (original particle size)	$578 \pm 6 \text{ m}^2/\text{g}$	N/A	0.14
Commercial AC (30–60 μm particle size)	$584 \pm 5 \text{ m}^2/\text{g}$	N/A	0.13
Home-made activated carbon	$1047 \pm 4 \text{ m}^2/\text{g}$	0.51	0.41

at high concentrations, and with regard to particle size, the best results were obtained with small sizes. Variations in these two parameters do not imply significant variations in results. The activated carbon, in agreement with the characterization results, is what really causes different results. The adsorption capability of the home-made activated carbon is about six times higher than that of the commercial membrane (see Fig. 6). Taking into account these results, we performed the following experiments using the home-made activated carbon.

3.3. Batch enzyme loading

As we stated earlier, the enzyme was immobilized with or without a metal ion intermediate but always on the carbon/polysulfone composite. In all cases, two enzyme concentrations were considered with a fixed amount of activated carbon in batch experiments. These concentrations were 100 and 250 mL of enzyme/L of dissolution. The concentrations were high so that the enzyme amount would not be the limiting factor.

All cases showed a reduction in the concentration of the enzyme, because a part of it was bound either to the activated carbon or to the activated carbon–copper system. The concentration decreased the most (about 27% in 48 h) when the initial enzyme concentration was low and with the system containing activated carbon–copper.

Note with regard to the presence of the metal, and despite the previous case, that in the first 24 h, the reduction of enzyme in the solution was greater with the systems that did not contain

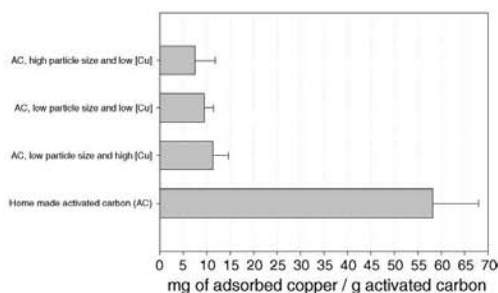


Fig. 6. Results of the metal adsorption capability of the activated carbons.

metal, though the difference in absolute terms was low (9 and 11% versus 4 and 6%). With regard to time, the reduction of enzyme in the solution was always greater at 48 h. It would therefore be suitable to consider longer times to check whether more enzyme can be bound to the precursors. Finally, with regard to concentration, results do not show an optimum configuration.

3.4. Enzymatic membrane reactors

3.4.1. EMR with solid enzyme

To obtain the EMR with the solid enzyme, one polymeric membrane supported the enzyme after dispersing it over the surface of the polymeric film and before immersing it in the coagulation bath to obtain the membrane. Another membrane without the enzyme was then also obtained. The system involved disposing the two membranes in the module, with the layer containing the enzyme located between the two membranes. The enzyme was therefore immobilized in one membrane and encapsulated between the two membranes, and could not escape because the particles were larger than the membrane pores.

The membrane obtained with 20% PSf in DMF and in a coagulation bath containing 50% v DMF and 50% v water has a permeate flux of 0.09 L/m² h bar and a molecular weight cut-off of 28 kDa, measured with the same dextrane samples [11].

Two membrane reactors containing different amounts of solid enzyme were prepared. One of these contained 0.5 g of enzyme and the other contained 3.0 g. Fig. 7 shows the chromatograms corresponding to the initial sample and the permeate of two experiments for each membrane.

These results clearly show that the reaction took place, and that a separation step occurred. In all cases, therefore, some reaction compounds with low molecular weights were produced, and those components with the highest molecular weight were removed from the permeate sample. With the EMR with the largest amount of enzyme, the main component produced in the reaction corresponded to the monomer (in agreement with the results of the batch study of the enzyme activity). With the EMR with the least amount of enzyme, monomer formation was very low and the main component produced was the one corresponding to a molecular weight of about 500 Da.

In the retentate we observed that no reaction products were obtained, which indicates that no reaction occurred, and that the enzyme was properly immobilized in the membranes (which was not in contact with the feed).

Finally, the fluxes measured for the membranes tested were 0.11 and 0.12 L/m² h bar, which is in good agreement to the nominal ones. Note the good agreement between the flux velocity across the membrane and the kinetics of the reaction. This does not occur with the commercial polysulfone membranes, which have larger fluxes (and also larger molecular weight cut-offs). Fig. 8 shows the results obtained using an EMR from a commercial membrane, with a permeability of 10 L/m² h bar and containing 3 g of enzyme, under the same conditions as the previous membrane reactors. Results show that no reaction occurred, though the amount of enzyme was high. This clearly indicates that, in this case, the kinetics of the reaction does not correspond to the membrane flux, which is too high.

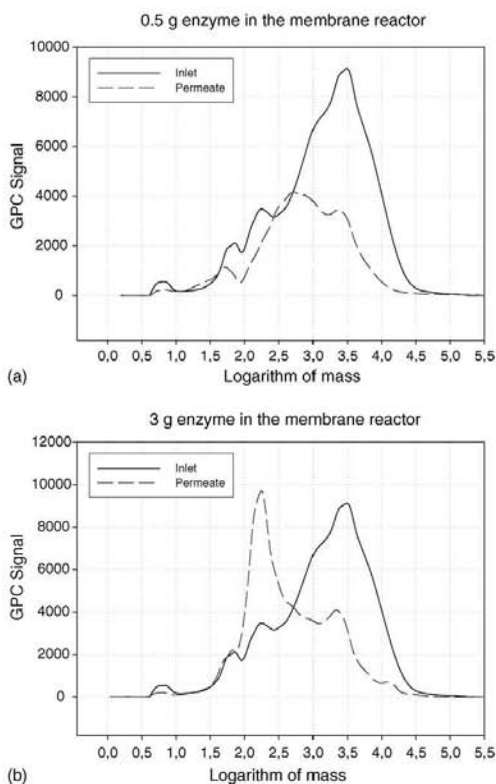


Fig. 7. Chromatographic results of oligosaccharides corresponding to the performance of the EMR containing the solid enzyme in two amounts: (a) 0.5 g and (b) 3 g.

3.4.2. EMR with liquid enzyme

Two types of EMR-containing liquid enzyme were obtained: one monolayer membrane reactor and a two-layer membrane reactor. Fig. 9 shows two photographs of the two type of

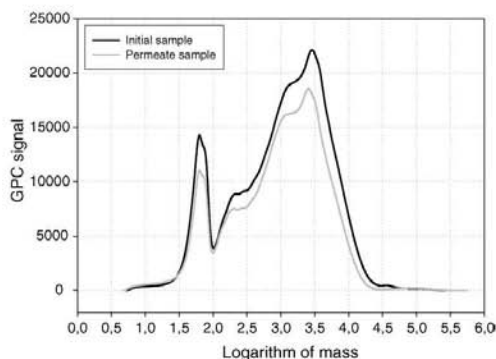


Fig. 8. Chromatographic results of oligosaccharides corresponding to the performance of the EMR containing 3 g of solid enzyme in a commercial membrane.

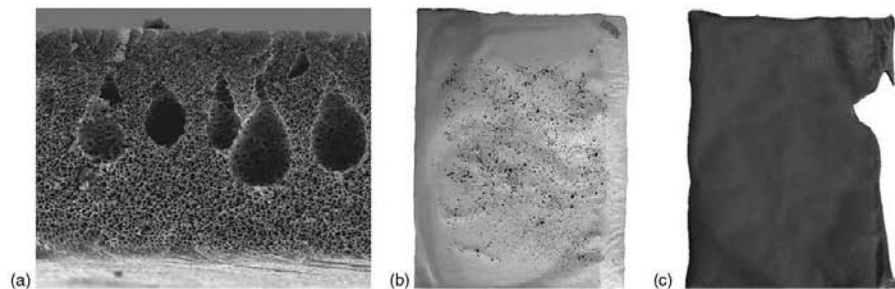


Fig. 9. (a) SEM micrograph of a polymeric membrane obtained with 20% PSF and 50% DMF and 50% H₂O in the coagulation bath. (b) Photograph of a two-layer membrane reactor and (c) one-layer membrane reactor.

membrane reactors, and a cross-section SEM micrograph of the structure of all membranes (which do not change).

For several reasons, the membrane reactors produced with one layer are those with the greatest potential. First, they are the most compact because they comprise a single layer containing the polymeric matrix and the complex-activated carbon–metal–enzyme (or activated carbon–enzyme). Second, the enzyme does not significantly affect the sample feed that does not cross the membrane, so no reaction products are expected to be detected in the retentate stream. Third, the morphological structure of the membrane, determined by the polymeric matrix, does not change when the complex is added (as shown in SEM images and in the conclusions of previous studies [11]). Finally, the presence of the complex throughout the membrane means it can be used in diffusive processes (without pressure and, therefore, without convection) because of the active sites provided by the complex.

On the other hand, this type of membrane reactor presents the most difficulties in its synthesis process because of the greater number of interactions between the components used in the process. Specifically, as is demonstrated in our previous studies [11], the interaction between the solvent (DMF) and the carbon is high. The solvent breaks the carbon particles and may break part of the complex made up of the activated carbon, the metal and the enzyme.

Fig. 10 shows the results from using the monolayer membrane reactor with a test fluid containing a 200 kDa commercial dextrane. These results show that the reaction and the separation were successful. The membrane cut-off is similar to the nominal one, and two basic reaction products were produced—one corresponding to a component of 630 Da and one corresponding to a component of 3200 Da. The signal of the permeate is lower than the one of the initial sample, but if we examine it alone we find that the area occupied by the reaction product is 32% of the total area.

As in the other cases, the retentate stream is free of reaction products. The superficial enzyme of the EMR therefore does not significantly affect the initial sample. The chromatogram shows that, because of the concentration effect of this stream after the most dilute sample crossed the membrane, the height of the signal related to the retentate is slightly higher than that of the initial sample.

Finally, the flux was 0.06 L/m² h bar, which is slightly lower than the nominal flux of the membrane.

The two-layer membrane reactor was obtained with the liquid enzyme. The main advantage of this reactor is the low interaction between the solvent and the enzymatic complex. These reactors can be obtained because the complex particles added on the top

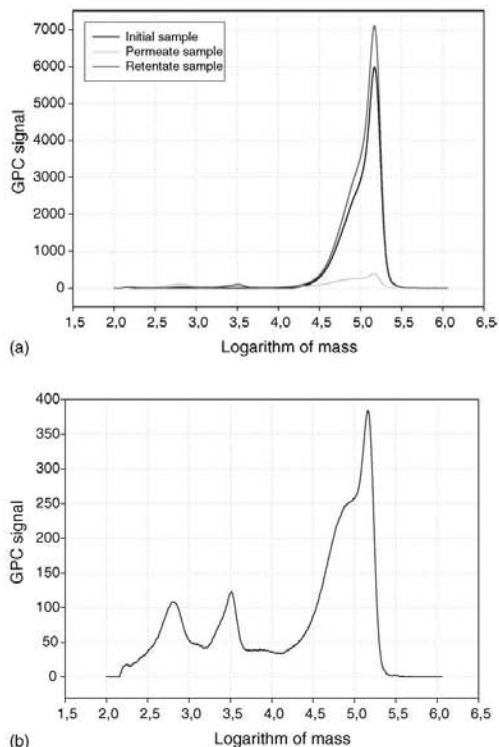


Fig. 10. Chromatographic results of dextrans corresponding to the performance of the monolayer EMR containing the liquid enzyme bound to the activated carbon–metal system: (a) signals corresponding to the initial sample, retentate and permeate, (b) signal corresponding to the permeate.

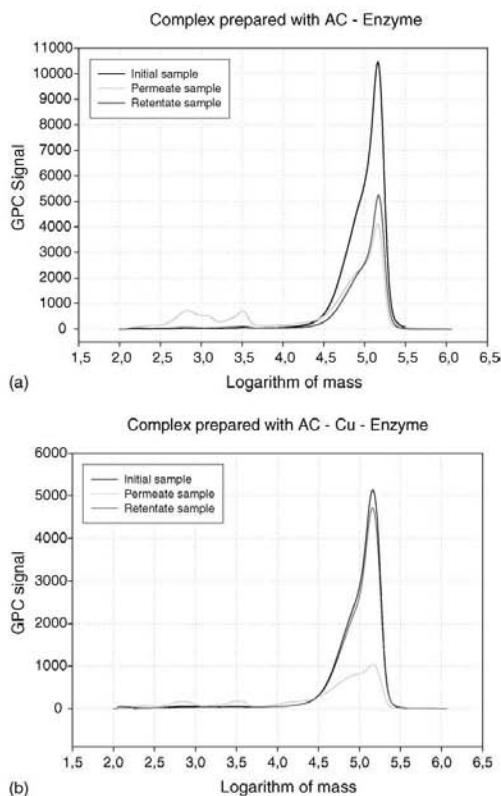


Fig. 11. Chromatographic results of dextrans corresponding to the performance of the two-layers EMR containing the liquid enzyme bound to: (a) activated carbon and (b) activated carbon–metal system.

of the film do not migrate from the membrane after it is immersed into the coagulation bath. In these types of membranes, the entire enzymatic complex is in contact with the initial sample and some reaction products can be formed on the retentate. Finally, this method requires a special technique, both to ensure that the complex deposition over the film is homogeneous and to control the amount of complex added.

Fig. 11 shows the results of the performance with this system. An EMR containing activated carbon–enzyme complex and another containing activated carbon–metal–enzyme were tested. Results are similar to those from the monolayer reactors. In these cases, the signals corresponding to the reaction products in the permeate are higher but they are also part of the feed component, which indicates that the MWCO of the membrane is higher. This always occurs with the two-layer membrane reaction, which suggests that the presence of the complex over the top surface slightly modifies the top nanoporous structure of the membranes. The experiments conducted with these membranes do not show that, overall, results are better with systems that contain metal.

4. Conclusions

In this study, several enzymatic membrane reactors were obtained from polymeric membranes using activated carbon as support to bind the enzyme directly or using a metal ion as precursor. Also, enzymatic membranes reactors were produced without a chemical bond by encapsulating the enzyme between two membrane layers.

Two types of activated carbons were used: a commercial one and a home-made one. Characterization results showed that the surface area was larger for the last one and spectrometer results obtained after the metal was adsorbed by the activated carbon show that adsorption capability was also higher. It is better, therefore, to use the home-made activated carbon.

Using copper to increase the enzyme immobilization with the activated carbon does not provide better overall results, though there is a tendency to increase enzyme adsorption. A more detailed study is needed to obtain more definitive conclusions.

With regard to the membrane reactors, a clear reactivity was demonstrated in all cases and the separation capability of the membrane was maintained, though in some cases this was slightly reduced. The immobilization of the enzymes was also successful in all cases since they were not detected in any stream (permeate and retentate). Also, though optimization was not the aim of this project since it corresponds to future work, there was good agreement in all cases between the kinetics of the reaction and the velocity of the flux across the membrane. The optimal ratio between kinetics and transport did not occur with commercial membranes, in which the velocity of the flux is too high and no reaction occurs.

With regard to the reactors in which the enzyme was encapsulated, although the system corresponds to the less compact EMR produced (two layers are required), it is easy to control the parameters to be considered in the synthesis process (especially the amount of enzyme), the interaction between the compounds that take part in the process is low, and the reactivity levels are satisfactory. In this case, the amount of enzyme should be carefully controlled to avoid the production of monomer.

With regard to the reactors in which the enzyme was adsorbed by the activated carbon or by the pair-activated carbon metal, the one made up of a single layer performs well, since it is compact, it facilitates diffusive transport, the reactivity is satisfactory without the production of monomer, and it maintains the separation capability of the membrane almost intact. The one made up of two layers is easier to produce (because of the fewer interactions between the compounds) and reactivity is higher, but it loses separation capability and is less compact. For these reasons, the reactive membrane with a single layer has the greatest potential.

These results correspond to basic research into this type of enzymatic membrane reactors based on polysulfone and activated carbon. A more detailed study is therefore needed to optimize the various parameters. Promising results are likely, not only in this field of application but also in others.

Acknowledgements

C. Torras acknowledges the Universitat Rovira i Virgili for the doctoral scholarship and Pepa Lázaro for her contribution to the experimental work. This work has been supported by the Spanish Ministry of Science and Technology; project PPQ2002-04201-C02.

Nomenclature

AC	Activated carbon
BET	Gas adsorption surface area analyzer
DMF	Dimethyl formamide
EMR	Enzymatic membrane reactors
GPC	Gel permeation chromatography
MWCO	Molecular weight cut off
PSf	Polysulfone

References

- [1] S. Bouhallab, Les separations par membranes dans les procédés de l'industrie alimentaire, Tech. Doc. Lavoisier, Paris, 1998.
- [2] C.-J. Moon, J.-h. Lee, Use of curdlan and activated carbon composed adsorbents for heavy metal removal, *Process Biochem.* 40 (2005) 1279–1283.
- [3] A. Üçer et al. Immobilisation of tannic acid onto activated carbon to improve Fe(III) adsorption, *Separ. Purif. Technol.*, in press.
- [4] S. Díez, et al., Immobilized soft-metal affinity system for amino acids based on an 8-hydroxyquinoline–Pd(II) complex; characterization using glycine as a model, *Anal. Chim. Acta* 315 (1995) 339–345.
- [5] L.L.E. Salins, S.K. Deo, S. Daunert, Phosphate binding protein as the biorecognition element in a biosensor for phosphate, *Sens. Actuators B* 97 (2004) 81–89.
- [6] M.E. Avramescu, et al., Preparation of mixed matrix adsorber membranes for protein recovery, *J. Membr. Sci.* 218 (2003) 219–233.
- [7] G.L. Lensmeyer, et al., Use of particle-loaded membranes to extract steroids for high-performance liquid chromatographic analyses, improved analyte stability and detection, *J. Chromatogr. A* 691 (1995) 239.
- [8] M. Mulder, *Basic Principles of Membrane Technology*, second ed., Kluwer Academic Publishers, Dordrecht (The Netherlands), 1997, ISBN: 0-7923-4247-8.
- [9] J. Rodríguez-Mirasol, T. Cordero, J.J. Rodríguez, Preparation and characterization of activated carbons from eucalyptus kraft lignin, *Carbon* 31 (1993) 87–95.
- [10] V. Fierro, V. Torné, D. Montané, R. Garcia-Valls, Removal of Cu(II) from aqueous solutions by adsorption on activated carbons prepared from kraft lignin, in: *Conference Proceedings Carbon*, Oviedo, Spain, 2003.
- [11] C. Torras, *Obtenció de Membranes polimèriques selectives*, Ph.D. Thesis, Tarragona (Spain), 2005, pp. 185–203, ISBN: 84-689-3628-6.

5.2.5. Removal of lignin and associated impurities from xylo-oligosaccharides by activated carbon adsorption

Este artículo se ha publicado en el journal Industrial Engineering Chemistry Research en 2006 en el volumen 45, páginas 2294 a 2302.

Removal of Lignin and Associated Impurities from Xylo-oligosaccharides by Activated Carbon Adsorption

Daniel Montané,* Débora Nabarlatz, Anna Martorell, Vanessa Torné-Fernández, and Vanessa Fierro

Departament d'Enginyeria Química, ETSEQ—Rovira i Virgili University, Av. Països Catalans 26, 43007 Tarragona (Catalunya), Spain

This paper studies purification with commercial activated carbons of the xylo-oligosaccharides produced by the autohydrolysis of almond shells. Almond shells are agricultural residues with a high content of xylan that are produced abundantly in some regions with a Mediterranean climate. Adsorption equilibrium was measured in a batch system for three commercial activated carbons using a constant concentration of 20 g/L of crude xylo-oligosaccharides and loads of activated carbon from 1.5 to 50.0 mg/mL. Adsorption for lignin-related products was higher than for xylo-oligosaccharides and the selectivity toward lignin adsorption was better when the carbon was highly microporous and had small mesopore diameters, a low volume of mesopores, a low concentration of basic surface groups to limit xylo-oligosaccharide adsorption, and acidic surface groups to favor the adsorption of the lignin-related products. Column tests were performed at a feed rate of crude xylo-oligosaccharide solution of 6.0 mL/min (35 g/L) in columns packed with 22 g of granular activated carbon and operated in up-flow mode. Average retention was around 64% for lignin products and 21% for carbohydrates for the fraction of treated solution collected during the first 2 h of operation (13.1 bed volumes circulated through the bed). Retention for lignin-derived products was limited because part of them is linked to the xylo-oligosaccharides.

Introduction

Xylose-based oligosaccharides (xylo-oligosaccharides or xylo-oligomers) derived from xylan-rich hemicelluloses are carbohydrates with a high potential for novel applications in food and pharmaceutical products. As they are not metabolized by the human digestive system, xylo-oligosaccharides can be used as low-calorie sweeteners and soluble dietary fiber. They act as prebiotics, providing a source of carbon for the development of intestinal microflora and probiotic microorganisms,^{1–4} and are already used in fortified foods intended for the development of intestinal microflora.^{5,6} In addition, xylo-oligosaccharides have acceptable organoleptic properties and do not exhibit toxicity or negative effects on human health. Ethers and esters prepared from xylan and xylo-oligosaccharides have been synthesized and used as thermoplastic compounds for biodegradable plastics, water soluble films, coatings, capsules, and tablets⁷ and also for the preparation of chitosan–xylan hydrogels.⁸ Xylo-oligosaccharides extracted by autohydrolysis of bamboo have recently been found to possess a cytotoxic effect on human leukemia cells.⁹

The autohydrolysis of xylan-rich biomass is a suitable process for the production of xylo-oligosaccharides. It eliminates the use of important amounts of the chemicals needed in other extraction processes, such as alkali and acid, and since autohydrolysis takes place in slightly acidic media, many of the side chains in the backbone xylose chains, such as acetyl, uronic acids, and phenolic acid substituents, remain in the xylo-oligosaccharides.^{10,11} The differential characteristics of the substituted xylo-oligosaccharides obtained by autohydrolysis have prompted renewed interest in the development of process strategies for achieving a high yield of xylo-oligosaccharides

with consistent reproducibility in purity and composition. Though xylo-oligosaccharides are the main component in the nonvolatile products of biomass autohydrolysis, they are mixed with monosaccharides, ferulic acids, uronic acids, and compounds formed by the partial hydrolysis of lignin, the dehydration and degradation of carbohydrates, and condensation reactions. Lignin-derived products are the largest fraction of the impurities associated with xylo-oligosaccharides. Lignin is a three-dimensional polymer made of phenylpropane units linked randomly through alkyl–aryl ether bonds. It acts as a protecting agent and binder in the cell-wall structure of lignocellulosic materials. During autohydrolysis, lignin is depolymerized partially through cleavage of the ether linkages and yields phenolic monomers and oligomers that are soluble in the aqueous media. Also, some of the xylose units in the xylan backbone are bonded to lignin through ether and ester linkages. Consequently, some of the xylo-oligosaccharides contain lignin oligomers linked to the xylose chain. Various impurities from minor constituents of the lignocellulosic biomass—including inorganic salts, extractives, and, in some cases, proteins—are also present.

Clearly, therefore, the crude xylo-oligosaccharides produced by the autohydrolysis of lignocellulosic biomass will contain large amounts of lignin-derived phenolics, carbohydrate dehydration and condensation products, and ash. For instance, the content of xylo-oligosaccharides in the nonvolatile products has been reported to be 58.3% for almond shells,¹² 54.8% for rice husks,¹³ and only 46.3% for barley residues.¹⁴ Crude xylo-oligosaccharides must be purified in order to obtain a final product that is well characterized chemically and structurally, homogeneous, repetitive, and suitable for food or pharmaceutical applications. Purification sequences based on liquid–liquid and solid–liquid extractions, solvent precipitation, and ion exchange treatments, as well as combinations of these techniques, have been thoroughly studied.^{13,14} Treatment with activated carbon has been shown to be an effective process for removing

* To whom correspondence should be addressed. E-mail: daniel.montane@urv.net. Phone: (+34) 977 559 652. Fax: (+34) 977 558 544.